Numerical Simulation of Ice Crystal Growth (Initial Frosting Process)

by

Eball Hifthy A. Ahmed

A Thesis Presented to the

FACULTY OF THE COLLEGE OF GRADUATE STUDIES

KING FAHD UNIVERSITY OF PETROLEUM & MINERALS

DHAHRAN, SAUDI ARABIA

In Partial Fulfillment of the
Requirements for the Degree of

MASTER OF SCIENCE

In

MECHANICAL ENGINEERING

February, 1992

Order Number 1354079

Numerical simulation of ice crystal growth (initial frosting process)

Ahmed, Eball Hifthy A., M.S.

King Fahd University of Petroleum and Minerals (Saudi Arabia), 1992

U·M·I
300 N. Zeeb Rd.
Ann Arbor, MI 48106

NUMERICAL SIMULATION OF ICE CRYSTAL GROWTH (INITIAL FROSTING PROCESS)

BY

EBALL HIFTHY A. AHMED

A Thesis Presented to the

FACULTY OF THE COLLEGE OF GRADUATE STUDIES

KING FAHD UNIVERSITY OF PETROLEUM & MINERALS

DHAHRAN, SAUDI ARABIA

In Partial Fulfillment of the
Requirements for the Degree of

MASTER OF SCIENCE

In

MECHANICAL ENGINEERING

FEBRUARY, 1992

KING FAHD UNIVERSITY OF PETROLEUM & MINERALS

DHAHRAN, SAUDI ARABIA

This thesis, written by **EBALL HIFTHY A. AHMAD** *under the direction of his thesis committee, and approved by all the members, has been presented to and accepted by the Dean, College of Graduate Studies, in partial fulfillment of the requirements for the degree of*

MASTER OF SCIENCE IN MECHANICAL ENGINEERING

Thesis Committee

Ahmet Sahin

Chairman (Dr. Ahmet Z. Sahin)

S.M. Zubair

Member (Dr. Sayd M. Zubair)

W. Stahl

Member (Dr. Wolfgang M. Stahl)

Dr. M.O. Budair
Department Chairman

Dr. Ala M. Al-Rabeh
Dean College of Graduate Studies

Date : 17-2-92

كلية الدراسات العليا
COLLEGE OF GRADUATE STUDIES

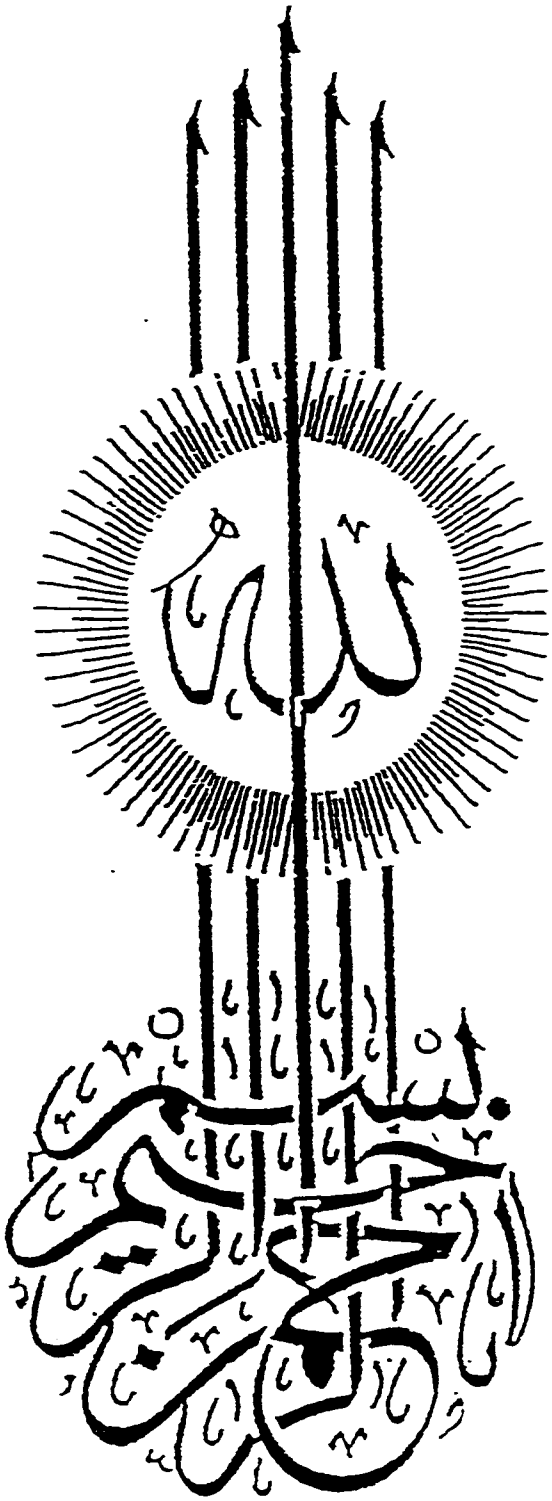
بسم الله الرحمن الرحيم

ACKNOWLEDGEMENT

First and foremost, praise and thanks be to Almighty ALLAH, the most Gracious, the most Merciful.

I wish to express my warmest and sincere gratitude to Dr. Ahmad Z. Sahin , my thesis committee chairman for his positive guidance, advice and relentless encouragement. I am also grateful to other members of my committee, Dr. Sayed Zubiar and Dr. W.H. Stahl, for their significant contribution and valuable suggestions.

I gratefully acknowledge the Mechanical Engineering department of King Fahd University of Petroleum & Minerals(KFUPM) for the support provided to carry out this research.

Thanks are also to Dr.Mohammed O. Budair, Chairman of Mechanical Engineering Department, for his cooperation and support during the research work.

I would like to express my sincere thanks and gratitude to Dr. Mohammad Hastouglu whose idea and advice attracted me to the field of such a work and helped me to initial understanding of this research.

I would like to express my special gratitude and warm thanks to my friends whose understanding, patience and loving in ALLAH have been a constant source of strength and confidence along the way.

Last,but certainly not least, other faculty and staff of Mechanical Engineering Department also deserve appreciation for their encouragement throughout the period which I spent among them.

TABLE OF CONTENTS

Chapter *Page*

ACKNOWLEDGEMENT iv

LIST OF TABLES ix

LIST OF FIGURES x

ABSTRACT -in English xvi

-in Arabic xvii

1. INTRODUCTION AND THEORETICAL BACKGROWND 1

1.1 INTRODUCTION 1

1.2 THEORETICAL BACKGROWND 3

1.2.1 Frost formation 3

1.2.2 Ice crystal formation 8

2. LETERATURE SURVEY 13

3. PROBLEM FORMULATION

3.1 Problem statement 20

3.2 Model selection 22

3.3 Model equations 24

3.2.1 Cylinrical model equations 24

3.3.1.1 Conservation equations for heat transfer 24

3.3.1.2 Boundary equations 28
3.3.1.3 Initial conditions 38
3.3.1.4 Boundary conditions 39
3.3.2 Sperical Model 40
3.3.2.1 Conservation equations for heat transfer 40
3.3.2.2 Boundary equations 43
3.3.2.3 Initial conditions 44
3.3.2.4 Boundary conditions 44

4. Numerical Solution 45

4.1 Finite difference solution for the cylendrical model 46
4.1.1 Model equations descritization 46
4.1.2 Stability of the method 50
4.1.3 Solution procedure 50
4.1.3.1 Sherwood and Nusselt numbers 51
4.1.3.3 thermal conductivity of ice crystal 52
4.1.3.4 Biot number 52
4.1.3.5 Reynold number 53
4.1.3.6 Prandl number and Schemidt number 53
4.1.3.7 Density of the ice crystal 53
4.1.3.8 difusion coeffecient 54
4.2 Numerical solution of the spherical
model of the ice crystal 55
4.2.1 Model equations descritization 55

4.2.2 Stability of the solution 60
4.2.3 Solution Procedure 60
4.2.3.1 Nusselt number and Sherwood number 61
4.2.3.2 Biot number 61

5. DISCUSSION OF RESULTS AND CASE STUDIES

5.1 Cylinrical model 64

5.1.1 Effect of ambient temperature 64
5.1.2 Effect of plate temperature 86
5.1.3 Effect of air velocity 99
5.1.4 effect of initial ratio 105
5.2 Spherical model 112

5.1.1 Effect of ambient temperature 112
5.1.2 Effect of plate temperature 120
5.1.3 Effect of air velocity 126

5.3 Experimental part 131

6. SUMMARY AND CONCLUSIONS 138

6.1 Conclusions 138
6.2 Recommendations 139

APPENDIX-A : 140

APPENDIX B 151

NOMENCLATURE 160

REFERENCES 165

VITA 170

LIST OF TABLES

table		*Page*
1.1	Ice crystal habits at different temperatures.	1
5.1	Comparison bctwwen the length of the crystal in the model and that obtained from experimental results. For cylindrical model.	134
5.2	Comparison bctwwen the radius of the crystal in the model and that obtained from experimental results.For cylindrical model	135
5.3	Comparison betwwen the radius of the crystal in the model and that obtained from experimental results.For spherical model	136

LIST OF FIGURES

figure		*Page*
1.1	Frost layer growth represented by cluster of rod type crystals	4
3.1	Cylindrical model assumed for the ice crystal.	22
3.2	Spherical model assumed for the ice crystal.	23
3.3	Control volume for cylindrical shape.	24
3.4	Concentration gradient at the interface between solid and air.	34
3.5	Control volume for spherical shape.	40
4.1	Grid points representation required for numerical solution in the case of Cylendrical model.	46
4.2	Grid points representation required for numerical solution in the case of Spherical model.	55
5.A	Length of the crystal vs. Time for different ambient temperatures	66
5.1	Dimensionless temperature vs. length of the crystal for cylindrical model $\Gamma_o = 1.0$, $V_{air} = 2\ m/s$ $T_v = 5.0°C$. , $T_s = -10°C$.	68
5.2	Dimensionless temperature vs. radius of the crystal for cylindrical model. $\Gamma_o = 1.0$, $V_{air} = 2\ m/s$ $T_v = 5.0°C$. $T_s = -10°C$.	69
5.3	Length of the crystal vs. Time for cylindrical model . $\Gamma_o = 1.0$, $V_{air} = 2\ m/s$ $T_v = 5.0°C$. $T_s = -10°C$.	70
5.4	Radius of the crystal vs. Time for cylindrical model . $\Gamma_o = 1.0$, $V_{air} = 2\ m/s$ $T_v = 5.0°C$. $T_s = -10°C$.	71
5.5	Dimensions of the crystal vs. Time for cylindrical model . $\Gamma_o = 1.0$, $V_{air} = 2\ m/s$ $T_v = 5.0°C$. $T_s = -10°C$.	72
5.6	Mass transfer flux vs. Time for cylindrical model. $\Gamma_o = 1.0$, $V_{air} = 2\ m/s$ $T_v = 5.0°C$. $T_s = -10°C$.	73

5.7 Dimensionless temperature vs. length of the crystal for cylindrical model .
$\Gamma_o = 1.0$, $V_{air} = 2\ m/s$ $T_v = 0.5°C$. , $T_s = -10°C$. 74

5.8 Dimensionless temperature vs. radius of the crystal for cylindrical model.

$\Gamma_o = 1.0$, $V_{air} = 2\ m/s$ $T_v = 0.5°C$. $T_s = -10°C$. 75

5.9 Length of the crystal vs. Time for cylindrical model .
$\Gamma_o = 1.0$, $V_{air} = 2\ m/s$ $T_v = 0.5°C$. $T_s = -10°C$. 76

5.10 Radius of the crystal vs. Time for cylindrical model .
$\Gamma_o = 1.0$, $V_{air} = 5\ m/s$ $T_v = 0.5°C$. $T_s = -10°C$. 77

5.11 Dimensions of the crystal vs. Time for cylindrical model .
$\Gamma_o = 1.0$, $V_{air} = 5\ m/s$ $T_v = 0.5°C$. $T_s = -10°C$. 78

5.12 Mass transfer flux vs. Time for cylindrical model.
$\Gamma_o = 1.0$, $V_{air} = 5\ m/s$ $T_v = 0.5°C$. $T_s = -10°C$. 79

5.13 Dimensionless temperature vs. length of the crystal for cylindrical model .
$\Gamma_o = 0.8$, $V_{air} = 2\ m/s$ $T_v = 10°C$. , $T_s = -10°C$. 80

5.14 Dimensionless temperature vs. radius of the crystal for cylindrical model.

$\Gamma_o = 0.8$, $V_{air} = 2\ m/s$ $T_v = 10°C$. $T_s = -10°C$. 81

5.15 Length of the crystal vs. Time for cylindrical model .
$\Gamma_o = 0.8$, $V_{air} = 2\ m/s$ $T_v = 10°C$. $T_s = -10°C$. 82

5.16 Radius of the crystal vs. Time for cylindrical model .
$\Gamma_o = 0.8$, $V_{air} = 2\ m/s$ $T_v = 10°C$. $T_s = -10°C$. 83

5.17 Dimensions of the crystal vs. Time for cylindrical model .
$\Gamma_o = 0.8$, $V_{air} = 2\ m/s$ $T_v = 10°C$. $T_s = -10°C$. 84

5.18 Mass transfer flux vs. Time for cylindrical model.
$\Gamma_o = 0.8$, $V_{air} = 2\ m/s$ $T_v = 10°C$. $T_s = -10°C$. 85

5.B Length of the crystal vs. Time for different surface temperatures 87

5.19 Dimensionless temperature vs. length of the crystal for cylindrical model .
Γ_o=0.8 , V_{air} = 2 m/s T_v= 5.0°C . , T_s= -20°C . 88

5.20 Dimensionless temperature vs. radius of the crystal for cylindrical model.
Γ_o=0.8 , V_{air} = 2 m/s T_v= 5.0°C . T_s= -20°C . 89

5.21 Length of the crystal vs. Time for cylindrical model .
Γ_o=0.8 , V_{air} = 2 m/s T_v= 5.0°C . T_s= -20°C . 90

5.22 Radius of the crystal vs. Time for cylindrical model .
Γ_o=0.8 , V_{air} = 2 m/s T_v= 5.0°C . T_s= -20°C . 91

5.23 Dimensions of the crystal vs. Time for cylindrical model .
Γ_o=0.8 , V_{air} = 2 m/s T_v= 5.0°C . T_s= -20°C . 92

5.24 Mass transfer flux vs. Time for cylindrical model.
Γ_o=0.8 , V_{air} = 2 m/s T_v= 5.0°C . T_s= -20°C . 93

5.25 Dimensionless temperature vs. length of the crystal for cylindrical model .
Γ_o=1.0 , V_{air} = 2 m/s T_v= 5.0°C . , T_s= -3°C . 94

5.26 Dimensionless temperature vs. radius of the crystal for cylindrical model.
Γ_o=1.0 , V_{air} = 2 m/s T_v= 5.0°C . T_s= -3°C . 95

5.27 Length of the crystal vs. Time for cylindrical model .
Γ_o=1.0 , V_{air} = 2 m/s T_v= 5.0°C . T_s= -3°C . 96

5.28 Radius of the crystal vs. Time for cylindrical model .
Γ_o=1.0 , V_{air} = 2 m/s T_v= 5.0°C . T_s=-3°C .

5.29 Dimensions of the crystal vs. Time for cylindrical model .
Γ_o=1.0 , V_{air} = 2 m/s T_v= 5.0°C . T_s= -3°C . 98

5.30 Mass transfer flux vs. Time for cylindrical model.
Γ_o=1.0 , V_{air} = 2 m/s T_v= 5.0°C . T_s= -3°C . 99

5.C Length of the crystal vs. Time for different air velocities 991

5.31 Dimensionless temperature vs. length of the crystal for cylindrical model .
Γ_o=1.2 , V_{air} = 6 m/s T_v = 5.0°C . , T_s = -10°C . 100

5.32 Dimensionless temperature vs. radius of the crystal for cylindrical model.
$\Gamma_o = 1.2$, $V_{air} = 6\ m/s$ $T_v = 5.0°C$. $T_s = -10°C$. 101

5.33 Length of the crystal vs. Time for cylindrical model.
$\Gamma_o = 1.2$, $V_{air} = 6\ m/s$ $T_v = 5.0°C$. $T_s = -10°C$. 102

5.34 Radius of the crystal vs. Time for cylindrical model.
$\Gamma_o = 1.2$, $V_{air} = 6\ m/s$ $T_v = 5.0°C$. $T_s = -10°C$. 103

5.35 Dimensions of the crystal vs. Time for cylindrical model.
$\Gamma_o = 1.2$, $V_{air} = 6\ m/s$ $T_v = 5.0°C$. $T_s = -10°C$. 104

5.36 Mass transfer flux vs. Time for cylindrical model.
$\Gamma_o = 1.2$, $V_{air} = 6\ m/s$ $T_v = 5.0°C$. $T_s = -10°C$. 105

5.37 Dimensionless temperature vs. length of the crystal for cylindrical model.
$\Gamma_o = 2.0$, $V_{air} = 3\ m/s$ $T_v = 5.0°C$., $T_s = -20°C$. 106

5.38 Dimensionless temperature vs. radius of the crystal for cylindrical model.
$\Gamma_o = 2.0$, $V_{air} = 3\ m/s$ $T_v = 5.0°C$. $T_s = -10°C$. 107

5.39 Length of the crystal vs. Time for cylindrical model.
$\Gamma_o = 2.0$, $V_{air} = 3\ m/s$ $T_v = 5.0°C$. $T_s = -10°C$. 108

5.40 Radius of the crystal vs. Time for cylindrical model.
$\Gamma_o = 2.0$, $V_{air} = 3\ m/s$ $T_v = 5.0°C$. $T_s = -10°C$. 109

5.41 Dimensions of the crystal vs. Time for cylindrical model.
$\Gamma_o = 2.0$, $V_{air} = 3\ m/s$ $T_v = 5.0°C$. $T_s = -10°C$. 110

5.42 Mass transfer flux vs. Time for cylindrical model.
$\Gamma_o = 2.0$, $V_{air} = 3\ m/s$ $T_v = 5.0°C$. $T_s = -10°C$. 111

5.D Length of the crystal vs. Time for different ambient temperatures. 112

5.43 Dimensionless temperature vs. X for spherical model.
$\Gamma_o = 1.0$, $V_{air} = 2\ m/s$ $T_v = 5.0°C$., $T_s = -10°C$. 113

5.44 Radius of the crystal vs. Time for spherical model.
$\Gamma_o = 1.0$, $V_{air} = 2\ m/s$ $T_v = 5.0°C$., $T_s = -10°C$. 114

5.45 Mass transfer flux vs. Time for spherical model.
$\Gamma_o = 1.0$, $V_{air} = 2\,m/s$ $T_\infty = 5.0°C$., $T_s = -10°C$. 115

5.46 Dimensionless temperature vs. X for spherical model.
$\Gamma_o = 1.0$, $V_{air} = 2\,m/s$ $T_\infty = 10°C$., $T_s = -10°C$. 116

5.47 Radius of the crystal vs. Time for spherical model.
$\Gamma_o = 1.0$, $V_{air} = 2\,m/s$ $T_\infty = 10°C$., $T_s = -10°C$. 117

5.48 Mass transfer flux vs. Time for spherical model.
$\Gamma_o = 1.0$, $V_{air} = 2\,m/s$ $T_\infty = 10°C$., $T_s = -10°C$. 118

5.E Length of the crystal vs. Time for different surface temperatures. 119

5.49 Dimensionless temperature vs. X for spherical model.
$\Gamma_o = 1.0$, $V_{air} = 2\,m/s$ $T_\infty = 5.0°C$., $T_s = -20°C$. 120

5.50 Radius of the crystal vs. Time for spherical model.
$\Gamma_o = 1.0$, $V_{air} = 2\,m/s$ $T_\infty = 5.0°C$., $T_s = -20°C$. 121

5.51 Mass transfer flux vs. Time for spherical model.
$\Gamma_o = 1.0$, $V_{air} = 2\,m/s$ $T_\infty = 5.0°C$., $T_s = -20°C$. 122

5.F Length of the crystal vs. Time for different air velocities 123

5.52 Dimensionless temperature vs. X for spherical model.
$\Gamma_o = 1.0$, $V_{air} = 4\,m/s$ $T_\infty = 5.0°C$., $T_s = -10°C$. 124

5.53 Radius of the crystal vs. Time for spherical model.
$\Gamma_o = 1.0$, $V_{air} = 4\,m/s$ $T_\infty = 5.0°C$., $T_s = -10°C$. 125

5.54 Mass transfer flux vs. Time for spherical model.
$\Gamma_o = 1.0$, $V_{air} = 4\,m/s$ $T_\infty = 5.0°C$., $T_s = -10°C$. 126

LIST OF APPENDICES

APPENDIX-A : 140

APPENDIX B 151

THESIS ABSTRACT

Name Of Student : Eball Hifthy A. Ahmad

Title of Study : Numerical Simulation Of Ice Crystal Growth

(Initial Frosting Process)

Major Field : Mechanical Engineering

Date of Degree : February 1992

A numerical model for ice crystal growth is presented. Two models are assumed to represent the ice crystal. The ice crystal is assumed to grow in cylindrical and spherical shapes.Principles of mathematical modelling of ice crystal and a procedures for solving the models equations are discussed.The models permits a continuous determination of the phase change interface and the temperature distribution.

The models equations obtained are transformed into finite difference approximations and solved by an explicit method.Models predictions are compared together with some available experimental data to obtain the best model representing the ice crystal.

The effect of the velocity and composition of vapour gas mixture ice crystal base temperature and biot number are considered for the determination of the growth rate of ice crystal.

Model predictions are analyzed to assess the potential application of such methods in the study of frosting process.

The important features of the model are :
(i) Explicit formulation is used to prevent extensive storage.
(ii) Exclusive use is made of two dimensional formulation.

MASTER OF SCIENCE DEGREE

KING FAHD UNIVERSITY OF PETROLEUM AND MINERALS
Dhahran, Saudi Arabia

February 1992

ملخص الرسالة

إسم الطالب : عبال حفظي عبد الرحيم أحمد .

عنوان الرسالة : التمثيل الرقمي لنمو البلوره الثلجية (بداية عملية التثليج) .

التخصص : الهندسة الميكانيكة .

تاريخ الرسالة : فبراير ١٩٩٢م .

لقد تمت في هذا البحث دراسة نمو البلوره الثلجية وقد مثلت البلورة الثلجية بتمثيلان رقميان .

في هذا البحث أفترض نمو البلورة الثلجية بشكل أسطواني وآخر كروي الطرق اللازمة للتمثيل الرقمي والحلول المتبعة للوصول الى هذا المثيل قد وضحت في البحث ، التمثيل الرقمي المستخدم في البحث يمكن من التحديد المستمر لنمو البلورة الثلجية وتغير درجة الحرارة بداخلها وعلى حدودها .

المعادلات التمثيلية المستخدمة حولت الى فروق محدودة العددية وحلت بالطريقة الظاهرة .
النتائج المستخرجة من التمثيل الرقمي درست وحللت وقورنت بالنتائج المستخرجة من التجارب .

تأثير سرعة ومكونات الخليط الجوي الرطب وتأثير درجة الحرارة القاعده التي تنمو عليها البلورة الثلجية وتأثير رقم بيوت درست بتركيز لتحديد تأثيرها على نمو البلورة الثلجية وتحليل نتائج هذا التمثيل تم لدعم استخدام هذه الطريقة لدراسة عمليات التثليج .

من الخواص المهمة لهذا التمثيل الرقمي :
١ ـ التقليل من الحاجة الى كمية هائلة من ذاكرة الحاسب الآلي باستخدام الطريقة الظاهرة في الفروق المحدودة العددية .
٢ ـ تم إستخدام تمثيل رقمي يعتمد اعتمادا كليا على التمثيل ثنائي الابعاد .

درجة الماجستير في العلوم

جامعة الملك فهد للبترول والمعادن

الظهران ـ المملكة العربية السعودية

فبراير ١٩٩٢م

CHAPTER ONE

INTRODUCTION AND THEORETICAL BACKGROUND

1.1-INTRODUCTION

It is known that when humid air is exposed to a surface which is colder than the dew point temperature of the air, condensation will take place as the air is cooled, and that the water vapor leaving the air will pass directly from gaseous to solid state of frost if the surface temperature is below $0°C$. This phenomena encountered in the field of air conditioning and refrigeration has a significant adverse effect upon the heat transfer and pressure drop. For instance, the frost formation on heat exchanger surface can be extremely important to their efficient operation since the frost will act as a thermal insulator, thus reducing the ability of the surface to transfer heat. Also, accumulations of the frost often become thick enough to restrict and block the air flow passage. There is a need for a fundamental understanding of the nature of frost formation including the vapor condensation process to assist the predicting rate of frost formation.

Frost formation is a common phenomena in aerospace environment as well. In particular, formation of frost on air craft wings has been known to cause

aerodynamic penalties on lift and drag during the take-off. The accurate calculation of frost growth on the airfoil and the corresponding aerodynamic penalties require better understanding of early stages of the frost formation process.

Early stages of frost formation process is characterized by ice crystals starting to form on the surface. Investigating the ice crystal growth process is a fundamental part in getting better view on the frost formation process.

Ice crystal growth is a very complicated transient process, in which a variety of heat and mass transfer mechanisms are at work, simultaneously. In this project, we have investigated the process of ice-crystal growth from vapor phase and the behavior of these crystals under different conditions.

1.2- THEORETICAL BACKGROUND

2.2.1 - Frost Formation

When a cold surface is exposed to the moist air, small dotted-like ice crystals first appear on it . These crystals seem to grow perpendicular to the surface for a short time (the exact duration depends on the conditions of deposition), after which a noticeable meshing of the crystals occurs and a smooth layer covers the surface. The initial period before a smooth layer is formed is referred to as the " nucleation regime " or " crystal growth period " according to different investigators. The second and third distinct regimes of frost formation are called " dry frost layer growth " or " frost layer growth period " and " wet frost layer growth " or " frost layer full growth period", respectively. This kind of a division is the result of studies by microscopic observations, Sahin(1988).

In the crystal growth period, a thin frost layer covers the surface initially. Next, frost crystals, which are relatively far apart from each other, appear on the thin frost layer, and grow in a vertical direction at about the same rate. Thus, the frost formation in this period is best characterized by the crystal growth in linear dimensions, such that the frost becomes like a forest of trees, without the growth of a homogeneous layer.

In the frost layer growth period, the rough frost which is assumed to be a cluster of rod type crystals as shown in Fig (1.1) changes its shape by the generation of branches around the top of a crystal or by the interaction of each crystal and then grows gradually into a meshed and more uniform frost layer until the frost surface becomes nearly flat. In this period, the frost density increases with the growth of frost layer, because of three-dimensional growth and the internal diffusion of water vapor in the frost layer.

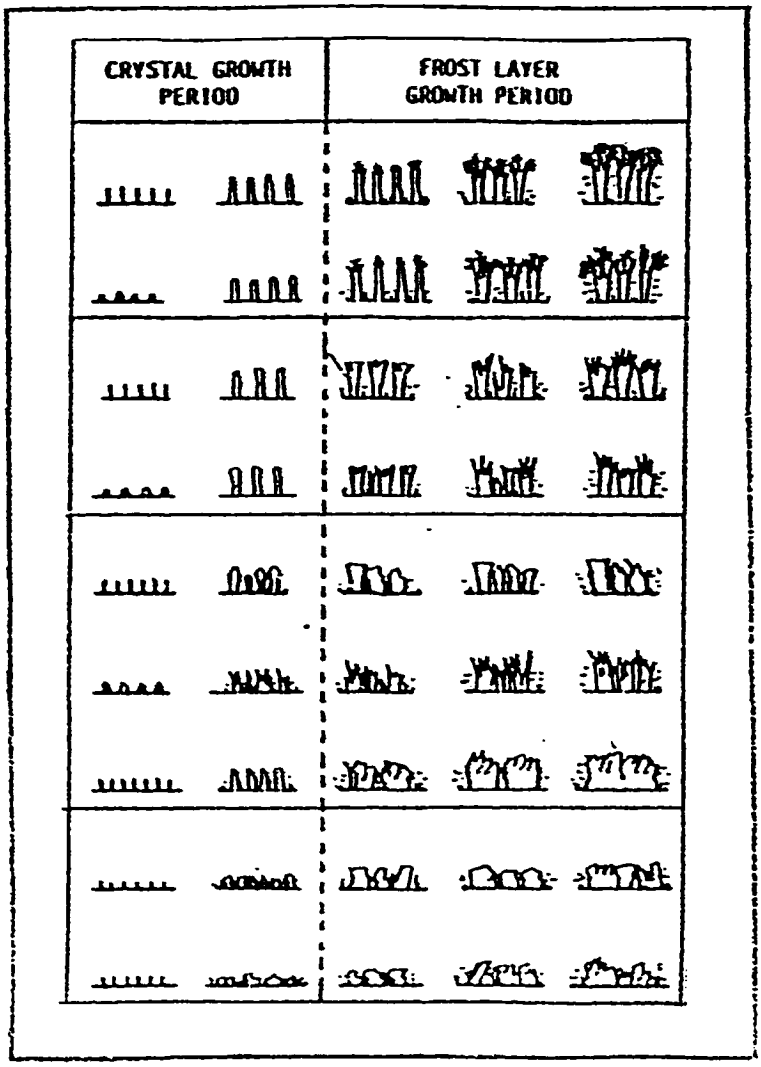

Fig(1.1) Frost layer growth represented by cluster of rod type crystals, Hallett (1984)

In the frost layer full growth period, the frost layer surface temperature is assumed to be $0°C$. Once the frost layer surface temperature increased over this temperature i.e. $0°C$, the frost surface will begin to melt. The resultant water soaks into the frost layer and freezes into an ice layer. The melting and freezing cause a sudden increase in the frost layer density and a sudden decrease in its thermal resistance, thus the frost deposition occurs again. Then a cyclic process of melting, freezing, and deposition continues, periodically, until the frost formation stops when the thermal equilibrium conditions is reached. During this period, the frost layer becomes a dense and tight layer and grows into aged frost.

When the humid air flows over a flat plate, the frost formation process does not occur uniformly over the whole plate but varies with longitudinal position. The frost layer grows faster in the upstream than in the downstream of the plate even for the same thermal conditions, and each phase moves gradually from the front to the rear of the plate. This means that the time required for each phase varies not only with the frost formation conditions but also with the frost deposition position. This longitudinal variation is insignificant during the frost nucleation process but becomes quite pronounced during the frost layer growth period, Gallily (1987).

It has been noticed that the higher stream velocity appears to increase the number of frost columns in the crystal growth period, and to advance the rate

of the frost growth even for the same frost deposition rate, Termizi (1987).

The detailed mechanism of frost formation and the shape of the frost layer during each phase are different in a microscopic viewpoint due to the various frost formation conditions, Hayashi (1977). classified frost formation into several types according to:

1- The structure and shape of crystals in the initial stage of frost formation, the temperature of the transition from the rod type crystal to the feather type crystal and the state of its transition at the end of the crystals growth period.

2- The regional position of frost formation conditions, crystal surface and plate tempratures.

In the first regime, namely " crystal growth period ", the initial frost layer can begin in one of the two ways. In the first case, initial condensation occurs at nucleation sites on the wall resulting from a critical supersaturation. In the other case (for a very cold wall), boundary layer fogging occurs and the fog becomes the major source for water droplet condensation on the wall. Thus the " frost-point ", temperature (i.e. the temperature at which frost actually begins to form) lies somewhere between the " fog-point " and the " dew-point " temperatures, depending on nucleation sites on the wall and on the wall temperature.

It has been well established that vapor diffusion does occur within the frost layer due to the vapor pressure gradient which is a consequence of the temperature gradient. The diffusion process is relatively slow process and it was concluded by Chung and Algren (1958) that the diffusion process has a little effect on changing the local frost density or thermal conductivity. Although the diffusion of vapor does play an important role in the density and thermal conductivity, Sahin (1988) have assumes that these variables are constant with time.

Several variables have been suggested in the literature as having an apparent effect on the density of frost. These include plate temperature, air temperature and air velocity. However, it is noted that none of these are properties of the frost layer in that they are all variables external to the frost layer and do not uniquely define properties within the frost layer itself. If a useful analytical tool it to be developed, it was felt that the frost model must include the correlation of the frost density with some other property (or properties).

1.2.2 - Ice crystal formation :

Ice crystals can grow in two distinct ways either by the freezing of liquid water or by direct sublimation from the vapor phase. In each case the mechanisms which determine the rate and habit of growth are the transport of water molecules to the point of growth and their accommodation into the growing interface, together with the transport of latent heat away from this interface. Many different physical situations can occur; of course, but they are all controlled by these basic mechanisms. If the system contains another components in addition to water, the situation will be more complicated because crystal growth depends upon the transport of this component as well and there may also be competing process occurring at the interface with the growing ice crystal.

The thermodynamic force driving any crystallization process is an excess of the chemical potential of molecules in the environment relative to its value in a bulk crystal. This excess may be specified as a supercooling in the case of freezing or as a supersaturation in the case of growth from the vapor. The total chemical potential excess may be divided into two parts. A component which is the driving force for transport of water molecules through the environment to the growing interface. and another component which is necessary to achieve the incorporation of molecules into the crystal itself. In this project the ice crystal

growth from vapor phase will be studied .

The growth of ice crystals from the vapor is a familiar phenomenon since a major part of the growth of snow flakes occur in this way. The beautifully symmetric growth forms of snow crystals like those shown in appendix (A) are well known and it is often supposed that all natural snowflakes are of this form. The shapes of ice crystals growing either artificially or experimentally is very complicated and may take different shapes. These shapes range from long thin needles through columns to plates, and each shape may be simple or eccentric. These different shapes are all related to the environment in which the crystal grow. In addition there are many other mixed forms, such as columns tipped with plates, representing crystals whose environment altered during the course of their growth.

The main parameter affecting the growth habits of ice crystals are the temperature .

Many scientists have done experiments on this factor that is effecting the growth rate of ice crystals. Results are summarized in table like table (1), Sahin (1988).

Temperature (°C)	*Form of ice crystal*
≥ -3.5	Solid hexagonal plane ice crystal
−3.5 to −4	Solid/hollow-type column
−4 to −6	Needle-type column
−6 to −8	Sheath-type column
−8 to −9.5	Solid/hollow-type column
−9.5 to −12	Thick plane-type ice crystal, often with hollow structure on prism faces
−12 to −14	Plane-type ice crystal with internal structure and ribs extending along the *a* axis over the basal faces of the crystal
−14 to −17	Stellar-type plane ice crystal
−17 to −19	Hexagonal plane ice crystal with internal structure
−19 to −23	Thick plane-type ice crystal with hollow structure on prism faces
−23 to −32	Mostly columnar ice crystals, sheath and solid/hollow types

TABLE (1.2) Ice crystal habits at different temperatures, Sahin(1988).

The striking feature of this table is the sharp effect of temperature on the growth regimes. These transition between the different growth regimes are very sharp extending over less than 1°C. The axial ratio (c/a) of the crystal is changing discontinuously from perhaps 10 for columns to 100 for needles to values from 0.1 to 0.01 for plates. It is also worth noting that transitional forms, such as plates growing on the end of needles can be produced if the crystals are transferred from one temperature regime to another during the growth process. The temperature dependence of crystals habits is thus extraordinarily specific in formulation, Show (1955).

There has been no convincing explanation of these changes of ice crystals at different temperatures because present theories of crystals growth do not contain parameters that are likely to be strongly face dependent and also sensitive to temperature changes of only few degrees, Hallett and Cho (1984).

From all the previous explanations we can see that any attempt to model the ice crystal growth will meet many uncertainties.

At the present time there are no theoretical expressions to allow direct computations of ice crystal growth, shapes and densities as a function of the temperature. Therefore any model must be based on experimental observations which contain many discrepancies between the different observers.

Models studied in this project for the ice crystal are approximations to the actual process since we are only assuming cylindrical and spherical shapes without any reference to changes from one type of growth to another, so what is being done is a method to approximate the crystal growth and this will not replace the need for experimental study of ice crystals to obtain more accurate results.

CHAPTER TWO

LITERATURE SURVEY

Many workers studied the ice crystal growth and the factors effecting this growth. Both experimental and theoretical investigations have been carried out.

Reynolds (1952) computed the growth rates of large ice crystals. He assumed the crystals to be in motion, because of this he supplemented the diffusion term by a ventilation. He was able to generate the beak of growth rates at $-5°C$ and $-15°C$ by choosing suitable values for the axial ratios and densities.

Mason (1953) studied using numerical approximation the growth of an ice particle by diffusion. He computed crystal growth rates at $-2.5°C$ and $-5°C$.

Braham (1968) compiled all known empirical evidence for the rates of growth of ice crystals and he compared all his evidence with some available approximations. He concluded that approximations done by Marson does not fit his observations.

Cotterill and Martin (1973) studied the micro-structure of an ice crystal. They studied an ice model containing two unit cells. They assumed that the individual model in the cell interact with one another through the effective pair potential. They, also, studied energies of the molecules using the method of molecular dynamics.

Jaweera (1970) calculated the growth rates and the masses to which the crystal grow at different times for various temperatures. He used the electrostatic analogy and assumed the crystals to follow the experimentally observed growth modes. He concluded that the resulting growth rates are best approximated by a spherical model.

Ono (1970) studied the growth modes of ice crystal in natural clouds. He reached a conclusion that the ice crystal growing in a water cloud may grow either with a constant axial ratio or with one axis fixed. Crystal whose minor axis is smaller than some limiting value (which he founded it to be a function of temperature and super saturation) seen to grow with constant axial ratio. After this limiting dimension is reached, the growth stands to be apparently along the major axis only.

Hindman (1972) presented an empirical approximation for the growth of ice crystal by diffusion. He assumed the crystal to have a shape of hexagonal prism with a starting dimensions along the major and minor axis to be 0.1mm and initial mass at 0.1mgm. He studied the ice crystal formation in a cloud from

super-cold water droplets. He founded that after 27 minutes from the starting point of the formation, the length of ice crystal will be one cm.

Allen (1973) presented a paper where he mentioned diffraction and thermal experiments carried out on the form of ice obtained from vapor phase. He mentioned various structural models of ice crystals where he studied them experimentally. He found that the actual behavior of the crystals is different from the models assumed.

Hobbs (1973) used the classical diffusion theory to determine the ice crystal growth under the assumption that the crystals grow as spheres until their radii reach 35 μm after which they grow as plates with the growth limited to one axis.

Heymsfied (1974) studied the growth of the ice phase in the clouds. He developed some equations to calculate the rate of growth of the ice in the clouds. He studied the growth of ice crystal with an updraft velocity of 100 cm/s. He calculated the growth of ice crystals assuming nucleation temperature of $-40°C$. He predicted the crystal to have a length of 1.00 mm after a long time.

Pruppacher and Hall (1976) did a theoretical study to determine the relevant micro-physical processes which control the survival distance af ice particles falling from cerrius clouds in subsaturated air. They also studied the heat exchange between an ice particle and its environment. They reached a

result that an ice particle falling could survive a distance of 2 km with a relative humidity of 70%. If humidity is larger, ice particles could survive to a large distances. They also compared their results with experimental results where they found good agreement.

A study on the effect of convection on the growth of ice crystals had been done by Kallungal and Barduhn (1977). They studied various aspects of ice crystals growth in forced and natural convection. They concluded that the dimensions of the crystals' major (c) and minor (a) axes vary widely among various experimental studies. They found that the crystals shapes, geometries and orientations depend on whether the crystals are forming under forced or natural convection.

Young and Miller (1978) discussed a detailed scheme for numerically integrating the diffusion equation for ice crystals growth. Their study was based on extensive survey of observed crystals habits, i.e., densitis and masses. They assumed that the ice crystals will take the shapes of hexagonal prisms with two based face and six prism faces and that growth of these crystals stand along both axis. Then after a critical limit, the growth along one axis will stop while it will continue along the other axis. They also concluded that the ice crystals shapes and growth mode depend mainly on temperature and to less degree on super saturation of water vapor.

Laudise and Barns (1984) studied the formation of the largest crystallization process in the world which is the formation of ice in a lake. They studied the process of ice crystal growth in two lakes under different conditions. they concluded that the orientation of the major (c) axis of the crystal depends on the ambient conditions under which the crystals are forming.

Stoyanova and Nenow (1984) studied the stability of ice crystals growing from vapor phase. They studied the stability of plate and column like ice crystals obtained at temperatures from (-1 to $-12°C$) Small ice crystals were found to be stable. They found that the instability of the crystals start to develop from the phase with higher growth rate.

Hallet and Cho (1984) studied ice crystal growing from vapor phase. They measured

the growth velocity as a function of temperature, super saturation and air pressure. They concluded that the growth velocity of the ice crystals increases with decreasing air pressure. They, also, concluded that the growth velocity of the ice crystals increases with decreasing temperature.

Colbeck (1985) did an experimental study on the growth of ice crystals under controlled conditions at temperatures between ($-0.6°C$ and $-20°C$). He studied the equilibrium form of the crystals which were found to be a temperature dependent. He concluded that the equilibrium form of the ice

crystals at temperatures below $-11°C$ is a hexagonal prism with a ratio of hexagonal diameter to thickness of about 2.5.

A study on the ice crystal formation and growth and how natural convection is effecting this growth and formation has been done by Termizi and Gill (1987). Their work is mainly experimental. They did quantative measurements of the growth rates and dimensions of ice crystals growing in pure water under forced convection. They concluded that natural convection is effecting the velocity of the growth of ice crystal.

Sahin (1988) presented a model of the frost formation on cold surfaces. He assumed the ice crystal to have a cylindrical shape. He proved experimentally that his model for the frost formation process was correct.

Many other scientists [20-26] studied the ice crystal properties like ice crystal thermal conductivity, density and many other properties under different conditions.

Numerical solution to moving boundary problems, which involve a phase change process, had been paid great attention.

Lazaridis (1970) solved a multi-dimensional heat transfer problem which involve a solidification process . He used the finite difference scheme to solve the pertinent equations numerically where he determined the temperature

distribution in both the media around the solid-liquid interface.

This type of problems has also been solved by Comini and Bonacina (1973) where they solved one dimensional phase-change problem using finite difference implicit method. They compared thier results with analytical solution, where they found satisfactory results.

Hastaoglu (1986) solved a one dimensional melting and solidification problem using finite difference implicit method.

Hastaoglu (1987) solved a three dimensional melting and solidification problem in which a second layer of solid is added at variable rates. He assumed the physical properties of the system to depend on the position and temperature. He solved the problem using finite difference method where he used explicit method in the solution.

Based on the literature survey, it appears that, this is the first time where the ice crystal growth (initial frosting process) will be studied using finite difference method.

CHAPTER THREE

PROBLEM FORMULATION

3.1- Problem Statement

As soon as a cooled surface is exposed to the humid air, ice crystals will start to form on the surface. Very soon ice crystal will start to grow in size. Since a temperature gradient exists through the crystal, water vapor diffuses through the gas phase of the layer under the vapor pressure gradient (corresponding to the temperature difference) and solidifies in the ice crystal. This process will cause the growth of the ice crystal.

A simple model is selected to study the growth of an ice crystal in which the ice crystal is assumed to grow in two shapes. the first shape will be considered is a cylindrical shape while the second one is the spherical shape. The study of the ice crystal growth will be investigated under the following assumptions:

1- ice crystal is assumed to grow in cylindrical and spherical models.

2- constant humidity ratio.

3- constant ice crystal surface temperature.

4- The physical properties of the ice in the crystal is independent of temperature and position .

5- the ice-gas interface is smooth.

6- low pressure application.

3.2- Models selection:

To approximate the ice crystal shape and growth a model should be selected. This model should be based on the best approximation that will give the best simulation of the ice crystal growth.

First model : Ice crystal is modeled as a cylinder as shown in Fig (3.1). All the assumptions assumed in sec(3.1) apply to this model. The shape of the ice crystal is assumed to be represented at any time with this model. The growth of the ice crystal is taking place along (r,z) directions. The growth is assumed to be homogeneous in which the ice crystal is growing equally in any direction.

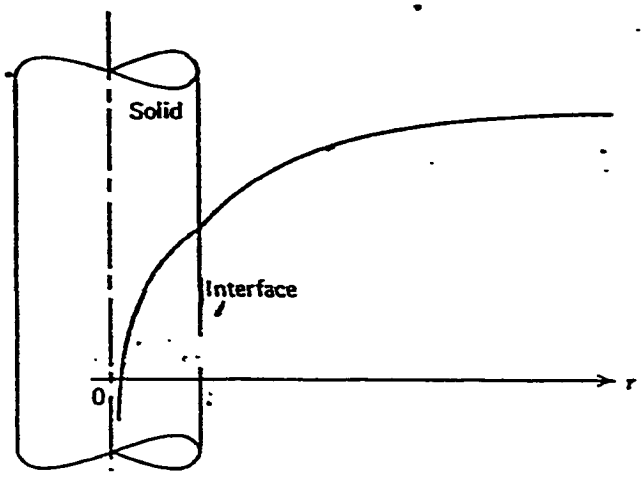

Fig(3.1) Cylendrical model assumed for the growth of ice crystals.

Second model : Ice crystal is modeled as a hemi-sphere as shown in Fig(3.2). All the assumptions assumed in sec(3.1) apply to this model. The shape of the ice crystal is assumed to be represented at any time with this model. The growth of the ice crystal is taking place along (r) direction. The growth is assumed to be homogeneous in which the ice crystal is growing equally in any direction. taking place along the (r) direction as shown in Fig(3.2).

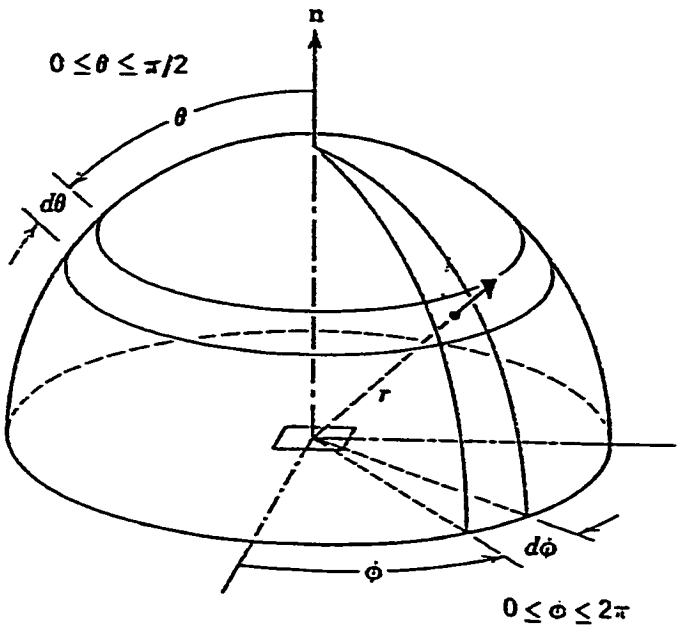

Fig(3.2) Spherical model assumed for the growth of ice crystals.

3.3- Models equations:

3.3.1- Cylindrical model equations:

3.3.1.1 - Conservation equations for heat transfer

To obtain the energy conservation equation for cylindrical model we apply the conservation of energy over a control volume. So the first thing is to identify the control surface. The next step is identifying the energy terms. These include the rate of energy entering and/or leaving through the control surface, $\dot{E}_{in} - \dot{E}_{out}$, ,the rate of change of energy stored with in the control volume $\frac{dE_{st}}{dt} = \dot{E}_{st}$. A general form of the energy conservation requirement may then be expressed on rate basis as $\dot{E}_{in} - \dot{E}_{out} = \dot{E}_{st}$. Taking a control volume for the cylindrical shape as shown in fig (3.3).

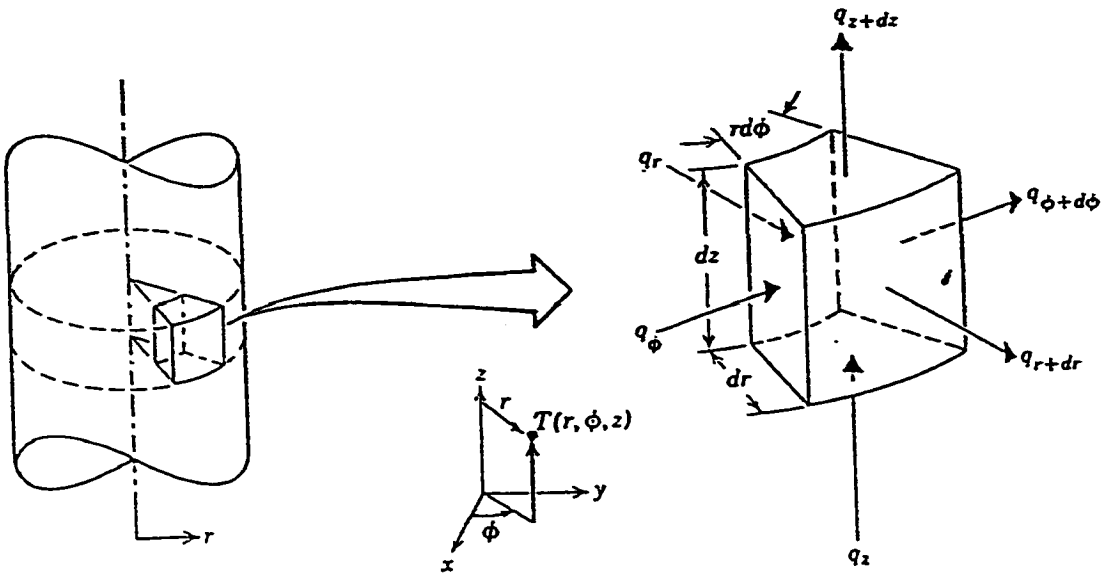

Fig(3.3) Differential control volume, $dr \cdot r\,d\phi \cdot dz$, for conduction analysis in cylindrical coordinates (r,ϕ,z).

Applying Energy conservation on this control volume for two dimensional case along (r,z) direction

$$q_z - q_{z+dz} + q_r - q_{r+dr} = \rho_s \frac{\partial T}{\partial t} (2\pi r\, dr\, dz) \tag{3.2}$$

substituting the following values for q_{z+dz} and q_{r+dr} we ger

$$q_{z+dz} = q_z + \frac{\partial q_z}{\partial z} dz + \text{higher order term.} \tag{3.3}$$

$$q_{r+dr} = q_r + \frac{\partial q_r}{\partial r} dr + \text{higher order term.} \tag{3.4}$$

into the energy balance equation gives.

$$-\frac{\partial q_z}{\partial z} dz - \frac{\partial q_r}{\partial r} dr = \rho_s \frac{\partial T}{\partial t} (2\pi r\, dz\, dr) \tag{3.5}$$

Using Fourier's equation we can get the following expressions

$$q_z = -kA_z \frac{\partial T}{\partial z} = -k\, 2\pi r\, dr \frac{\partial T}{\partial z} \tag{3.6}$$

$$q_r = -k\, 2\pi r\, dz \frac{\partial T}{\partial r} \tag{3.7}$$

substituting these expressions into the differential form of the energy equations gives :

$$-\frac{\partial}{\partial z}(-K2\pi\, r\,dr\frac{\partial T}{\partial z})\,dz - \frac{\partial}{\partial r}(K2\pi\, r\,dz\frac{\partial}{\partial r})\,dr = \rho_s\frac{\partial T}{\partial t}(2\pi\, r\,dr\,dz)$$

$$2\pi\, r\,dr\,dz\frac{\partial^2 T}{\partial z^2} + 2\pi\,dz\,dr\frac{\partial}{\partial r}(r\frac{\partial T}{\partial r}) = \frac{1}{\alpha_s}\frac{\partial T}{\partial t}(2\pi\, r\,dr\,dz)$$

dividing by $2\pi\, r\,dr\,dz$ gives

$$\frac{\partial^2 T}{\partial z^2} + \frac{1}{r}\frac{\partial}{\partial r}(r\frac{\partial T}{\partial r}) = \frac{1}{\alpha_s}\frac{\partial T}{\partial t} \qquad (3.9)$$

Where $\alpha_s = \frac{k}{\rho_s c_s}$.

Equation (3.9) represents the conservation of energy in cylindrical coordinate system for two dimensional case where conduction is assumed to be dominant factor for heat transfer in the solid ice.

Since the dimensions involved in this problem are very small (in the order of microus) the equations used will be non dimensionalized. non dimensionalizing equation (3.9) is made by the following dimensionless variables.

$R = \frac{r}{r_o}$ dimensionless radius (3.10)

$Z = \frac{z}{z_o}$ dimensionless length (3.11)

$$0 = \frac{T - T_s}{T_{des} - T_s} \qquad \text{dimensionless temperature.} \qquad (3.12)$$

$$\tau = \frac{\alpha t}{z_o^2} \qquad \text{dimensionless time.} \qquad (3.13)$$

Using the forgoing dimensionless parameters equation (3.10) becomes

$$\frac{\partial \theta}{\partial \tau} = [\frac{z_o^2}{r_o^2} \frac{1}{R} \frac{\partial}{\partial R}(R \frac{\partial \theta}{\partial R}) + \frac{\partial^2 \theta}{\partial Z^2}]$$

When defining $\Gamma_o = \frac{z_o}{r_o}$, equation (3.9) becomes :

$$\frac{\partial \theta}{\partial \tau} = [\frac{\Gamma_o^2}{R} \frac{\partial}{\partial R}(R \frac{\partial \theta}{\partial R}) + \frac{\partial^2 \theta}{\partial Z^2}] \qquad (3.14)$$

3.3.1.2- Boundary equations

We now present a discussion of the boundary equations at the ice-vapor interface for the present model. The fundamental relations that should be satisfied at such an interface are.

1- The temperature of the adjacent phases should be equal to the same temperature which is equal to the desublimation temperature of the vapor gas.

2- Energy balance must be satisfied at the interface, generally the densities at the vapor and solid ice are not the same therefore some motion at the vapor resulting from density change is expected in actual situation.

The requirements on the continuity of temperature at the solid ice-gas interface.

$$T_s(r,z,t,) = T_v = T_{des} \quad \text{at} \quad f(r,z,t) = 0. \tag{3.15}$$

where ($f(r,z,t) = 0$) accounts for the definition at the sharp interface separating the ice-vapor in the energy equation at the ice-gas interface for desublimation as in Fig(3.a), Ozisik(1980).

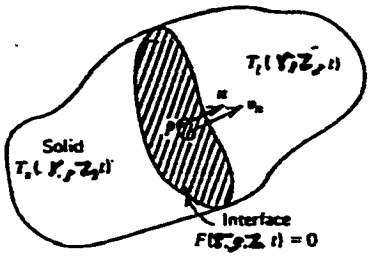

Fig(3.a)

Energy balance at the interface should satisfy the following relation .

[Heat flux through the solid phase] −

[Heat flux through the vapor phase]=

[Rate of heat liberated during desublimation per unit area of interface]

In the models, we are assuming that the heat transfer mode between the interface and the vapor is by convection, conduction is the only mode of heat transfer in the ice-crystal.

For cylindrical coordinates the change along (r or z) direction through the interface is given by

$$[k_s \frac{\partial T}{\partial n} + h(T_{des} - T_\infty)] = \rho \Delta H V_n \qquad (3.16)$$

where $(\frac{\partial}{\partial n})$ is the derivation at the interface along the normal direction vector (n) which could be r or z depending on the direction assumed for the change of the interface. V_n is the velocity of the intervace in the positive n direction. This form of the equation is not suitable for development af analytical or numerical solution so another form of this equation could be obtained in the following manner. The previous equation could be written in the form

$$k_s \, grad\, T_s \, grad\, f + h(T_{des} - T_s) = -\rho_s \Delta H \frac{\partial f}{\partial t} \qquad (3.17)$$

where $$grad\, T_s \, grad\, f = \frac{\partial T_s}{\partial r}\frac{\partial f}{\partial r} + \frac{\partial T}{\partial z}\frac{\partial f}{\partial z} \qquad (3.18)$$

relating

$$\frac{\partial T_s}{\partial r} \text{ to } \frac{\partial T_s}{\partial z}$$

through

$$\frac{\partial T_s}{\partial r} = \frac{\partial f / \partial r}{\partial f / \partial z}\frac{\partial T}{\partial z} \qquad (3.19)$$

now introducing this into $\partial T_s \, \partial f$

$$grad\, T_s \, grad\, f = \frac{\partial T}{\partial z}\frac{\partial f}{\partial z} + \left(\frac{\partial f}{\partial z}\right)^2. \qquad (3.20)$$

substituting this back into the energy balance equation gives

$$\frac{\partial f}{\partial z}\left[1 + \left(\frac{\partial f / \partial r}{\partial f / \partial z}\right)^2\right]\left[k_s \frac{\partial T_s}{\partial z} + h(T_{des} - T_s)\right] = -\rho_s \Delta H \frac{\partial f}{\partial t} \qquad (3.21)$$

if the equation of interface is expressed in the form of

$$f(r,z,t) = z - s(r,t) = 0 \qquad (3.22)$$

then

$$\frac{\partial f}{\partial r} = -\frac{\partial s}{\partial r} \quad , \quad \frac{\partial f}{\partial z} = 1 \quad \text{and} \quad \frac{\partial f}{\partial t} = -\frac{\partial s}{\partial t}$$

this provides the interface equation for this part

$$[1+(\frac{\partial s}{\partial r})^2][k_s\frac{\partial T_s}{\partial z} + h\ (T_{des} - T_\infty)] = \rho_s \Delta H\frac{\partial s}{\partial t} \quad \text{at} \quad z = s(r,t) \qquad (3.23)$$

where $s(r,t) = Y_z$

same procedure could be followed to obtain the change in the interface along r direction. The previous form of the interface equation is represented in general form. The boundary equations for this model is assumed to take the following forms:

For two dimensional moving boundary problem in cylindrical coordinates the boundary equations are :

$$\rho_s \Delta H\frac{\partial Y_z}{\partial t} = [1 + (\frac{\partial Y_z}{\partial r})^2]\ [h_g(T_{des} - T_\infty) + k_s\frac{\partial T}{\partial z}] \qquad (3.24)$$

$$\rho_s\Delta H\frac{\partial Y_r}{\partial t} = [1 + (\frac{\partial Y_r}{\partial z})^2]\ [h_g(T_{des} - T_\infty) + k_s\frac{\partial T}{\partial r}] \qquad (3.25)$$

In which the change of the interface boundary is occuring in the r and z directions respectevely.

To nondimensionalize the previous equations the following dimensionless parameters will be used.

$$Y_Z = \frac{Y_z}{z_o} \ , \ Y_R = \frac{Y_r}{r_o} \ , \ \tau = \frac{\alpha_s t}{z_o^2}$$

The following form of the interface equation will be obtained after non dimensionalizing the interface equation along Z direction.

$$G\frac{\partial Y_Z}{\partial \tau} = [1 + \Gamma_o^2(\frac{\partial Y_Z}{\partial R})^2] \ [\frac{\partial \theta}{\partial Z} + B_i(1 - \theta_s)] \qquad (3.26)$$

$$\text{Where } G = \frac{\Delta H}{C_s(T_v - T_s)} \qquad (3.27)$$

$$B_i = (\frac{h_g z_o}{k_s}) \qquad B_i = \textit{Biot number} \qquad (3.28)$$

Non dimensionalizing the boundary equation along the R direction gives :

$$\frac{G}{\Gamma_o^2}\frac{\partial Y_R}{\partial \tau} = [1 + \frac{1}{\Gamma_o^2}(\frac{\partial Y_R}{\partial Z})] \ [B_{ir}(1 - \theta_s) + \frac{\partial \theta}{\partial R}] \qquad (3.29)$$

Where

$$G = \frac{\Delta H}{C_s(T_v - T_s)} \ , \ B_{ir} = \frac{B_i}{\Gamma_o} \qquad (3.30)$$

In desublimation, the phase change would occur due to heat transfer but the desubliming component has to be transferred via mass transfer to the solid gas interface. Therefore it is imperative to compare these two rates.The phase change due to mass transfer can be obtained using an F-type mass transfer coefficient (Treybal 1980) or by using the latent heat of desublimation as a factor relating the heat rate with the mass rate (Young 1978, Pruppacher 1976).

When there exists a gas system in contact with solid like ice-water vapor system, some vapor molecules will instantly transfer from the gas to the solid crossing the interfacial surface separating the two phases as long as the chemical potential at the vapor is not equal in the two phases. It should be noted that the chemical potential of the two phases and not the concentration is the driving force for the transport phenomena, Treybal(1980).

Since in our case the vapor is diffusing from the gas phase into the solid, there must be a concentration gradient in the direction of mass transfer with in each phase. This is shown in fig (3.4).

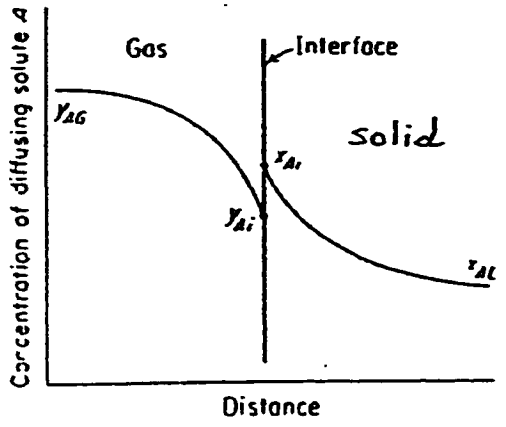

Fig(3.4) Concentration gradient at the interface between solid and air.

As shown the concentration of vapor in the main body of the gas is y_{AG} mole fraction and it falls to Y_{Ai} at the interface, in the solid the concentration falls from X_{Ai} at the interface to X_{AS} in the bulk liquid, the bulk concentrations Y_{AG} and X_{AS} are not equilibrium values since other wise diffusion of the water vapor molecules would not occur. At the same time, these bulk concentrations can't be used directly with a mass transfer coefficient to describe the rate of interface mass transfer since the two concentrations are differently related to chemical potentials which is the real driving force to mass transfer. To get around this problem, we can assume that the only diffusion resistance are those residing in the solid and that there is no resistance to solute transfer across the interface separating the phases.

It may be noticed according Fig(3.4) that X_{Ai} is greater than Y_{Ai} and this may be an obstacle infront of mass transfer across the phases but this is not true since both of these concentrations are equilibrium concentration according to the two film theory and hence corresponds to equal chemical potentials of vapor in both phases at the interface.

For the case shown in fig (3.4) for the mass transfer between two phases and assuming the applicability of Ficks equation which will be written for mass transfer in the z direction

$$J_A = -D_{AB}\frac{\partial C_A}{\partial z} = -CD_{AB}\frac{\partial X_A}{\partial z} \qquad (3.31)$$

where the negative sign emphasizes that diffusion occurs in the direction at a drop of concentration. If diffusion is occurring between two components then the net flux is

$$N_A + N_B = N \qquad (3.32)$$

Where the movement of A is made up into two parts namely that resulting from the bulk motion N, and the fraction X_A of N which is N_A, and that resulting from diffusion J_A:

$$N_A = X_A N + J_A \qquad (3.33)$$

$$N_A = (N_A + N_B)\frac{C_A}{C} - D_{AB}\frac{\partial C_A}{\partial z} \qquad (3.34)$$

Applying this case to the case where diffusing is only taking place in the z direction and same thing could be done for diffusion in the (r) direction with N_A and N_B both constants (steady state) we can separate the variables and assuming D_{AB} is constant we can integrate.

$$\int_{C_{A1}}^{C_{A2}} \frac{-dC_A}{N_A C - C_A(N_B + N_A)} = \frac{1}{CD_{AB}} \int_{z_1}^{z_2} dz$$

Letting

$z_2 - z_1 = z$

The integration of the previous equation gives

$$N_A = \frac{N_A}{N_B + N_A} \frac{CD_{AB}}{z} \ln \frac{N_A/(N_A+N_B) - (C_{A2}/C)}{N_A/(N_A+N_B) - (C_{A1}/C)} \tag{3.35}$$

The general form of the equation (3.35) is :

$$N_A = \frac{N_A}{\Sigma N} F \ln \frac{(N_A/\Sigma N) - Y_{Ai}}{N_A/\Sigma N - Y_{AG}} = \frac{N_A}{\Sigma N} F \ln \frac{N_A/\Sigma N - X_{Ai}}{N_A/\Sigma N - X_{AS}} \tag{3.36}$$

Applying the previous expression for the case of diffusion of one component

$\Sigma N = N_A$ gives

$$N_A = F \ln \frac{1 - X_{Ai}}{1 - X_{Ao}} \tag{3.37}$$

In this F-type mass transfer coefficient, the rate of mass flux due to the transfer of water-vapor molecules to the ice crystal can be claculated using equation (3.37). Writing the previous equation in a general form where the diffusing component A is water-vapor gives :

$$N_{water\text{-}vapor} = F \ln \frac{1 - X_{Ai}}{1 - X_{Ao}} \tag{3.38}$$

Where the interphase mole fraction X_{Ai} is calculated from the interface concentration C_{Ai}, which is determined from the vapor pressure-temperature relation and the perfect gas law. X_{Ao} is the mole fraction of desubliming component in the vapor gas mixture and F equals to $\frac{D\,c}{Z}$

3.3.1.3- Initial Conditions

The initial ice crystal temperature is assumed to be constant and equal to the plate temperature over which the ice crystal is growing so initially in the ice crystal ($T = T_s$) which is represented in dimensionless form by

$$\theta = 0.0 \qquad (3.39)$$

The vapour initial temperature is also assumed to be constant and this temperature is not a function of time . The air-water vapor temperature is given as (T_v) which is represented in dimensionless form by

$$\theta = \theta_v = constant \qquad (3.40)$$

To start the numerical solution, there should be some grid points available initially in the model. This requires initial values for the length and radius of the crystal. These initial values are taken to be for most cases about 100 μm

Ice crystal initial dimensions are represented as :

$$Y_R = Y_{RI} \tag{3.41}$$

$$Y_Z = Y_{ZI} \tag{3.42}$$

Where Y_{RI} and Y_{ZI} represents initial dimensions assumed for the ice crystal

3.3.1.4- Boundary conditions

$$\theta = 0.0 \quad at \quad Z = 0 \tag{3.43}$$

$$\theta = 1.0 \quad at \quad Z = Y_Z \tag{3.44}$$

$$\frac{\partial \theta}{\partial R} = 0.0 \quad at \quad R = 0 \tag{3.45}$$

$$\theta = 1.0 \quad at \quad R = Y_R \quad \text{(the Ice-gas interface)}. \tag{3.46}$$

$$C = C_{Ai} \quad at \quad R = Y_R \quad \text{(the Ice-gas interface)}. \tag{3.47}$$

Previous equations with initial and boundary conditions have to be solved simultaneously. Numerical finite difference procedure will be used.

3.3.2- Spherical Model :

The second model assumed for the shape of an ice crystal is a hemi-spherical shape. The ice crystal is assumed to have the shape of hemi-sphere with temperature profile varying along (r, φ). The growth of the spherical ice crystal is assumed to be along (r) direction only.

3.3.2.1- Conservation equations for heat and mass transfer

For spherical coordinates to obtain the energy conservation equation a mass balance should be made on a segment shell along (r and φ) directions as shown in fig (3.5).

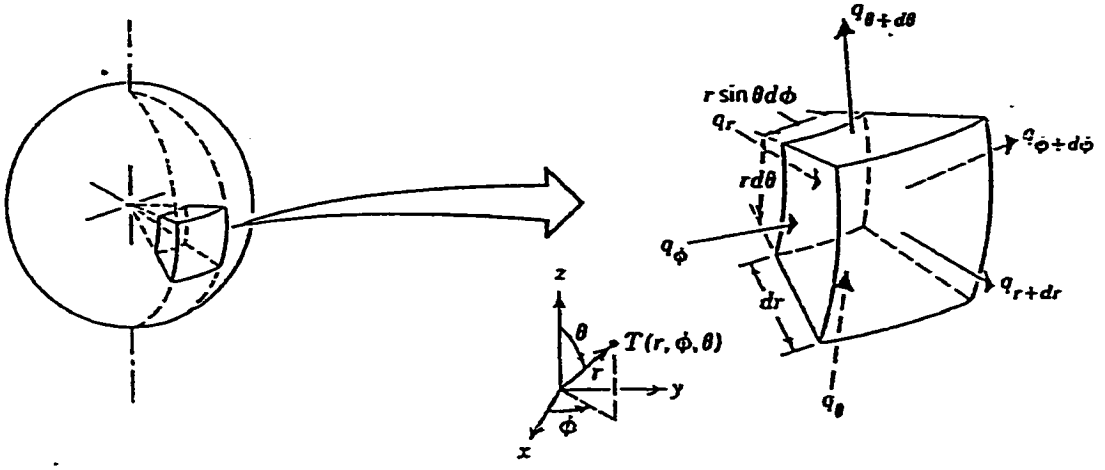

Fig(3.5) Differential control volume, $dr \cdot r\sin\theta d\phi \cdot r d\theta$, for conduction analysis in spherical coordinates (r,ϕ,θ).

$$q_r - q_{r+dr} - q_\varphi - q_{\varphi+d\varphi} = 2\pi r \sin(\varphi)\, r\, d\varphi\, dr\, \rho_s \frac{\partial T}{\partial t} \tag{3.48}$$

$$-\frac{\partial q_r}{\partial r} dr - \frac{1}{r}\frac{\partial q_\varphi}{\partial \varphi} d\varphi = 2\pi r \sin(\varphi)\, r\, d\varphi\, dr\, \rho_s \frac{dT}{dt} \tag{3.49}$$

From forier equation

$$q_r = -k A_r \frac{\partial T}{\partial r} = -k\, 2\pi \sin\varphi\, r\, d\varphi \frac{\partial T}{\partial r} \tag{3.50}$$

and

$$q_\varphi = -kA_\varphi \frac{\partial T}{\partial \varphi} = -k\, 2\varphi\, r\, d\, r \sin\varphi \frac{\partial T}{\partial \varphi} \tag{3.51}$$

substituting these values into the energy balance equation.

$$-\frac{\partial}{\partial r}\left(-k\, 2\pi\, r \sin\varphi\, r\, d\varphi \frac{\partial T}{\partial r}\right) dr$$

$$-\frac{\partial}{\partial \varphi}\left(-k\, 2\pi\, r\, dr \sin(\varphi) \frac{\partial T}{r\partial \varphi}\right) d\varphi = 2\pi\, r \sin\varphi\, r\, d\varphi\, dr\, \rho_s \frac{\partial T}{\partial t}$$

$$2\pi\, k \sin\varphi\, d\varphi\, dr \frac{\partial}{\partial r}\left(r^2 \frac{\partial T}{\partial r}\right)$$

$$+ 2\pi\, r\, k\, dr\, d\varphi \frac{\partial}{r\,\partial \varphi}\left(\sin\varphi \frac{\partial T}{\partial \varphi}\right) = 2\pi\, r \sin\varphi\, r\, d\varphi\, dr\, \rho_s \frac{\partial T}{\partial t}$$

dividing by $2\pi K r^2 \sin\varphi \, d\varphi \, dr$ gives.

$$\frac{1}{r^2}\frac{\partial}{\partial r}\left[r^2 \frac{\partial T}{\partial r} + \frac{1}{r^2 \sin\varphi}\frac{\partial}{\partial \varphi}\left(\sin\varphi \frac{\partial T}{\partial \varphi} \right) \right] = \frac{1}{\alpha_s}\frac{\partial T}{\partial t}. \qquad (3.52)$$

Where $\alpha_s = \dfrac{k}{\rho_s c_s}$

which is the energy equation in spherical coordinates, with neglecting the effect of temperature change with θ.

So the conservation equation for heat and mass transfer for two dimensional case where conduction is assumed to be the dominant factor for heat transfer in the solid ice is given in another form by

$$\frac{\partial^2 T}{\partial r^2} + \frac{2}{r}\frac{\partial T}{\partial r} + \frac{1}{r^2 \sin\varphi}\frac{\partial}{\partial \varphi}\left[\sin\varphi \frac{\partial T}{\partial \varphi} \right] = \frac{1}{\alpha_s}\frac{\partial T}{\partial t} \qquad (3.53)$$

nondimensionlizing the previous equation with the following dimensionless parameters:

$$R = \frac{r}{r_o} \quad , \quad \theta = \frac{T - T_s}{T_{des} - T_s} \quad , \, , \quad \tau = \frac{\alpha_s t}{z_o^2}$$

gives

$$\frac{\partial^2 \theta}{\partial R^2} + \frac{2}{R}\frac{\partial \theta}{\partial R} + \frac{1}{R^2 \sin\varphi}\frac{\partial}{\partial \varphi}\left(\sin\varphi \frac{\partial \theta}{\partial \varphi}\right) = \frac{\partial \theta}{\partial \tau} \qquad (3.54)$$

3.3.2.2- Boundary equations

The equation for the ice-liquid interface in spherical coordinates system by assuming the change in the solid liquid interface is along (R) direction is given by (Ozisik 1980):

$$[1 + \frac{1}{Y_r^2}(\frac{\partial Y_r}{\partial \varphi})^2]\ [k_s\frac{\partial T}{\partial r} + h_g(T_{dew} - T_v)] = \rho_s \Delta H \frac{\partial Y}{\partial r} \qquad (3.55)$$

nondimensioning the previous equation with

$$Y_R = \frac{Y_r}{r_o}, \qquad , \quad \tau = \frac{\alpha_s t}{z_o^2}$$

so the final form of the previous equation is

$$[1 + \frac{1}{Y_R^2}(\frac{\partial Y_R}{\partial \varphi})^2\ ]\ [\frac{\partial \theta}{\partial R} + B_{ir}(1 - \theta_v)] = G\ \frac{\partial Y_R}{\partial \tau} \qquad (3.56)$$

$$\text{Where } G = \frac{\Delta H}{C_s(T_v - T_s)} \qquad (3.57)$$

to calculate the mass flux equation (3.38) will be used.

3.3.2.3- Initial conditions for spherical method

The initial ice crystal temperature in this model is assumed to be constant and equal to the plate temperature over which the ice crystal is growing. So the initial ice crystal temperature is given by $\theta = 0.0$

The initial length of the crystal, which is a requirement for the numerical solution to start , is given by Y_{RI} which is assumed to be equal to $100\mu m$

3.3.2.4- Boundary conditions

$$\theta = 0 \quad at \quad \varphi = 0 \quad \text{and} \quad \varphi = \pi \tag{3.58}$$

$$\theta = 1.0 \quad at \quad R = Y_R \tag{3.59}$$

CHAPTER FOUR

NUMERICAL SOLUTION

The standard procedure in the numerical method to be used is to decide on the number of grid points to be used in the region. Then write down the system of equations in finite difference form using new time step values and previous time step values. For this purpose, an implicit, explicit or Crank - Nicolson types of approach can be used, Lapidus(1982). Implicit methods are less restrictive to the size of time step. The advantage of the implicit method over the explicit one is that the former is stable for all sizes of time step thus there is no size restriction on the time step, the only restriction on the time step is due to the consideration of the truncation error.

Because of the nature of the system, in which the boundary is moving, with the increasing availability of parallel computers and their greater throughout, the explicit method of solution not only offer simplicity but also the capability that the solution could be obtained at many points concurrently, this important factor may enable explicit methods to compete with implicit methods. In this problem because of the previous factor besides the nature of the boundary conditions the number of grid points to be used it is possible to use the explicit method since it requires less memory storage compared to the implicit method.

Finite defference explicit method will be used in this thesis.

To apply the explicit method the ice crystal is divided into four parts:

1.The solid ice.

2.Horizonal boundary between the solid and the vapor gas mixture.

3.Vertical boundary between the solid and the vapor gas mixture.

4.Boundary between the basement and the ice crystal.

4.1- Finite Difference Solution for the Cylindrical Model.

4.1.1- Model equations descritization .

The solution of the cylindrical model includes dividing the crystal into grid points along the R and Z directions. The grid points in the solid are designed so that the length of the grid points will be constant while the number of grid points could be changed since the dimensions of the ice crystal are time-dependent. The grid points used in the numerical solution for the case of cylindrical coordinates are shown in fig(4.1)

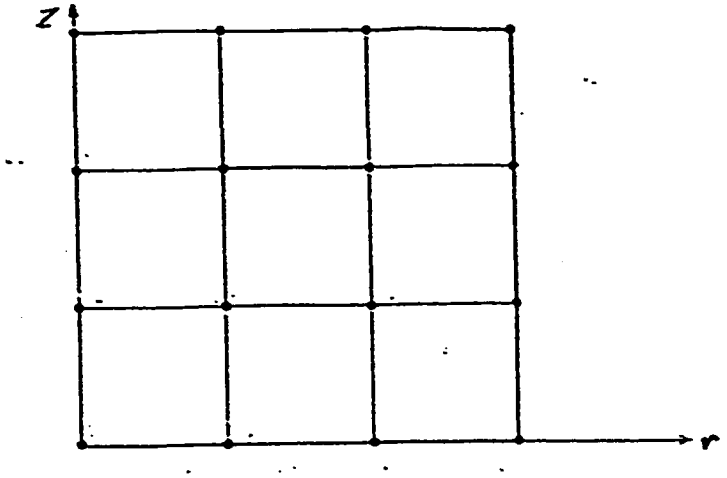

Fig(4.1) Grid points representation required for numerical solution in the case of Cylendrical model.

The location of the i^{th} grid points in the radial direction is obtained from the following equation.

$$R_i = i\,\delta R \qquad (4.1)$$

Where (δR) is related to the number of grid points (nR) along the radial direction.

Similarly, for the location of the j^{th} grid point in the axial direction is given by

$$Z_j = (j\,\delta Z)$$

where δZ is related to the number of grid points (nZ) along the length of the crystal.

The model equations are discretized by finite difference approximations.

The time derivative is discretized as

$$\frac{\partial \theta}{\partial 0} \sim \frac{\theta_{ij}^{n+1} - \theta_{ij}^{n}}{\delta \tau} \qquad (4.2)$$

To illustrate the features of the numerical technique, the discritization of the equations are given below.

For cylindrical geometry, the energy equation which is given by

$$\frac{\partial \theta}{\partial \tau} = \Gamma_{\bullet}^{2} \left[\frac{1}{R} \frac{\partial}{\partial R} \left(R \frac{\partial \theta}{\partial R} \right) \right] + \frac{\partial^2 \theta}{\partial Z^2} \qquad (4.3)$$

could be discretized to give :

$$\theta_{ij}^{n+1} = \theta_{ij}^{n} + \Gamma_{\bullet}^{2}(\delta\tau) \left\{ \left[\theta_{i-1,j}^{n} - 2\theta_{ij}^{n} + \theta_{i+1,j}^{n} \right] \frac{1}{(\delta R^2)} + \right.$$

$$\left. + \frac{1}{2\, i\, (\delta R)^2} \left[\theta_{i+1,j}^{n} - \theta_{i-1,j}^{n} \right] \right\} + \frac{\delta\tau}{(\delta Z)^2} \left[\theta_{i,j-1}^{n} - 2\theta_{ij}^{n} + \theta_{i,j+1}^{n} \right] \qquad (4.4)$$

The explicit form of finite difference approximation given by the equation (4.4) provides a relatively straight forward expression for the determination of the unknown θ_{ij}^{n+1} at a new time step from the knowledge of θ_{ij}^{n} at the previous time step.

The change of the boundaries of the crystal equations (3.26), (3.29) along the Z and R axis can be written in discretized form as follows:

$$Y_{Z(i,j)}^{n+1} = Y_{Z(i,j)}^{n} + \frac{\delta\tau}{G} \left[1 + \Gamma_{\bullet}^{2} \left[\frac{Y_{Z(i+1,j)} - Y_{Z(i-1,j)}}{2(\delta R)} \right]^2 \right] *$$

$$\left[\frac{\theta_{ij} - \theta_{i,j-1}^{n}}{(\delta Z)} + B_i (1 - \theta_{ij}) \right] \qquad (4.5)$$

$$Y^{n+1}_{R(i,j)} = Y^{n}_{R(i,j)} + \delta\tau\frac{\Gamma_e^2}{G}\left[1+\frac{1}{\Gamma_e^2}\left(\frac{Y^{n}_{R(i,j+1)} - Y^{n}_{R(i,j-1)}}{2(\delta Z)}\right)^2\right]*$$

$$\left[\frac{0_{i,j}-0^{n}_{i-1,j}}{\delta R} + B_{ic}(1-0_{ic})\right] \qquad (4.6)$$

Where the first part of the second term on the right accounts for the curvature effect at the ice crystal-gas interface. This equation only applies when the deposition profile is developed otherwise the terms which account for the curvature effect are omitted.

4.1.2- Stability of the method

Stability is effected by the time step chosen. However, the error between numerical and actual solution increases as (δR or δZ) increases, which is an added consideration in the selection of (δR and δZ).
This time step is chosen to satisfy the following conditions.

$$\delta\tau \leq [\ \delta Z^2\ ] \quad \text{and} \quad \delta\tau \leq [\ \delta R^2\ ] \qquad (4.7)$$

4.1.3- Solution Procedure

The energy equation is solved separately and the temperature distribution in the ice crystal is first evaluated.

Equation (4.4) is used to evaluate the temperature distribution in the ice crystal. The movement of the ice crystal boundaries along the (Z,R) axis is determined through the interface equations (4.6)-(4.7).

The flow chart of the numerical algorithm is presented in Fig (4.2). The time is advanced by one time step and new temperature profiles and ice-gas interface are determined for a new time. Then the temperature and thicknesses are updated for a new time step. The process will continue until the length and height of the ice crystal is achieved.

Spherical Model :

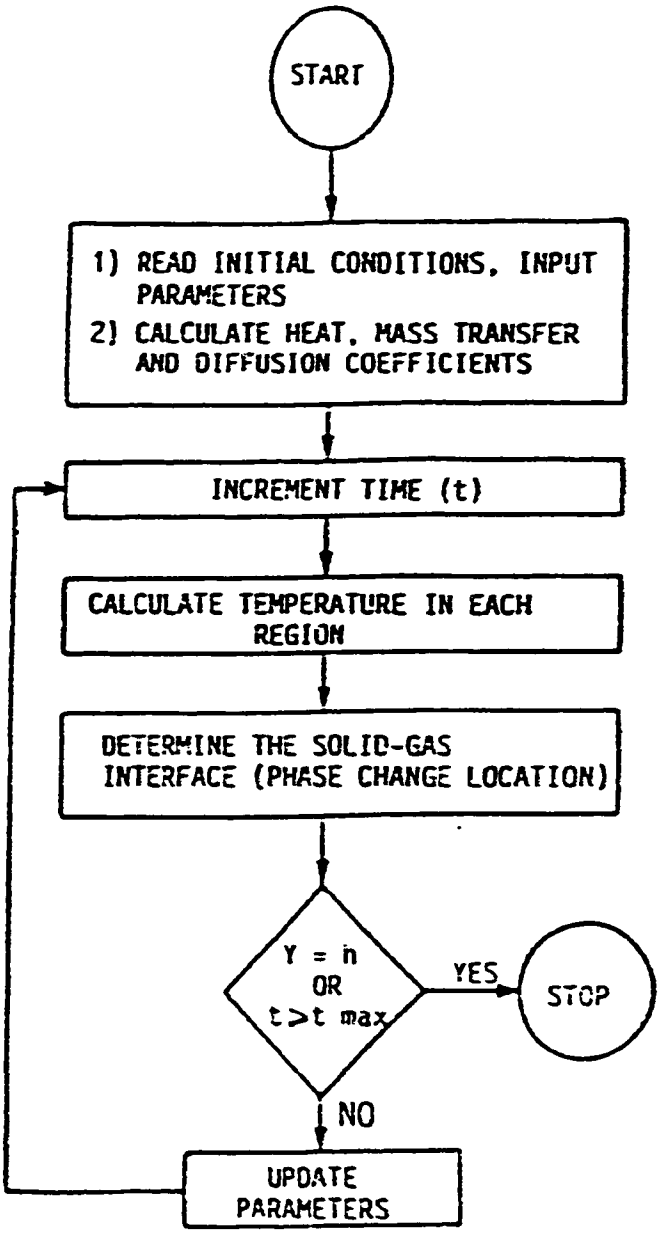

Fig(4.2) Flow Chart of the Numerical Algorithm

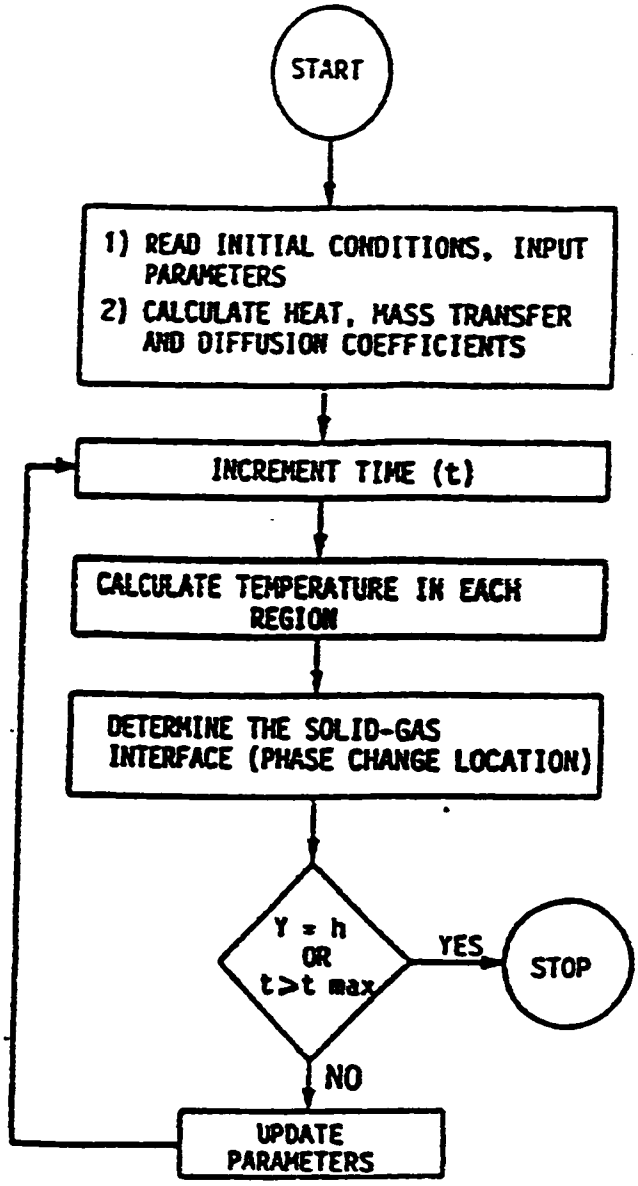

Fig(4.3) Flow Chart of the Numerical Algorithm

The equations used for the calculation of the molecular diffusivity, viscosity of the vapor gas mixture, thermal conductivities of ice and vapor gas mixture and heat and mass transfer coefficients are presented as follows.

Heat and mass transfer coefficients are calculated from empirical correlations. Their magnitudes are dependent on geometry used to represent the ice crystal shape, velocity and physical properties of vapor-gas mixture.

The external heat and mass transfer coefficients are calculated from well established correlations.

4.1.3.1 Sherwood and Nusselt numbers .

For cylindrical shaped ice crystals, a formula for Sherwood and Nusselt numbers is assumed by (Jaweera 1970) to be.

$$Sh = 0.315 + 0.87\ Sc^{1/3}\ Re^{1/2} \qquad (4.8)$$

$$Nu = 0.315 + 0.87\ Pr^{1/3}\ Re^{1/2} \qquad (4.9)$$

These previous equations are applicaple for $2 \leq Re \geq 400$ which is the range of applicability of the model.

Thermal conductivity of ice crystal (k_s)

To obtain the thermal conductivity of ice crystal experimental results are used. In these results the thermal conductivity of ice at different temperature is obtained. Thermal conductivity of ice increases with decreasing temperature. But since this correlations and results are made for thick ice layers, these correlations may be not suitable for the present study. Sahin (1988) offers a correlation for the thermal conductivity together with the density of ice at early stages of the formation process based on the temperature of the surface on which the ice is forming .

$$k_s = 1.2020 * 10^{-3} \ (\rho_s)^{0.963}$$

Where k_s is the thermal conductivity of the ice layer, ρ_s is the average sublimation density which is given by the following correlation

$$\rho_s = \begin{cases} 926.376 + 41.574 T_s & -18°C \le T_s \le 0°C \\ 180 & T_s \le -18°C \end{cases} \qquad (4.10)$$

4.1.3.4- Biot Number

Biot number plays an important role in conduction problems that involve surface convection effects. Biot number provides a measure of the temperature drop in the solid relative to the temperature difference between the surface and the fluid. Simply, Biot number can be defined as the ratio of conduction

resistance to the resistance to convection.

For a cylindrical shaped ice crystal, Biot number according to Jaweera(1970) could be obtained using the following correlation:

$$B_i = \frac{k_s}{k_{vz}}\{\ 0.315\ +\ 0.87 Pr^{1/3}\ \mathrm{Re}^{1/2}\ \} \qquad (4.11)$$

4.1.3.6- Prandtle number and Schmidt number

According to Jaweera (1970), Prandtle and Schmidt number could be approximated to be $\approx$ 0.729.

4.1.3.7- Density of ice crystal

The density of ice crystal is assumed to be a function of the crystal temperature. The density of ice crystal may be found using the figure represented by (Young and Miller (1978)). The least square approximation of the experimental data as presented by (Sahin 1988) is

$$\rho_s = \begin{cases} 926.376 + 41.574 T_s & -18^\circ \le T_s \le 0^\circ \\ 180 & T_s \le -18^\circ \end{cases} \qquad (4.12)$$

where T_s is the crystal base temperature.

4.1.3.8- Diffusion Coefficient

Pruppacher (1976) presented the diffusion coefficient of water vapor in air for temperatures between $-40°C$ and $40°C$ as

$$D = 2.11 \times 10^{-5} \left(\frac{T_v}{T_o}\right)^{1.94} \left(\frac{P_{atm}}{P}\right) \qquad (4.13)$$

where

P_{atm} = atmospheric pressure in Pascals.

$T_o = 273.14°K$

4.2- Numerical Solution of the Spherical Model of the Ice Crystal

4.2.1- Model equations descretization

The model will be divided into grid points along R and φ. In this model the grid points in the solid are designed so that both the length and number of grid points could be changed as the radius of the crystal increases. In another way, every time step there will be a change in the radius of the crystal, this means that the number of grid points will increase but if the the length of every grid is kept constant we will have fraction of grid. To avoid this problem in this model, the length of the grid points in the R directions will be changed so we will have always integer number of grid points. The grid points for the model are shown in fig (4.3).

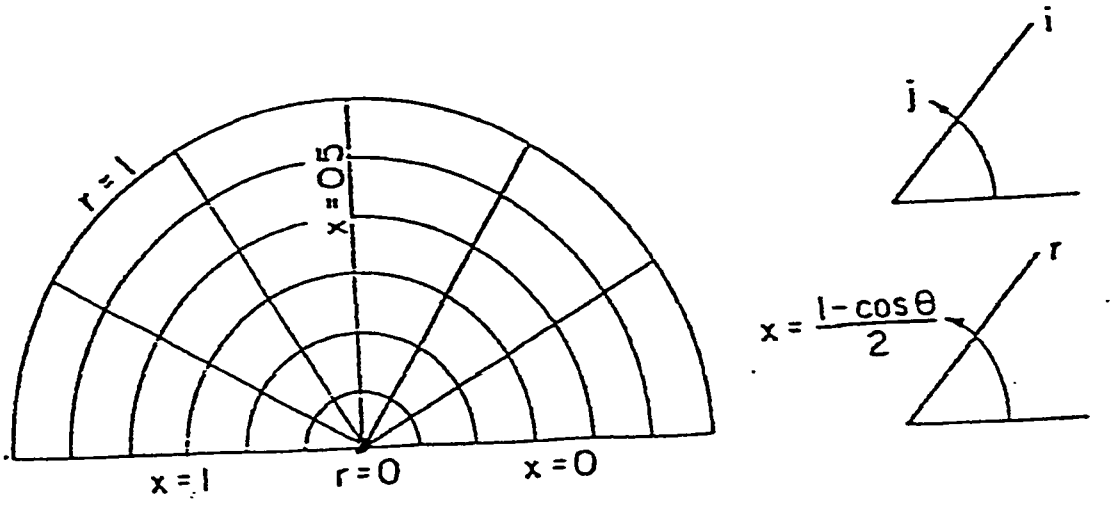

Fig(4.3) Grid points representation required for numerical solution in the case of Spherical model.

In this model, as mentioned previously, the ice crystal is assumed to have a hemi-spherical shape. The energy equation will be solved for two dimensional case (r,φ) with axial symmetry. The radius of the hemi-sphere varies with time. because of the moving boundary situation and also due to the convective heat transfer on the boundary.

The nondimensional energy equation for spherical coordinates together with the interface equation are given in equation (3.53) , (3.56) for the spherical model.

The energy equation is given as

$$\frac{\partial\theta}{\partial\tau} = \frac{\partial^2\theta}{\partial R^2} + \frac{2}{R}\frac{\partial\theta}{\partial R} + \frac{1}{R^2\sin\varphi}\frac{\partial}{\partial\varphi}\left(\sin\varphi\frac{\partial\varphi}{\partial\varphi}\right) \qquad (4.14)$$

The domain of interest for the problem is the interior and the boundary of the sphere, i.e $0 \le R \le 1$ and $0 \le \varphi \le \pi$ The solution ($\theta(r,\varphi,t)$) of the above equation is required subjected to the initial and boundary conditions as follows

Initial conditions

$$\theta\ (r, \varphi, 0) = 0, \tag{4.15}$$

and

$$Y_R(R, 0) = Y_{RI} \tag{4.16}$$

The boundary conditions

$$\varphi = 0\ ,\ \theta = 0 \tag{4.17}$$

$$\varphi = \pi\ ,\ \theta = 0 \tag{4.18}$$

$$r = Y_R\ ,\ \theta = 1.00 \tag{4.19}$$

The energy equation mentioned previously when solved for $r=0, \varphi=0$, or π will have a singularity. The singularities at $\varphi = 0$ or π can be removed by the following transformation of the φ coordinates

$$\text{let } X = \frac{1 - Cos(\varphi)}{2} \qquad \text{where } 0 \le \varphi \le \pi \tag{4.20}$$

The energy equation now becomes

$$\frac{\partial \theta}{\partial \tau} = \frac{\partial^2 \theta}{\partial R^2} + \frac{2}{R}\frac{\partial \theta}{\partial R} + \frac{1}{R^2}\frac{d}{dX}\left\{ (X - X^2)\frac{d\theta}{dX}\right\} \tag{4.21}$$

The initial coordinates also can be transformed to

$$\theta(R, X, 0) = 0. \tag{4.22}$$

The boundary conditions will become.

$$\theta = 0 \quad at \quad X = 0 \tag{4.23}$$

$$\theta = 0 \quad at \quad X = 1.0 \tag{4.24}$$

$$\theta = 1.0 \quad at \quad R = Y_R \tag{4.25}$$

The interface equation which is

$$\left[1 + \frac{1}{Y_R^2}\left(\frac{\partial Y R}{\partial \varphi}\right)^2\right]\left[\frac{\partial \theta}{\partial R} + B_{iR}(1 - \theta_v)\right] = G\frac{\partial Y_R}{\partial \tau} \tag{4.26}$$

can be simplified by neglecting the effect of curvature and assuming that $\frac{\partial Y_R}{\partial \varphi} = 0$, so Y_R increase by the same amount (with φ),

The interface equation now will become.

$$G\frac{\partial Y_R}{\partial \tau} = \left[\frac{\partial \theta}{\partial R} + B_{iR}(1 - \theta_v)\right] \tag{4.27}$$

where $G = \frac{\Delta H}{C_s(T_v - T_s)}$ (4.28)

To solve the previous problem numerically, we super impose a plane polar grid on the region of interest. The mesh points in the R-X plane are now points of intersection of the semi-circles.

$$R_i = i\delta R \quad i = 1,2,\text{---}m \quad \delta R = \frac{YR}{m} \tag{4.29}$$

$$X_j = j\delta X \quad J = 1,2,\text{---}n \quad \delta X = \frac{1}{n} \tag{4.30}$$

The discretization of the energy equation using finite difference explicit method.

$$\theta^{n+1}{}_{ij} = \theta^{n}{}_{ij} + \delta\tau\{\frac{i+1}{i\delta R^2}\theta^{n}{}_{i+1,j} - \frac{2}{(\delta R)^2}\theta^{n}{}_{ij} + \frac{i-1}{i(\delta R)^2}\theta^{n}{}_{i-1,j} +$$

$$\frac{1}{(i\delta R)^2}\,[(j\delta X - j^2\delta X^2)(\frac{\theta^{n}{}_{ij+1} - 2\theta^{n}{}_{ij} + \theta^{n}{}_{ij-1}}{(\delta X)^2}) + (1 - 2j\delta X)(\frac{\theta^{n}{}_{ij+1} - \theta^{n}{}_{ij-1}}{2\delta X})]\} \tag{4.32}$$

and for the interface equation, the discretization of equation(4.27) reduces to

$$Y^{n+1}_{R(i,j)} = Y^{n}_{R(i,j)} + \frac{\delta\tau}{G}[\frac{\theta^{n}{}_{ij} - \theta^{n}{}_{i-1,j}}{\delta R} + B_{ir}(1 - \theta_v)] \tag{4.33}$$

where $G = \dfrac{\Delta H}{C_s(T_v - T_s)}$

4.2.2- Stability of the solution

Applying the fourier method for stability, the increments are restricted approximately by (Teller and Churchill 1965)

$$\Delta\tau \le \frac{1}{5}\ Y_R(\Delta R)^2 \quad \text{and} \quad \Delta\tau \le \frac{1}{5} Y_R\ (\Delta X)^2 \tag{4.34}$$

4.2.3- Solution Procedure

The energy equation is solved separately the temperature distribution in the ice crystal is first evaluated. Equation (4.32) is used to evaluate the temperature distribution in the ice excluding the interface. The movement of the ice crystal boundaries along the (R) axis is determined through the interface equation (4.33). The flow chart of the numerical algorithm is presented in Fig(4.2). The time is advanced by one time step and new temperature profiles and ice-gas interface are determined for a new time. Then the temperature and thicknesses are updated for a new time step. The process will continue until the length and height of the ice crystal is achieved.

4.2.3.1- Nusselt number and Shewood number:

$$Nu = 2.00 + 0.216\ Pr^{1/3}\ \mathrm{Re}^{1/2} \qquad (4.35)$$

For sherwood number

$Sh = 2.0 + 0.216 Pr^{1/3}\mathrm{Re}^{1/2}$

These previous equations are applicaple for $2 \leq \mathrm{Re} \geq 400$ which is the range of applicability of the model.

(as given by Hall and Pruppacher 1976)

4.2.3.2Biot number :

For spherical body Biot number can be represented in the following form

$$B_{iR} = \frac{k_s}{K_v}\ [2.0 + 0.216 Pr^{1/3}\mathrm{Re}^{1/2}]$$

(as given by Hall and Pruppacher 1976)

In these constants the characteristic length is assumed to be the initial value of r

CHAPTER FIVE

DISCUSSION OF RESULTS AND CASE STUDIES

THEORETICAL PREDICTIONS .

As explained in the foregoing chapters, ice crystal growth is a very complicated phenomena. Inevitably, some simplifying assumptions have to be made in order to come up with models for complicated phenomena of this nature. However, it is also important that the assumptions that are made do not lead to results far from real situations. In that case the assumptions are said to be unrealistic.

From experimental evidence, it is anticipated that ice crystal density at the moment of formation under certain conditions is very critical and crucial in the process of ice crystal growth. In other words, if the crystal density and thermal conductivity under certain conditions is determined correctly, the development of the model could be accurate.

Unfortunately, no theoretical model of crystal density exists in the literature. Cloud physicists who have been extensively studying ice crystals growth in the atmosphere under different conditions have not explained why thousands of different ice crystal structures exist in nature and how they attain their forms or shapes.

Crystal shapes of ice were examined and data related to their weight and density have been collected experimentally. In this model constant ice crystal density is assumed with other properties like thermal conductivity .

Ice crystals model that is developed in this study utilizes the above considerations. This should be kept in mind while examining the following results.

There are many variables that effect ice crystals growth such as plate temperature, air temperature,air velocity, initial axial ratio, roughness of the surface, radiation from the surrounding environment, nucleation agents in the air, etc. The effect of the first four parameters of the above which are dominant on ice crystal growth are demonstrated through several ice crystals properties such as ice crystal length and radius, ice crystal temperature distributions and the rate of mass flux into the ice crystal.

5.1 Cylindrical Model

5.1.1 Effect Of Air-Water-Vapour Mixture Temperature .

One of the factors that effect the ice crystals growth is the temperature of air-water vapour mixture, since the deposition of water molecules into the crystal is occurring from this temperature. From Fig(5.A)it is very clear that as the ambient temperature is becoming higher the length of the crystal is also becoming higher ranging from 250 μm when the ambient temperature is (0.5°C) to 1600 (μm) when the ambient temperature reaches (10.0°C). The reasons for this is that the temperature gradient in the boundary layer is greater and therefore the development of ice crystals and phase change of water molecules is faster. As a matter of fact, water molecules passing through the boundary layer encounter a temperature gradient and arrive at the surface of the crystal to take their places in the ice crystal lattice. For small temperature gradients, which means less difference in temperature between the surface temperature and the ambient air temperature more time is required for the development of ice crystals, but for the case of higher temperature gradient less time is required to develop big ice crystals. The radius of the crystal is also effected in the same manner so as the ambient temperature is becoming higher the radius of the crystal is also increasing due to the same reasons mentioned previously. It is also very clear from the figures representing both the radius and length of the crystal versus time that the crystal is growing in plate like structure . Temperature distributions along the length and radius of the crystal are shown in Fig (5.1) and (5.2) It is very clear that as the dimensions of the crystal are increasing a

new temperature distribution is occurring. It is concluded that as the boundary conditions are moving away from the center of the crystal the temperature at ($R=0$) is decreasing with time. Cooling effect is really occurring in the crystal as it's boundaries move away from the center of the crystal. Fig(5.3) shows the change of the length of the crystal with time. The change is linear and with the ice crystal growing in length from 100 μm to 620 μm in 100 seconds. Fig (5.4) shows the change in the radius of the crystal with time. The behavior of radius of the crystal is the same as that for the length as shown in Fig(5.5), this is mainly due to assuming Γ_o to be equal to one .Fig(5.6) represents the variation of mass flux with time. It is shown that the mass flux inside the ice crystal is decreasing wit time, this implies that their is a variation in the density of the crystal as the crystal is growing but due to the shortage of information about the variation of the density of ice crystals with time, a constant ice crystal density is assumed which is causing a source of error in the model. Fig(5.7) represents the temperature profile of the ice crystal with it's length at 0.5°C ambient temperature. the variation of temperature with length has the same behavior as in Fig (5.1) but now the length of the crystal is less due to lower temperature gradient. The temperature variation of with radius for this temperature is represented in Fig(5.8). As the radius of the crystal is increasing the temperature in the crystal is becoming lower and since the radius is increasing slowly the slope of the temperature profile increase causing the crystal to become shorter with the length approaches a certain final limiting value as the case in Fig(5.9). This is expected due to the low ambient temperature. The radius of the crystal also takes the same behavior as it's length as it is in Fig(5.10). Fig(5.11) declears that the radius and length of the crystal have the

same curve. This is mainly due to the assumption of equal initial length and radius. The mass flux at lower temperature is higher leading to more dense ice crystals as shown in Fig(5.12).

To complete the study of the effect of the ambient temperature on the growth of the ice crystal, the ambient temperature increased in the model up to $10°C$ and to show how the initial assumed length and radius will effect the dimensions of the crystal, the value of Γ_o is assumed to be equal to 0.8. Fig(5.13) and (5.14) shows the temperature distribution in the crystal along it's length and radius The crystal is becoming cooler as it's dimensions increase in length and radius due to higher ambient temperature as n Fig(5.15) and Fig(5.16). Fig(5.17) gives the effect of initial assumed ratios to limit the growth along one direction. By assuming value of Γ_o to be 0.8, the growth along the radius of the crystal could be limited and controlled. The case represents allowing the crystal to grow in a shape of a column. This gives the model more flexibility to represent the growth of the ice crystal in plate or column shapes. The density of the ice crystal at higher ambient temperature is becoming lower, due to lower mass flux effect Fig(5.18) the previous discussed behavior of the model variation of ambient temperature is satisfied by the work done by Schneider (1977) where he studied the frost formation process and found that as the ambient temperature increases the frost layer is becoming higher which means the formation of higher ice crystals . In

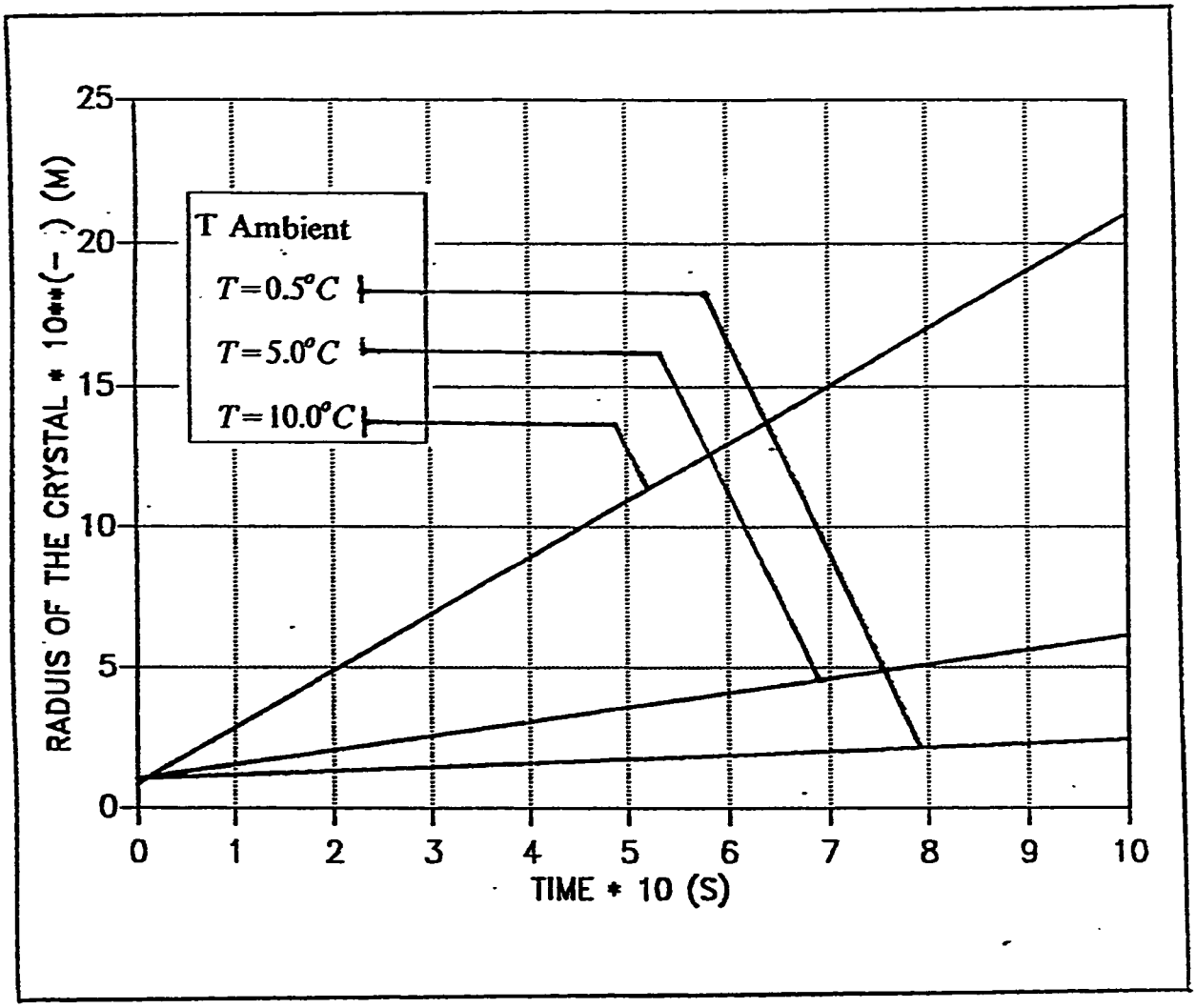

Fig(5.A) Length of the crystal vs. Time for different ambient temperatures

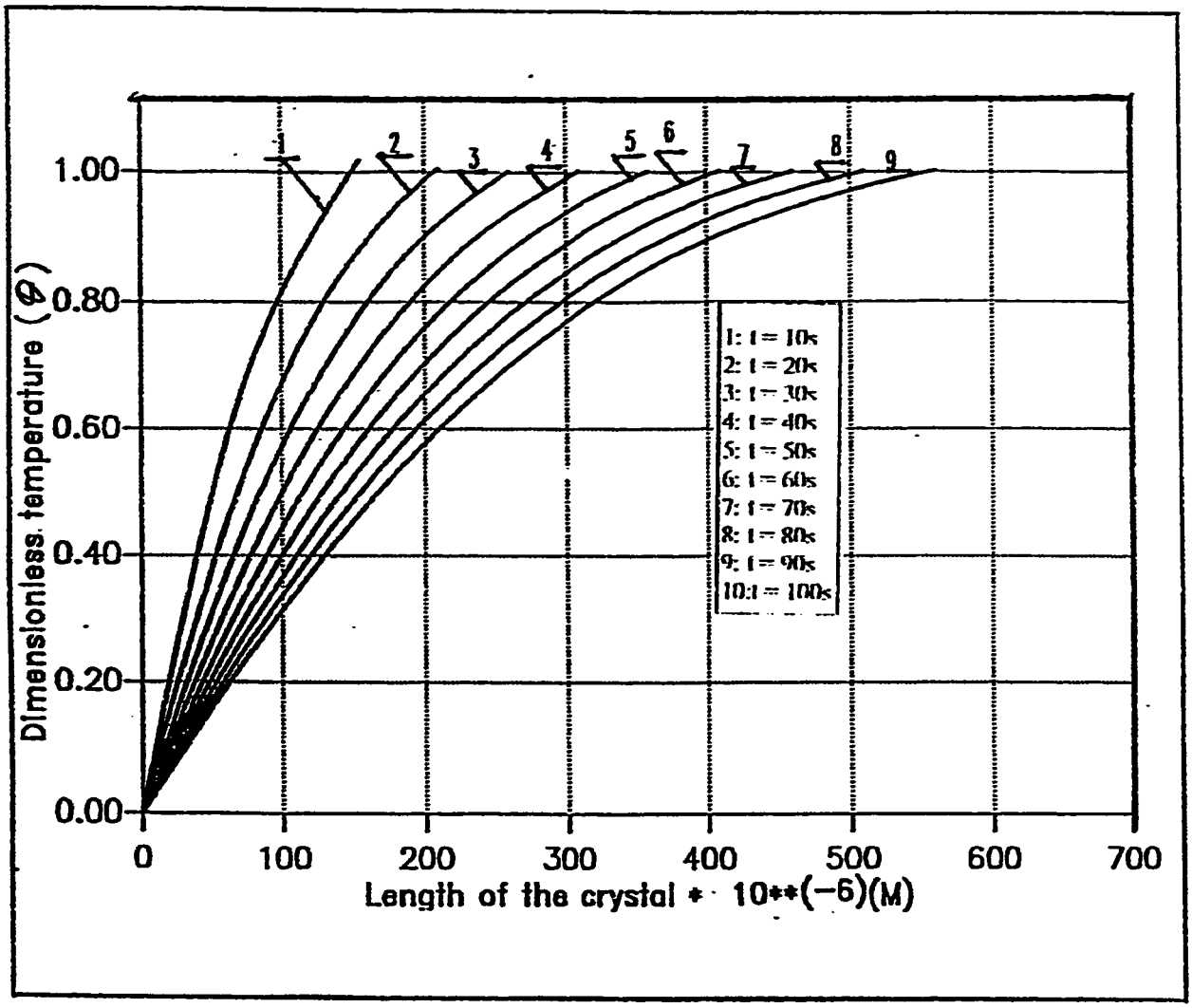

Fig(5.1) Dimensionless temperature vs. length of the crystal. For cylindrical model

$r_o = 1.0$, $V_{air} = 2\ m/s$

$T_v = 5.0^oC$. , $T_s = (-10)^oC$.

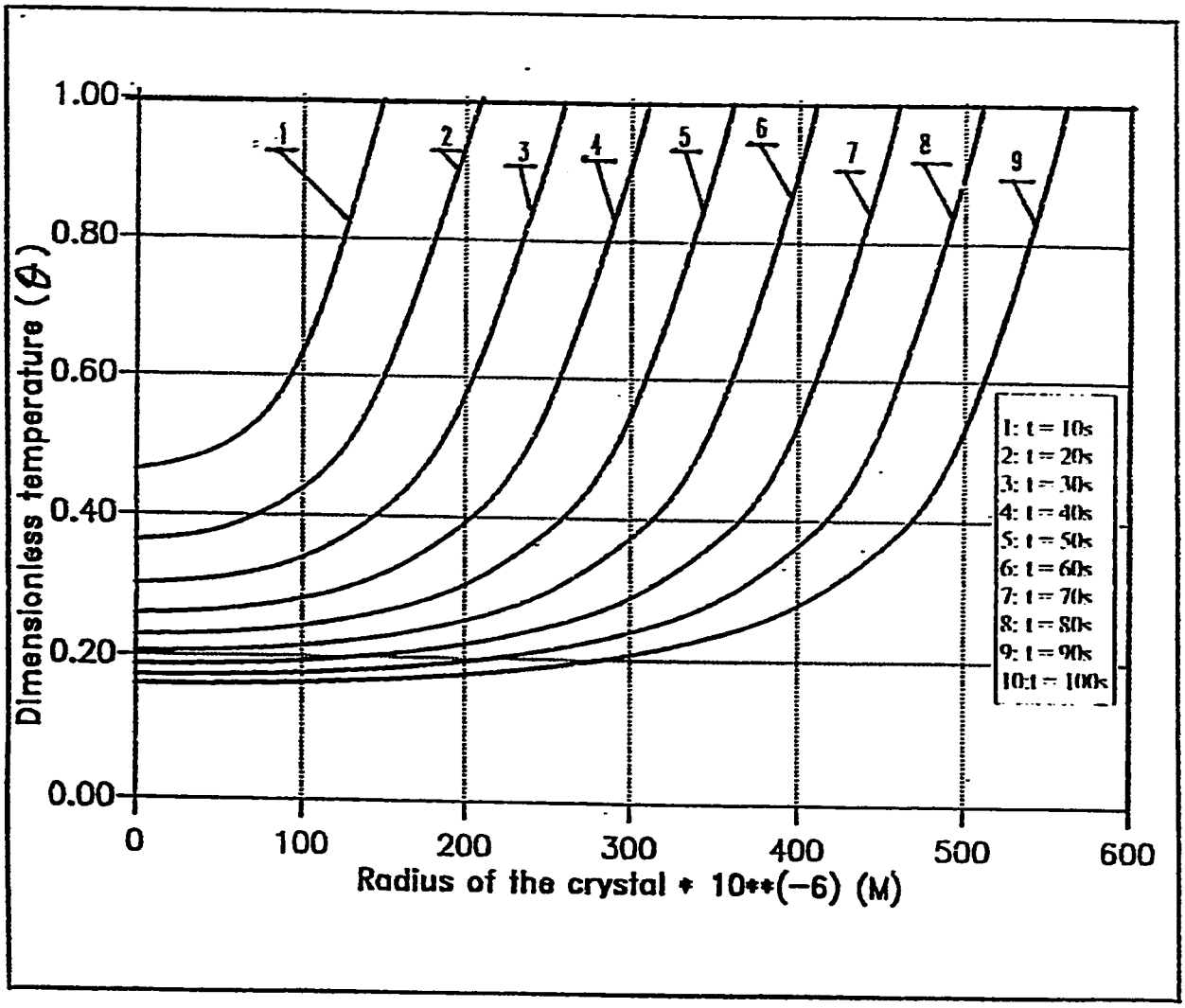

Fig(5.2) Dimensionless temperature vs. radius of the crystal For cylindrical model.

$r_o = 1.0$, $V_{air} = 2\ m/s$

$T_v = 5.0^oC$. $T_s = (-10)^oC$.

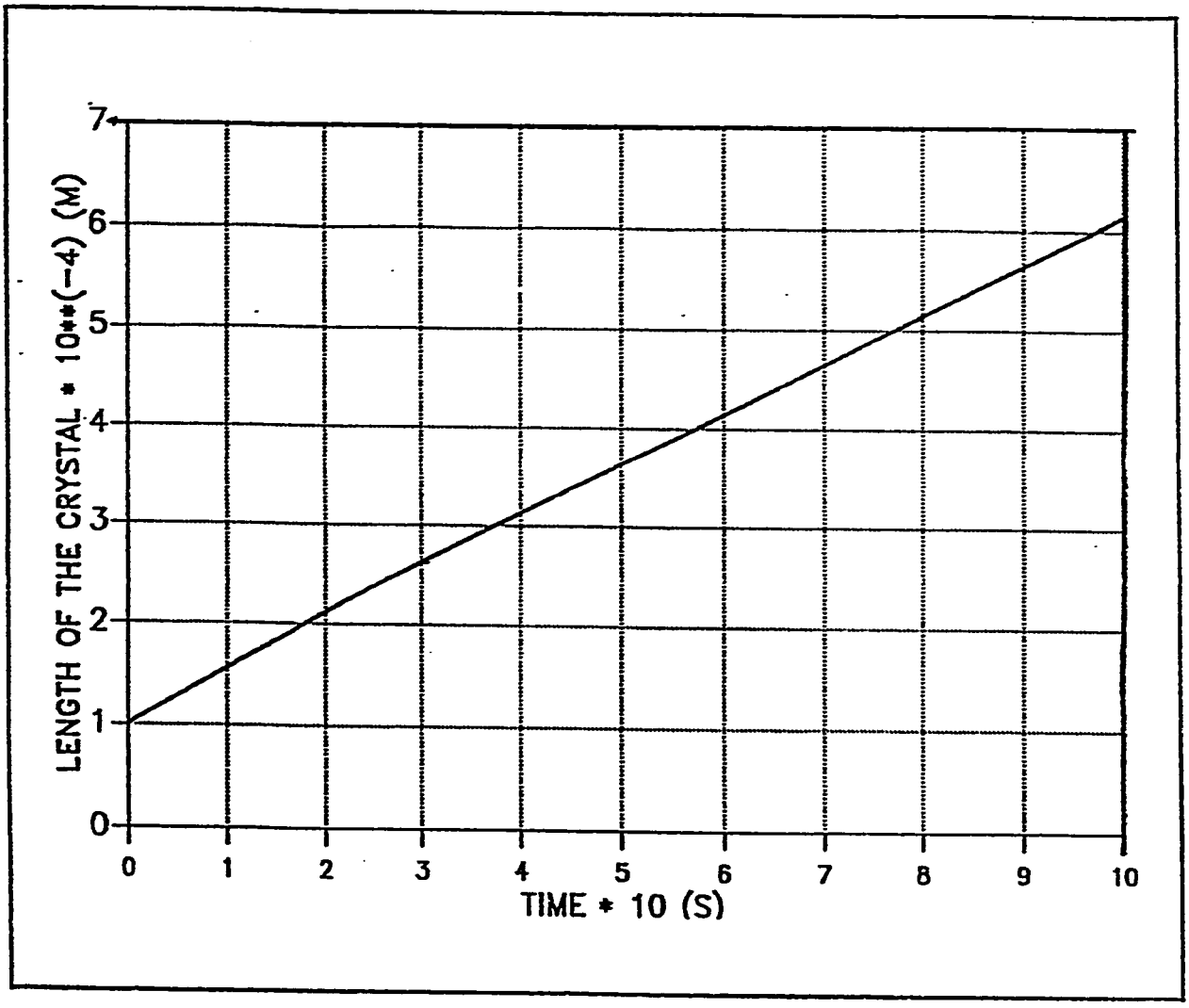

Fig(5.3) Length of the crystal vs. Time

For cylindrical model .

$r_o = 1.0$, $V_{air} = 2\ m/s$

$T_v = 5.0^oC$. $T_s = .(-10)^oC$.

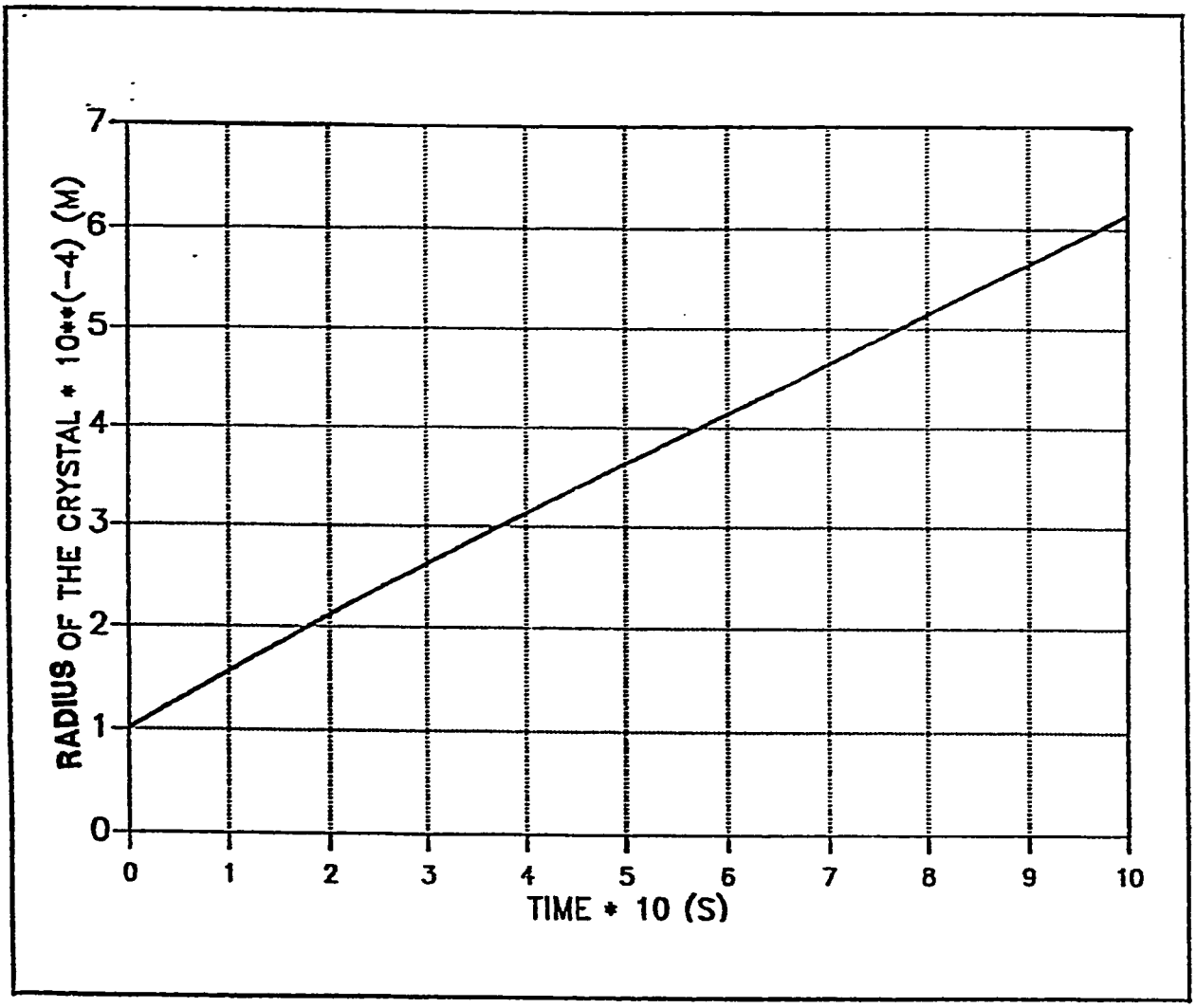

Fig(5.4) Radius of the crystal vs. Time

For cylindrical model .

$r_o = 1.0$, $V_{air} = 2\ m/s$

$T_v = 5.0^{\circ}C$. $T_s = (-10)^{\circ}C$.

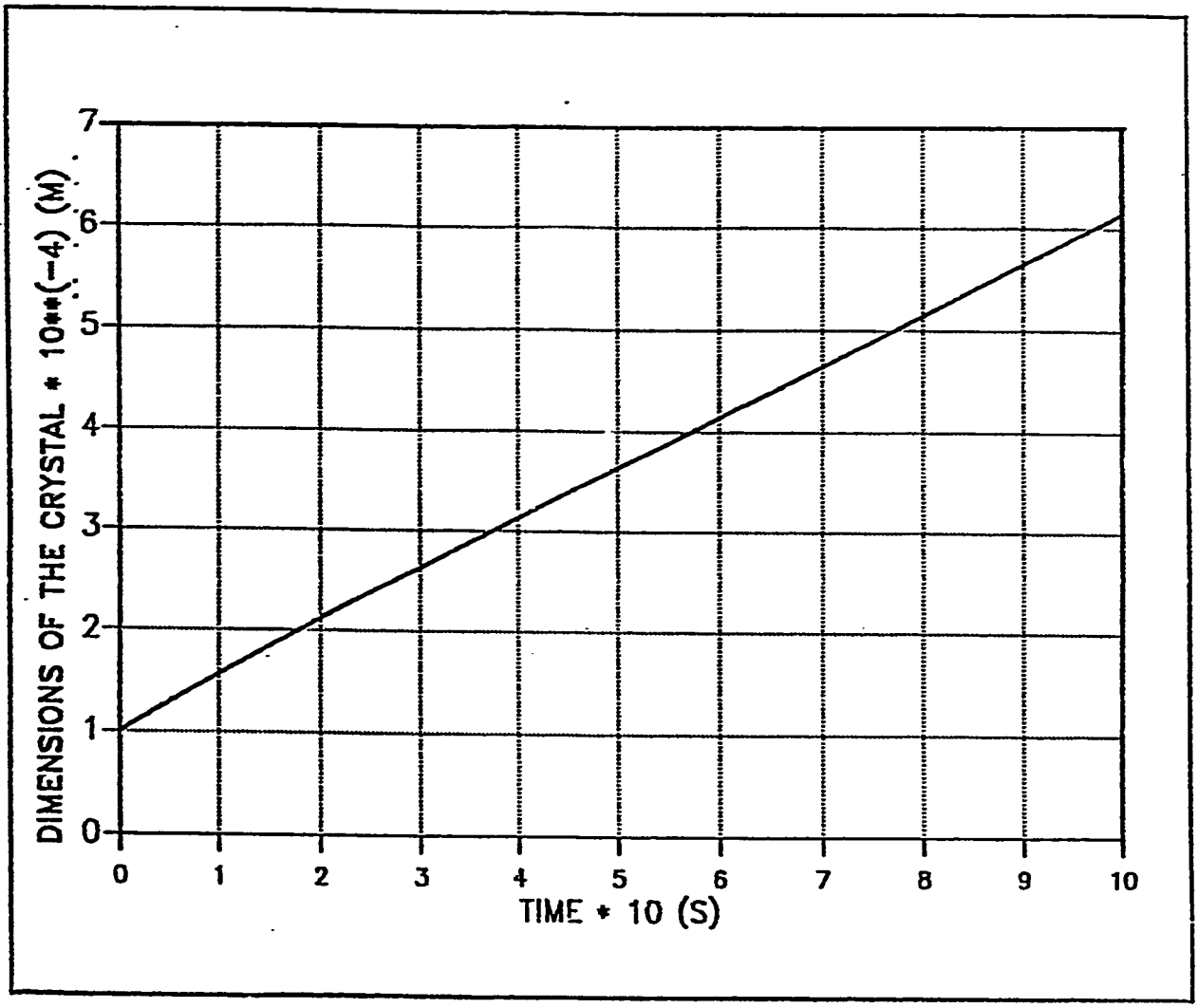

Fig(5.5) Dimensions of the crystal vs. Time

For cylindrical model .

$r_o = 1.0$, $V_{air} = 2\ m/s$

$T_v = 5.0^{o}C$. $T_s = (-10)^{o}C$.

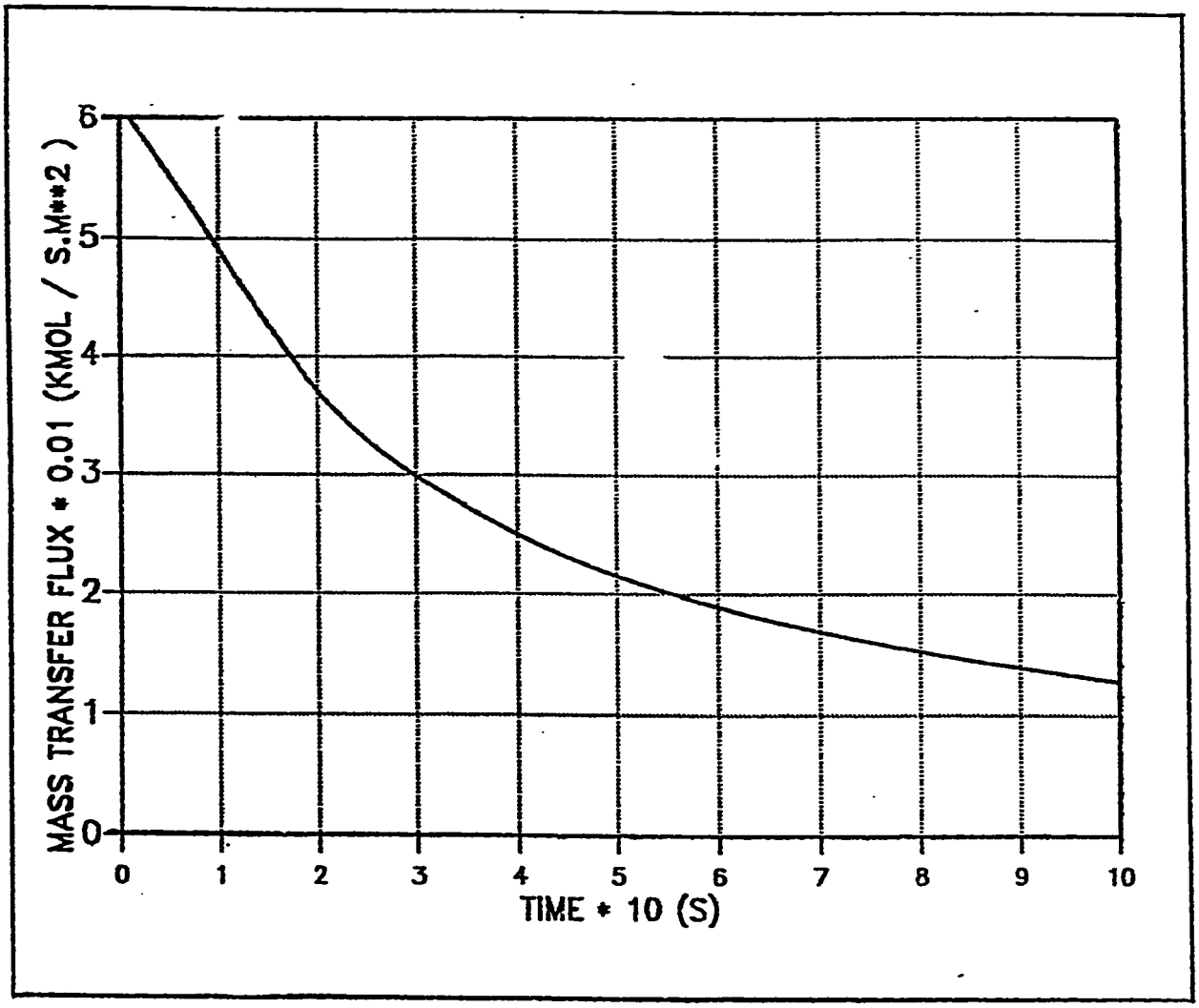

Fig(5.6) Mass transfer flus vs. Time

For cylindrical model.

$r_o = 1.0$, $V_{air} = 2\ m/s$

$T_v = 5.0^oC$. $T_s = (-10)^oC$.

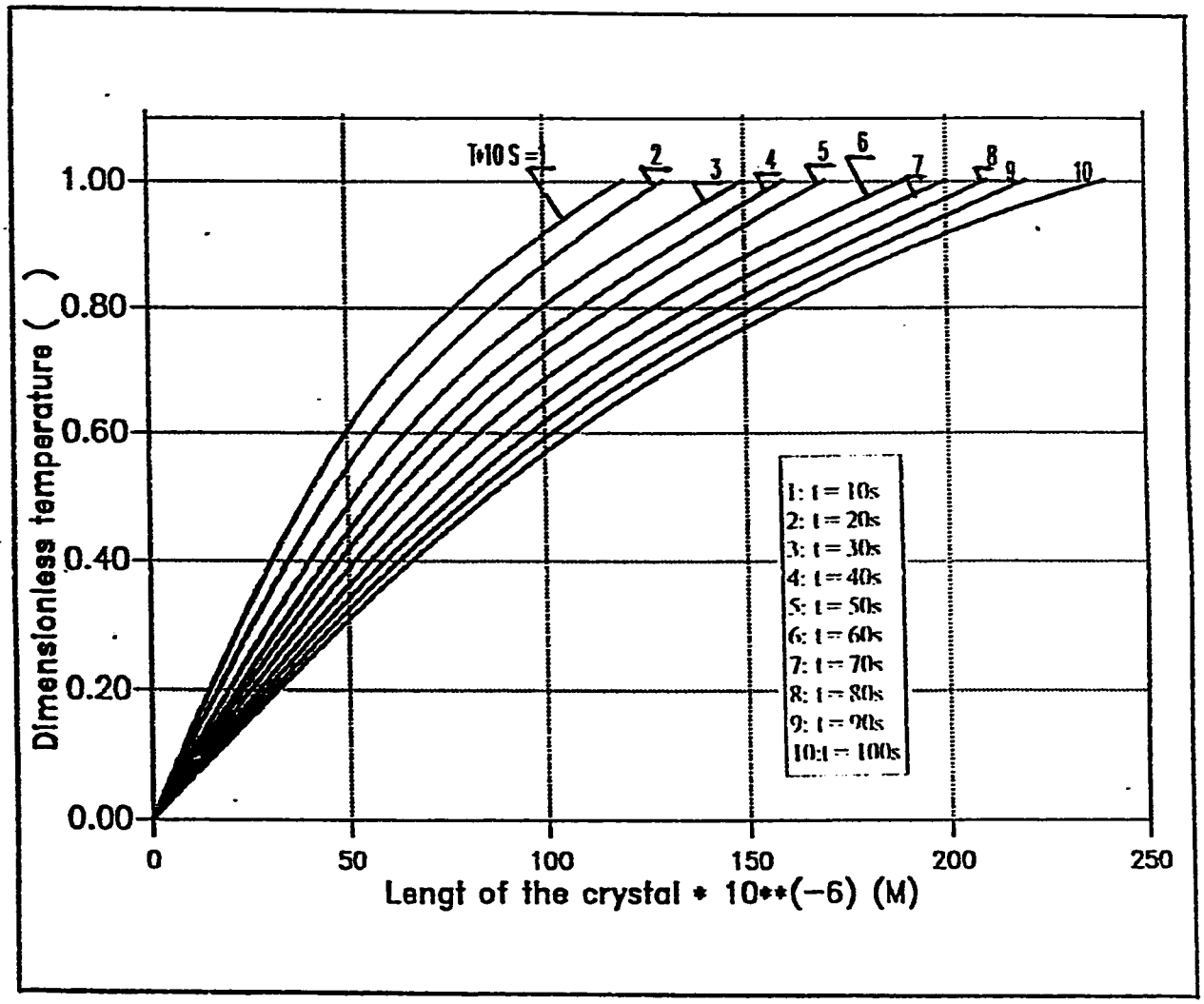

Fig(5.7) Dimensionless temperature vs. length of the crystal. For cylindrical model .

$r_o = 1.0$, $V_{air} = 2\ m/s$

$T_v = 0.5^oC$. , $T_s = (-10)^oC$.

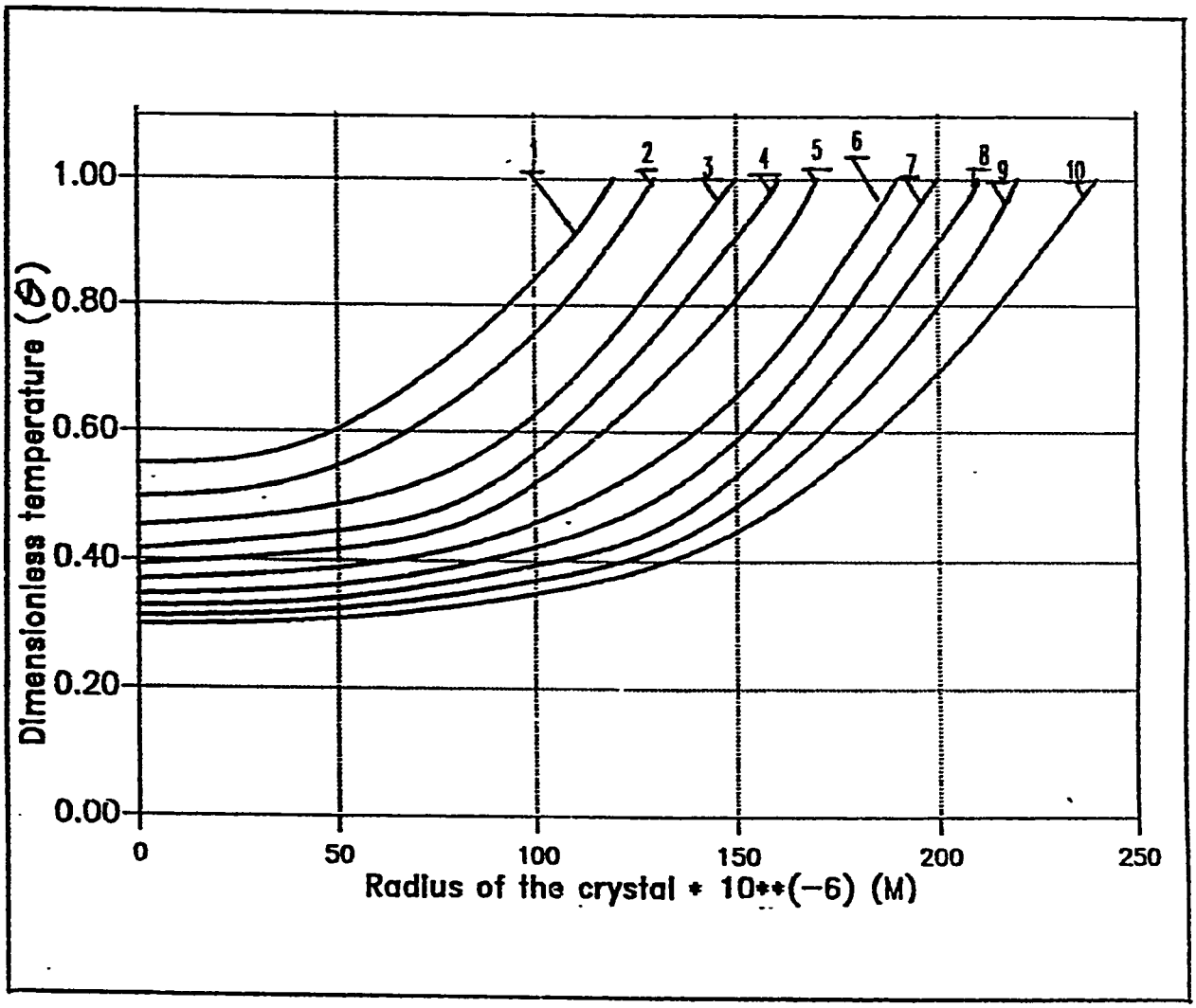

Fig(5.8) Dimensionless temperature vs. raduis of the crystal For cylindricalmodel.

$r_o = 1.0$, $V_{air} = 2\ m/s$

$T_v = 0.5^oC$. $T_s = (-10)^oC$.

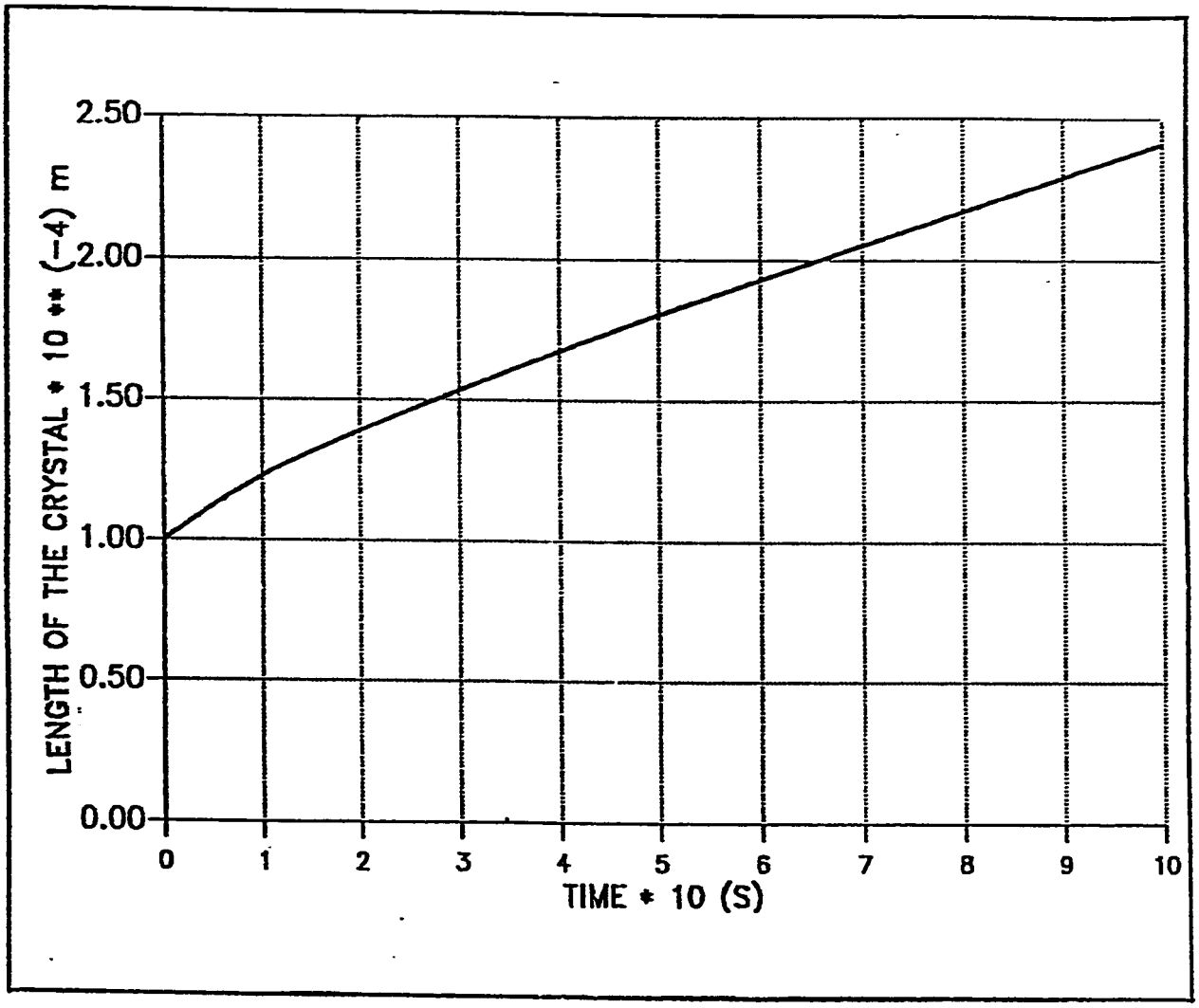

Fig(5.9) Length of the crystal vs. Time

For cylindrical model .

$r_o = 1.0$, $V_{air} = 2\ m/s$

$T_v = 0.5^oC$. $T_s = (-10)^oC$.

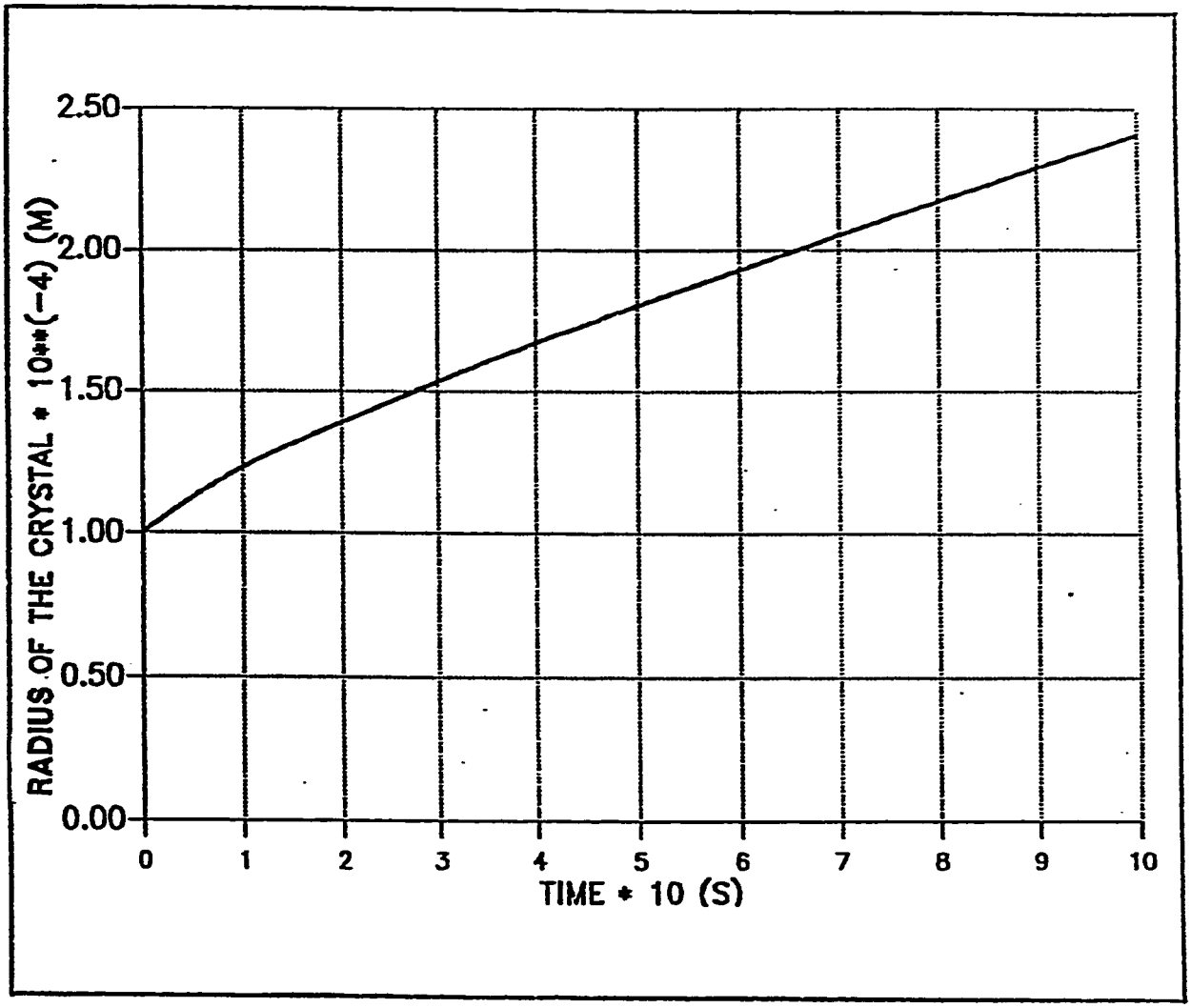

Fig(5.10) Radius of the crystal vs. Time

For cylindrical model .

$r_o = 1.0$, $V_{air} = 2\ m/s$

$T_v = 0.5^oC$. $T_s = (-10)^oC$.

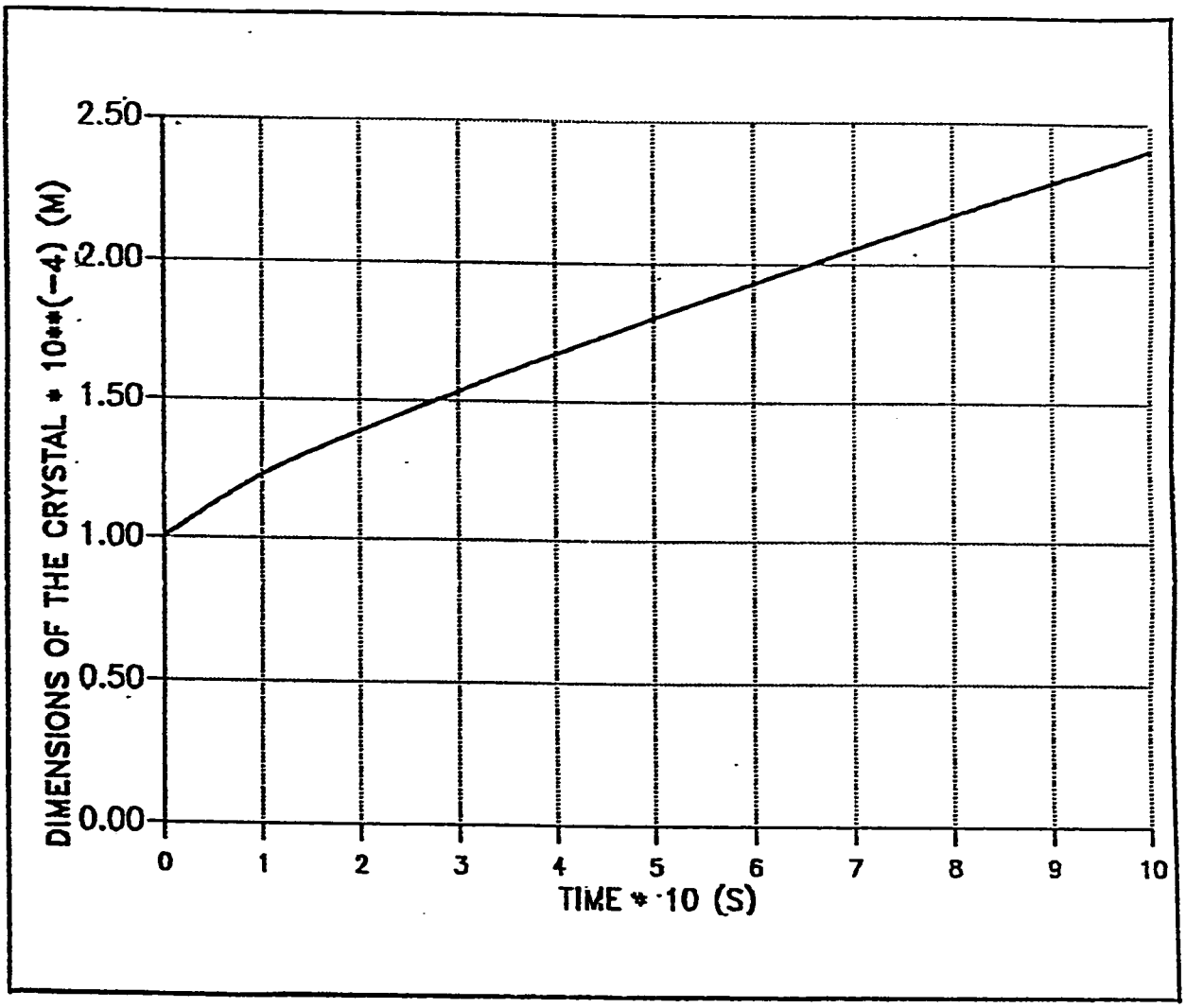

Fig(5.11) Dimensions of the crystal vs. Time

For cylindrical model .

$r_o = 1.0$, $V_{air} = 2\ m/s$

$T_v = 0.5^oC$. $T_s = (-10)^oC$.

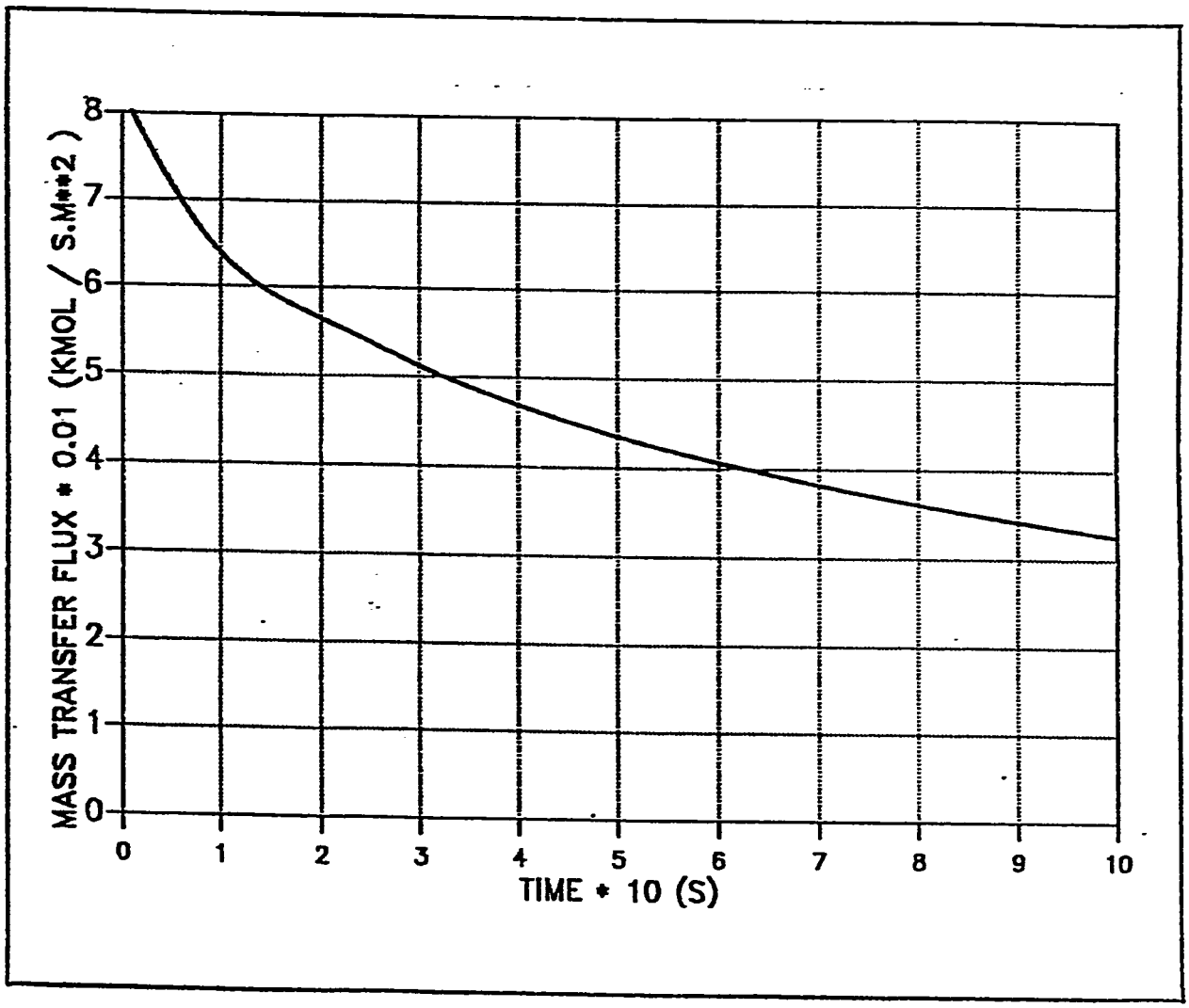

Fig(5.12) Mass transfer flus vs. Time

For cylindrical model.

$r_o = 1.0$, $V_{air} = 2\ m/s$

$T_v = 0.5^oC$. $T_s = (-10)^oC$.

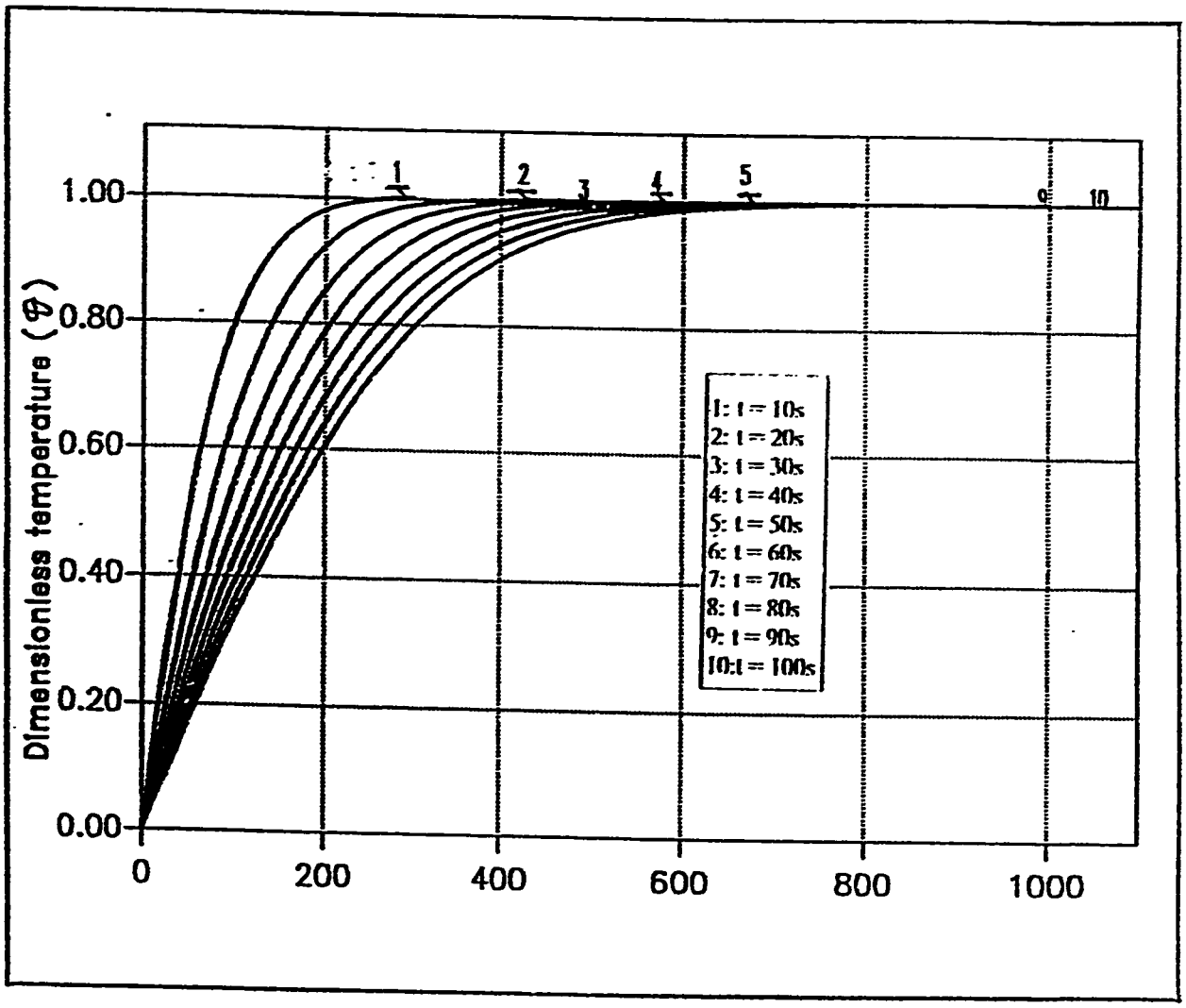

Fig(5.13) Dimensionless temperature vs. length of the crystal. For cylindrical model .

$r_o = 0.8$, $V_{air} = 2\ m/s$

$T_v = 10^oC$. , $T_s = (-10)^oC$.

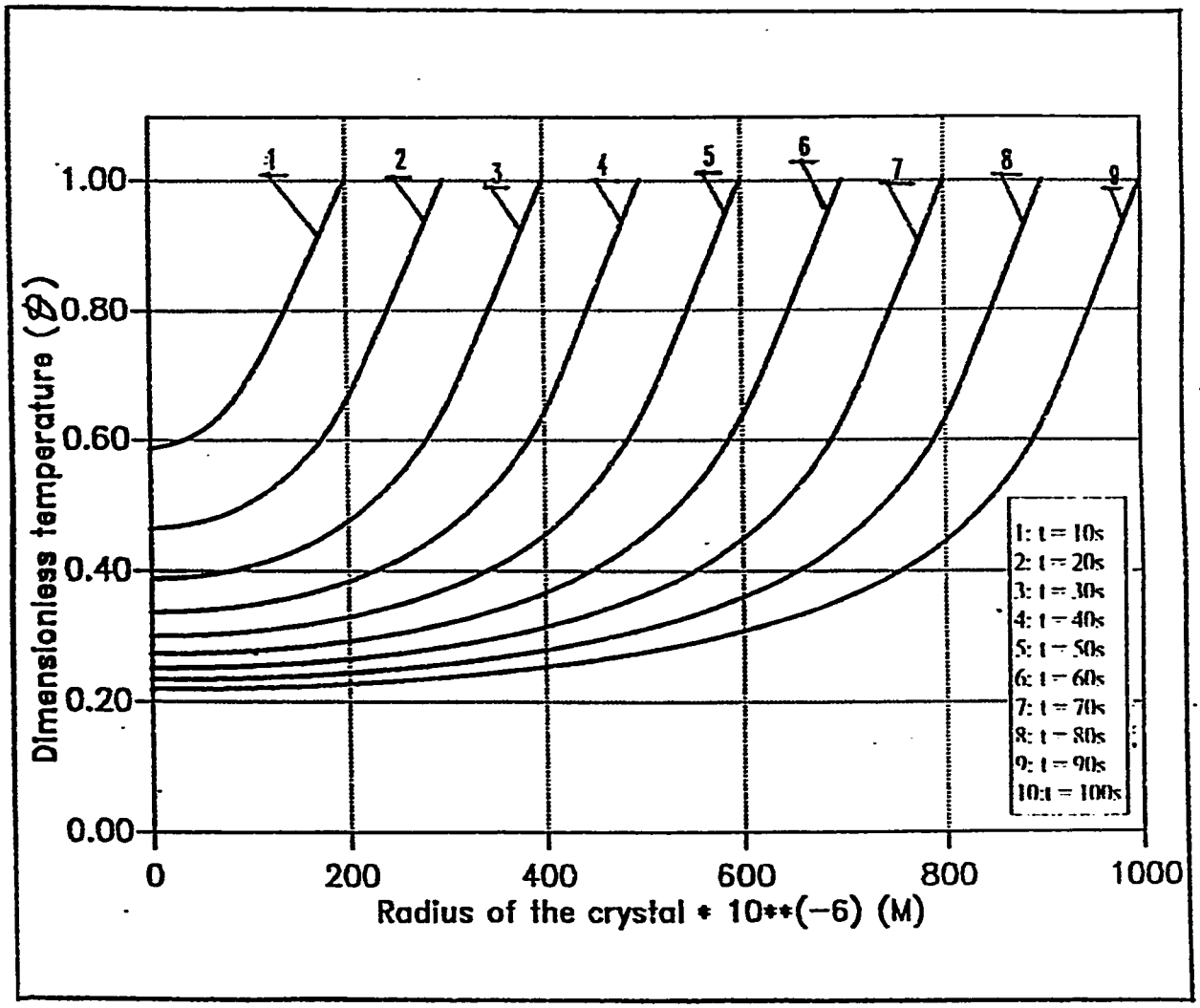

Fig(5.14) Dimensionless temperature vs. raduis of the crystal For cylindrical model.

$r_o = 0.8$, $V_{cir} = 2\ m/s$

$T_v = 10^oC$. $T_s = (-10)^oC$.

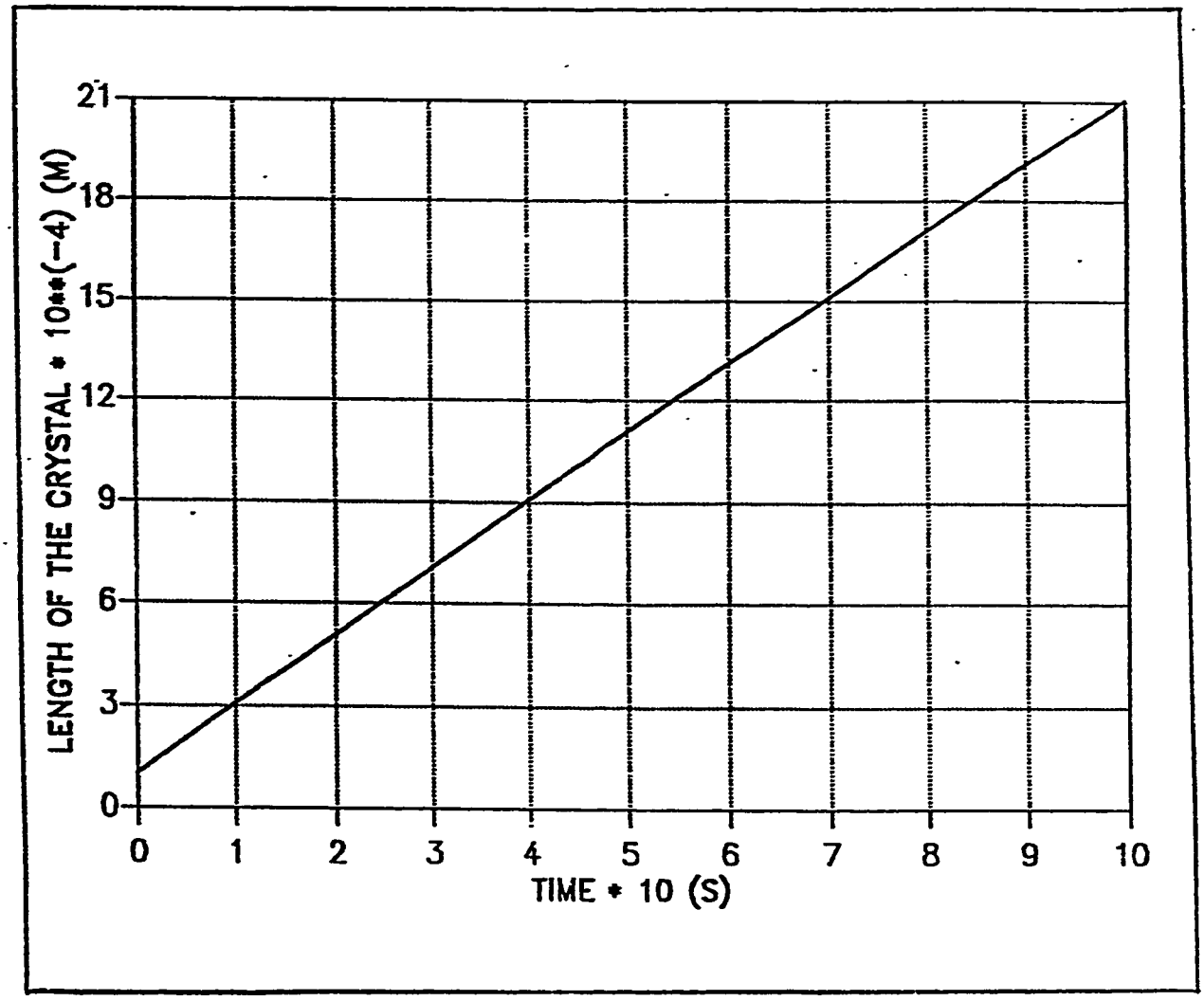

Fig(5.15) Length of the crystal vs. Time

For cylindrical model .

$r_o = 0.8$, $V_{air} = 2\ m/s$

$T_v = 10^oC$. $T_s = (-10)^oC$.

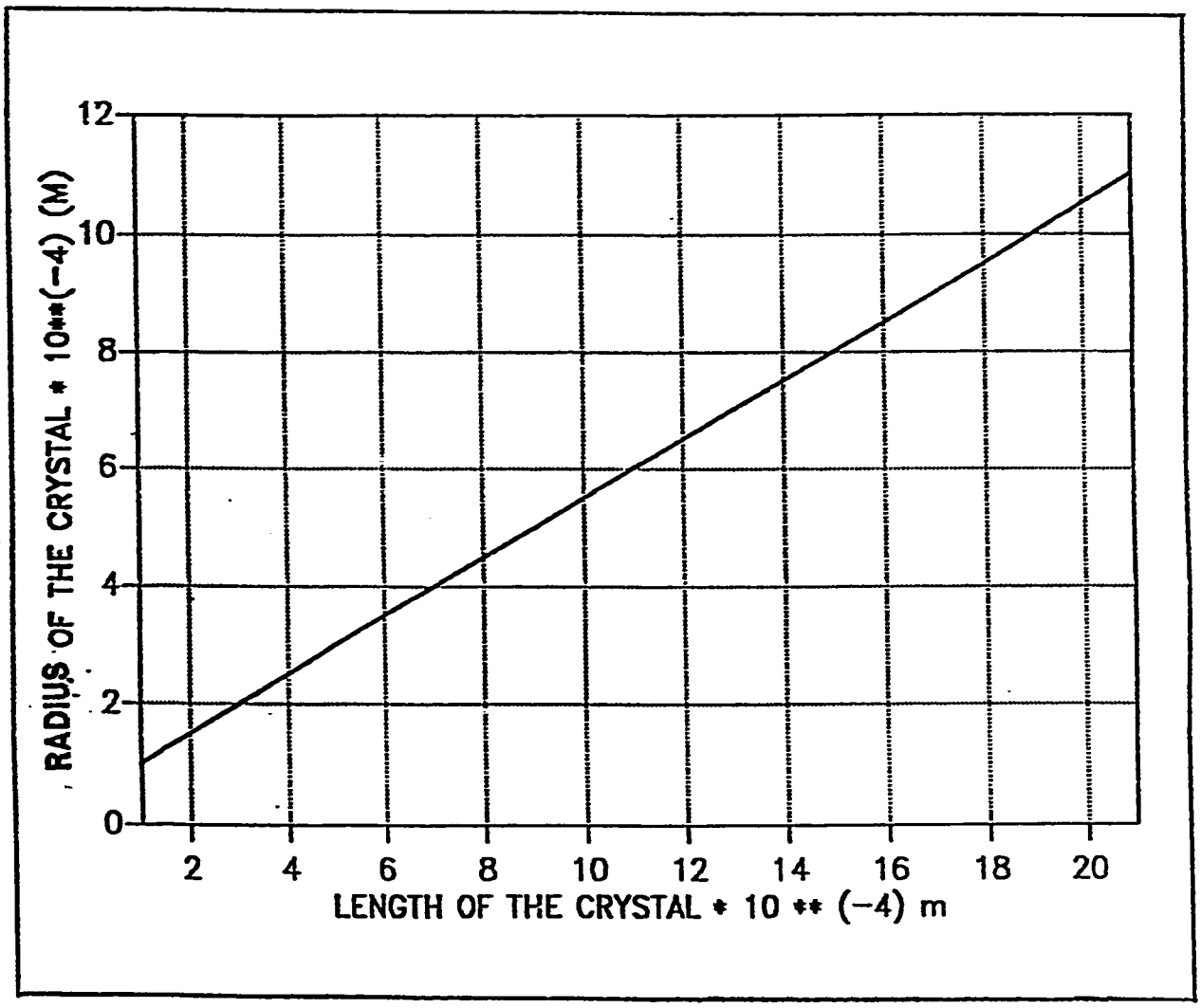

Fig(5.16) Radius of the crystal vs. Time

For cylindrical model .

$r_o = 0.8$, $V_{air} = 2\ m/s$

$T_v = 10^oC$. $T_s = (-10)^oC$.

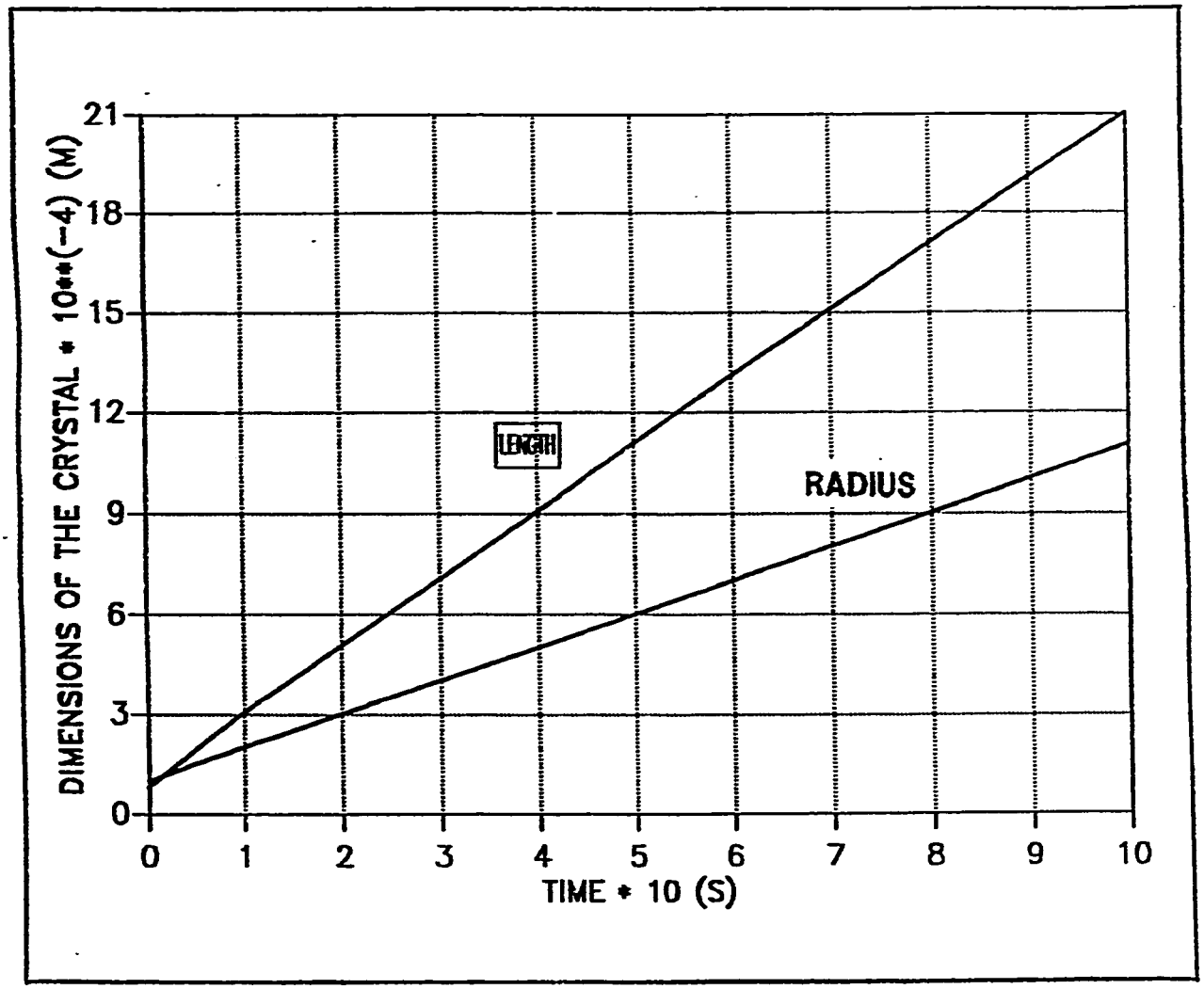

Fig(5.17) Dimensions of the crystal vs. Time

For cylindrical model .

$r_o = 0.8$, $V_{air} = 2\ m/s$

$T_v = 10^oC$. $T_s = (-10)^oC$.

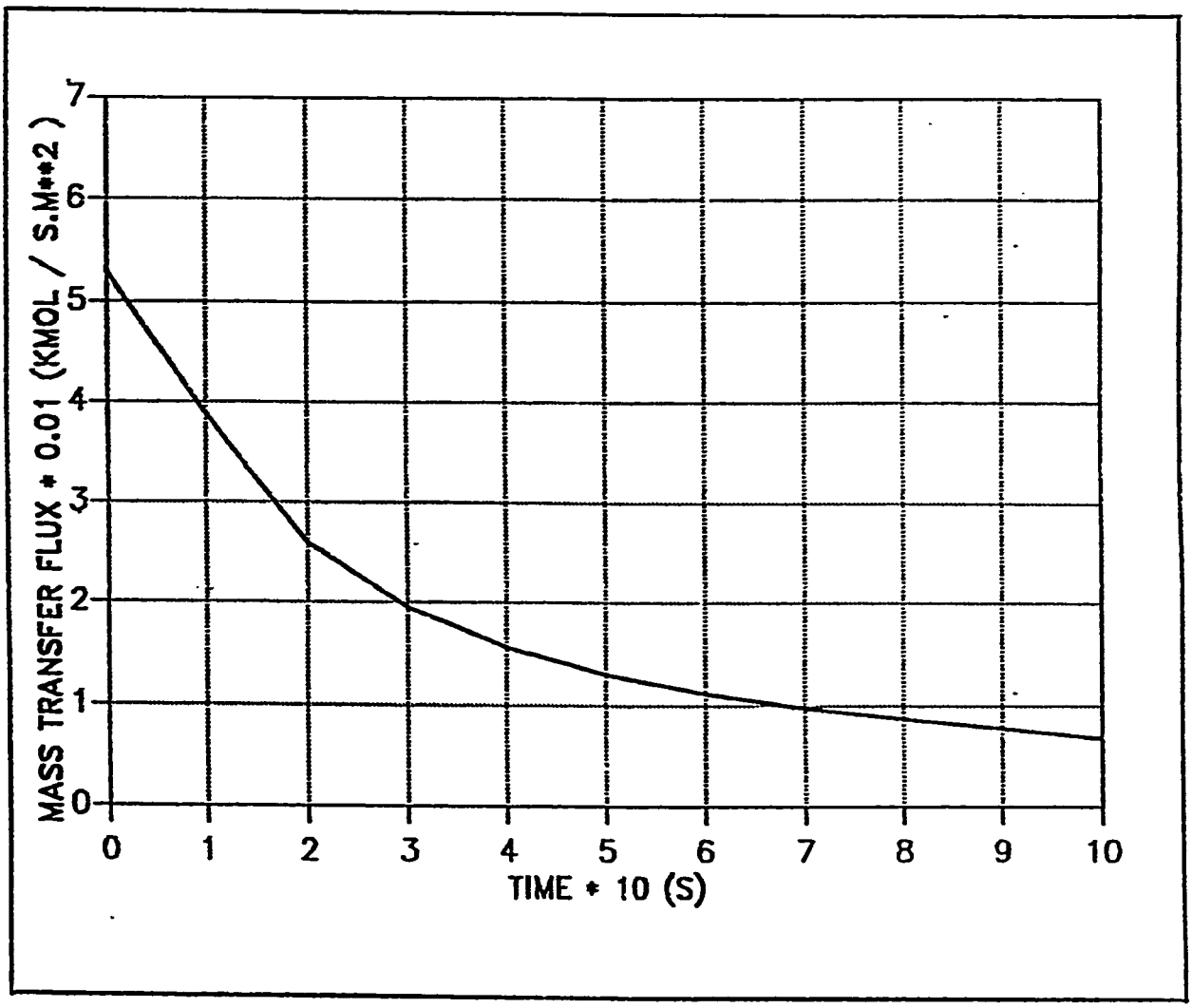

Fig(5.18) Mass transfer flus vs. Time

For cylindrical model.

$r_o = 0.8$, $V_{air} = 2\ m/s$

$\bar{T}_v = 10^oC$. $T_s = -10^oC$.

5.1.2 Effect Of Plate Temperature

In this model the effect of plate temperature is shown by fixing the ambient temperature to $5°C$ and allowing the plate temperature to vary from $(-3°C\ -20°C)$. It is shown in fig (5.B) that as the plate temperature decreases a higher ice crystals could be obtained this mainly could be explained by referring the reasons to the temperature this temperature gradient is becoming higher which is the case of lower plate temperature, it is expected to have bigger ice crystal in both length and diameter. As explained previously in (5.1.1) about the effect of ambient temperature increase it is observed that the same behavior is occurring in this case where the plate temperature is becoming lower, so when the plate temperature is $(-3°C)$ the maximum length that could be reached by the ice crystal is $(250\mu m)$ after 100 s of growing while if the plate temperature is about $(-20°C)$ it is possible to reach about 1600 (μm) of length.

The study of the effect of the plate temperature on the growth of the ice crystal, starts by lowering the plate temperature to $-\ 20°C$ while keeping the ambient temperature fixed to $5°C\ \ 10°C$ and with the value of Γ_o is assumed to be equal to 0.8. Fig(5.19) and (5.20) shows the temperature distribution in the crystal along it's length and radius The crystal is becoming cooler as it's dimensions increase in length and radius due to lower plate temperature as in Fig(5.21) and Fig(5.22). Fig(5.23) gives the effect of initial assumed ratios to limit the growth along one direction. By assuming value of Γ_o to be 0.8, the growth along the radius of the crystal could be limited and controlled. The case

represents allowing the crystal to grow in a shape of a column. This gives the model more flexibility to represent the growth of the ice crystal in plate or column shapes. The density of the ice crystal at higher ambient temperature is becoming lower, due to lower mass flux effect Fig(5.24) Fig(5.25) represents the temperature profile of the ice crystal with it's length at $-3°C$ plate temperature. the variation of temperature with length has the same behavior as in Fig (5.1) but now the length of the crystal is less due to lower temperature gradient. The temperature variation of with radius for this plate temperature is represented in Fig(5.26). As the radius of the crystal is increasing the temperature in the crystal is becoming lower and since the radius is increasing slowly the slope of the temperature profile increase causing the crystal to become shorter with the length approaches a certain final limiting value as the case in Fig(5.27). This is expected due to the low ambient temperature. The radius of the crystal also takes the same behavior as it's length as it is in Fig(5.28). Fig(5.29) declears that the radius and length of the crystal have the same curve. This is mainly due to the assumption of equal initial length and radius. The mass flux at higher plate temperature is higher leading to more dense ice crystals as shown in Fig(5.30).

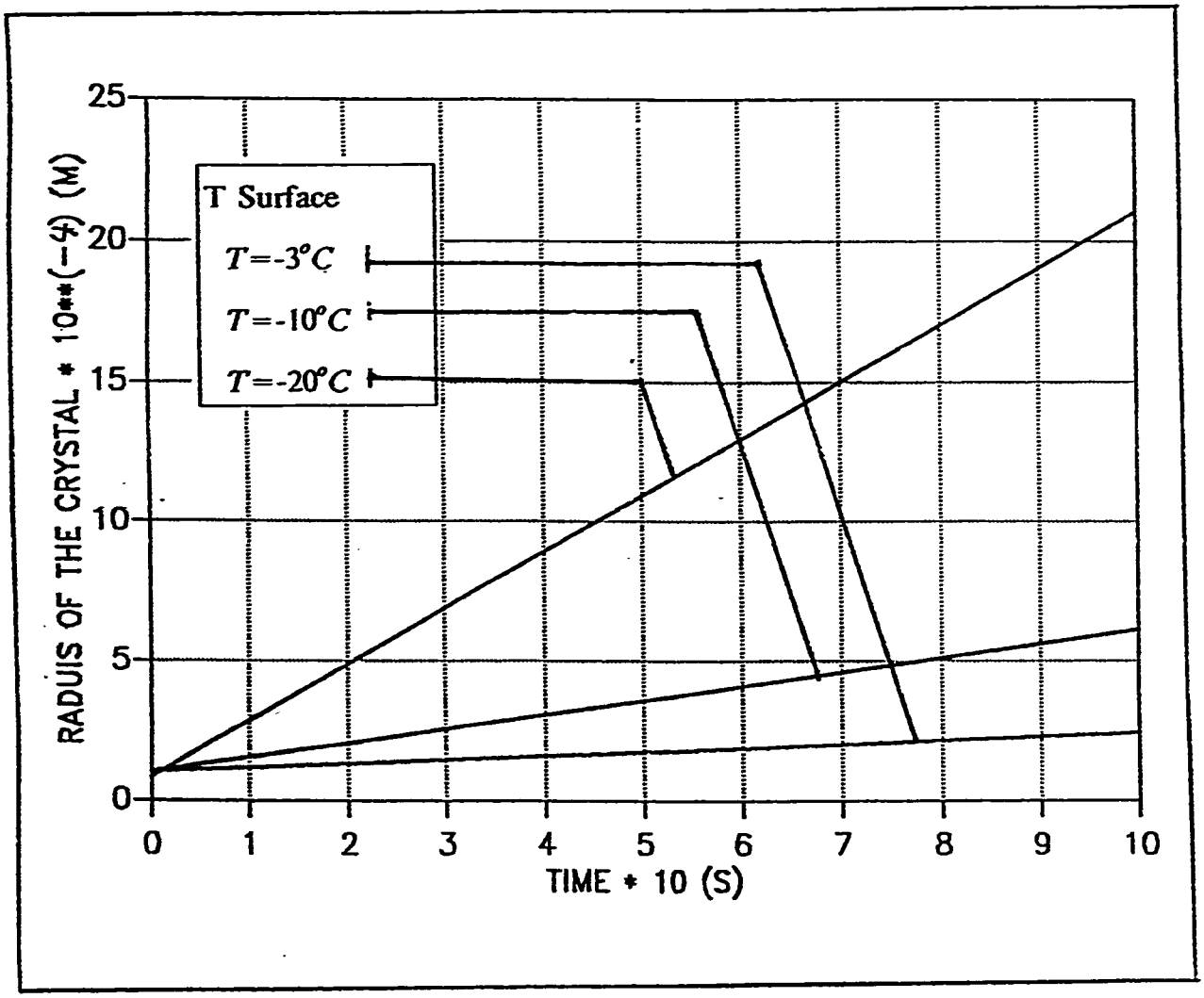

Fig(5.B) Length of the crystal vs. Time for different surface temperatures.

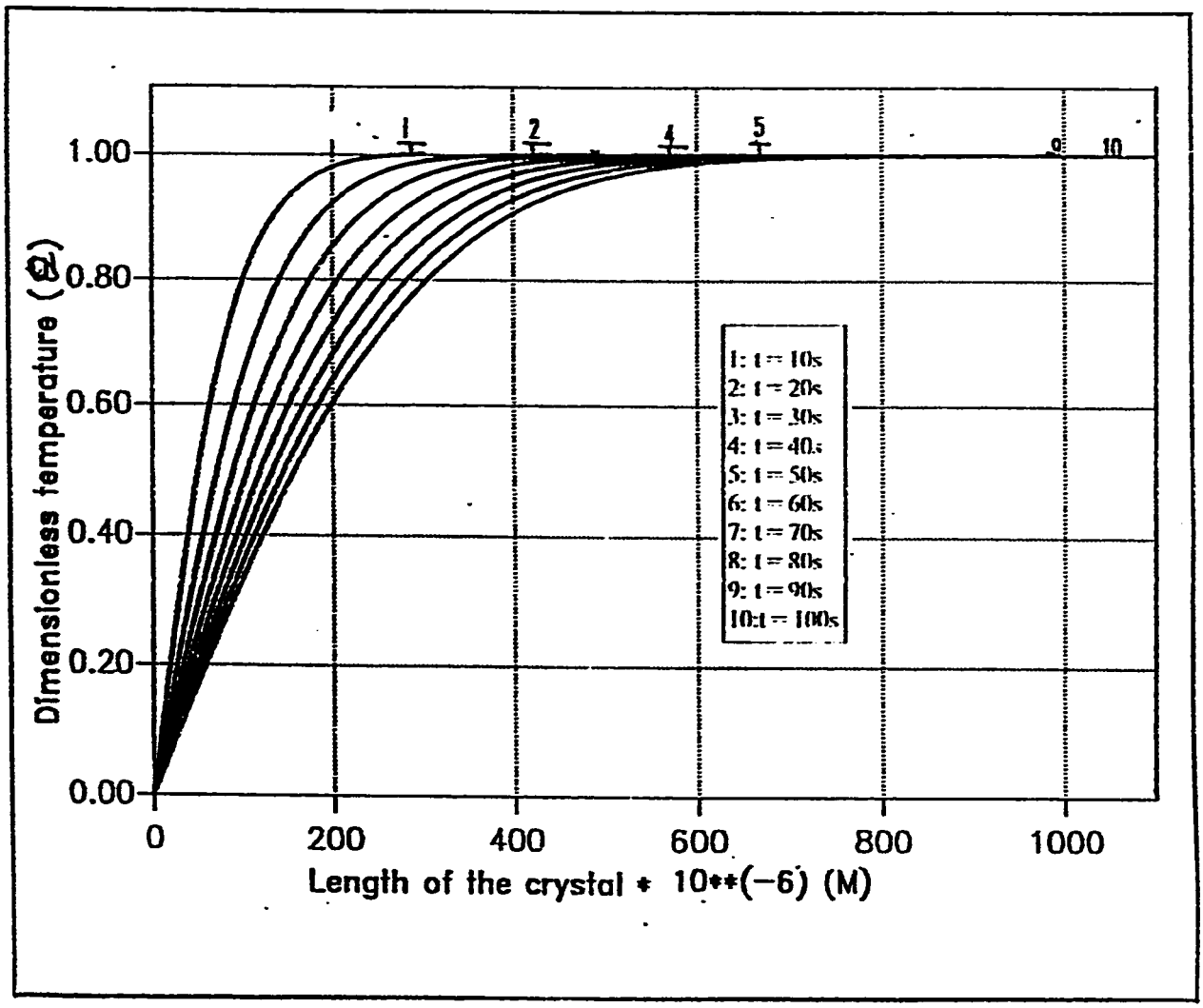

Fig(5.19) Dimensionless temperature vs. length of the crystal. For cylindrical model .

$r_o = 0.8$, $V_{air} = 2\ m/s$

$T_v = 5.0^oC$. , $T_s = (-20)^oC$.

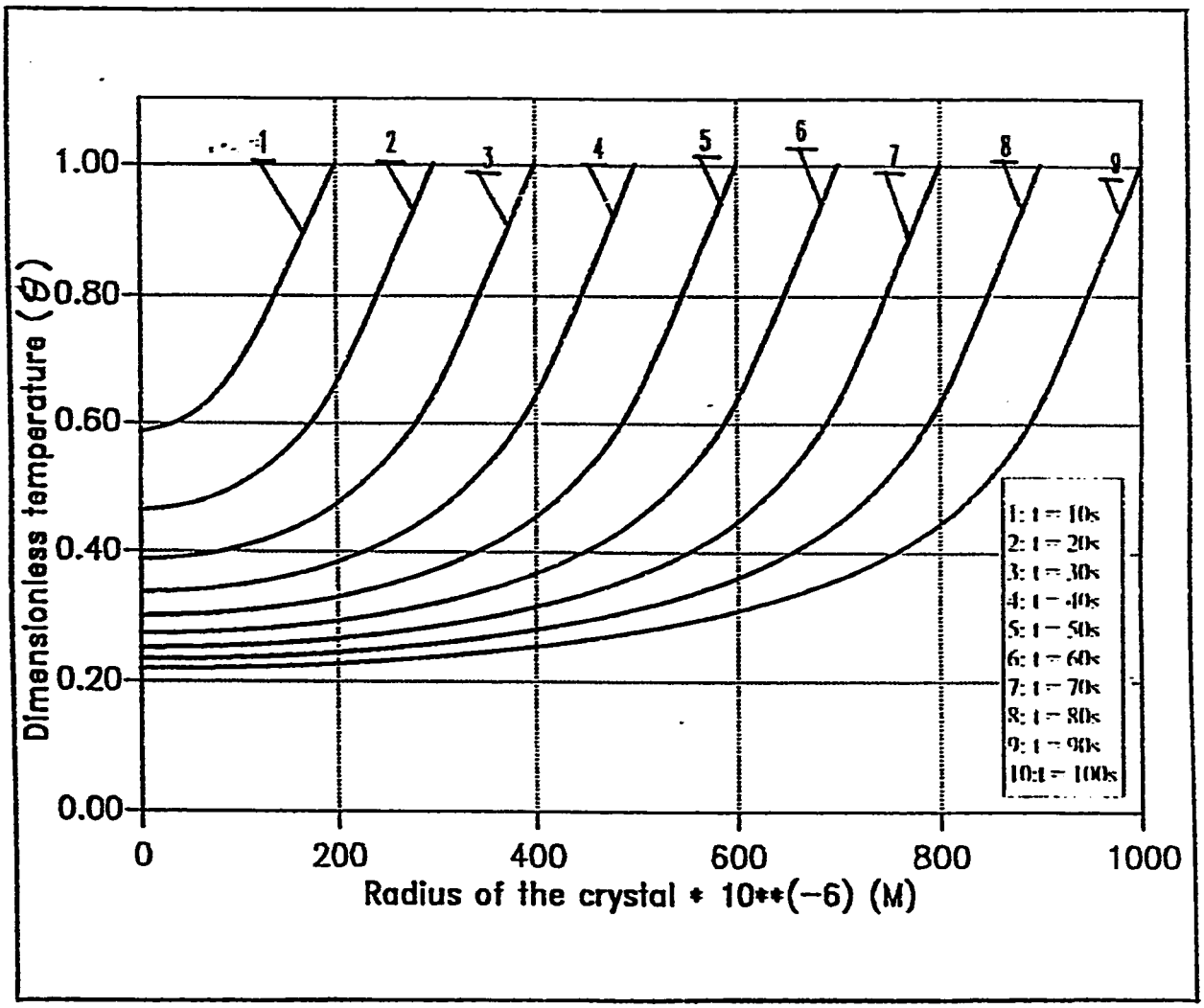

Fig(5.20) Dimensionless temperature vs. raduis of the crystal For cylindrical model.

$\Gamma_o = 0.8$, $V_{air} = 2\ m/s$

$T_v = 5.0^oC$. $T_s = (-20)^oC$.

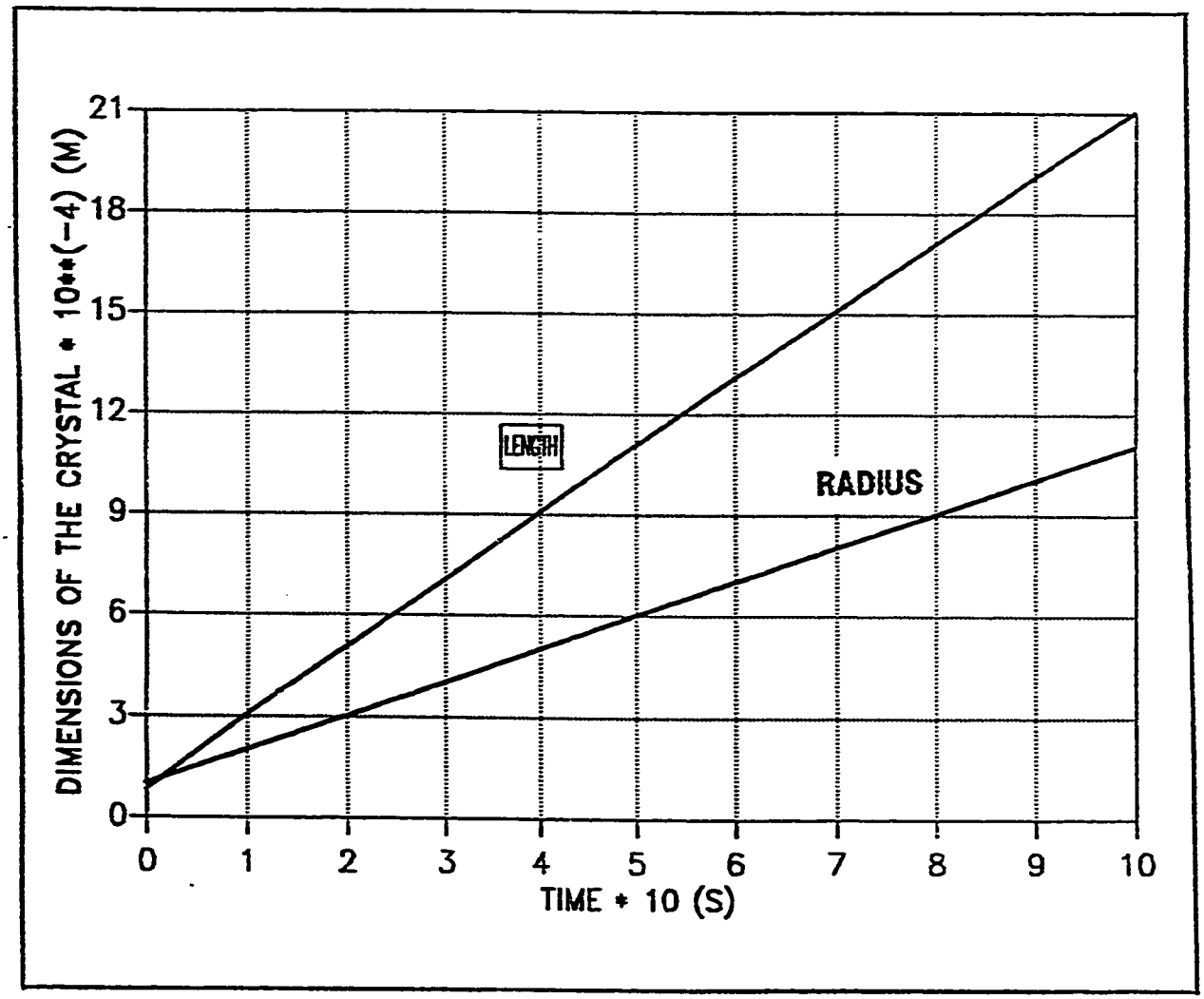

Fig(5.21) Dimensions of the crystal vs. Time

For cylindrical model .

$r_o = 0.8$, $V_{air} = 2\ m/s$

$T_v = 5.0^oC$. $T_s = (-20)^oC$.

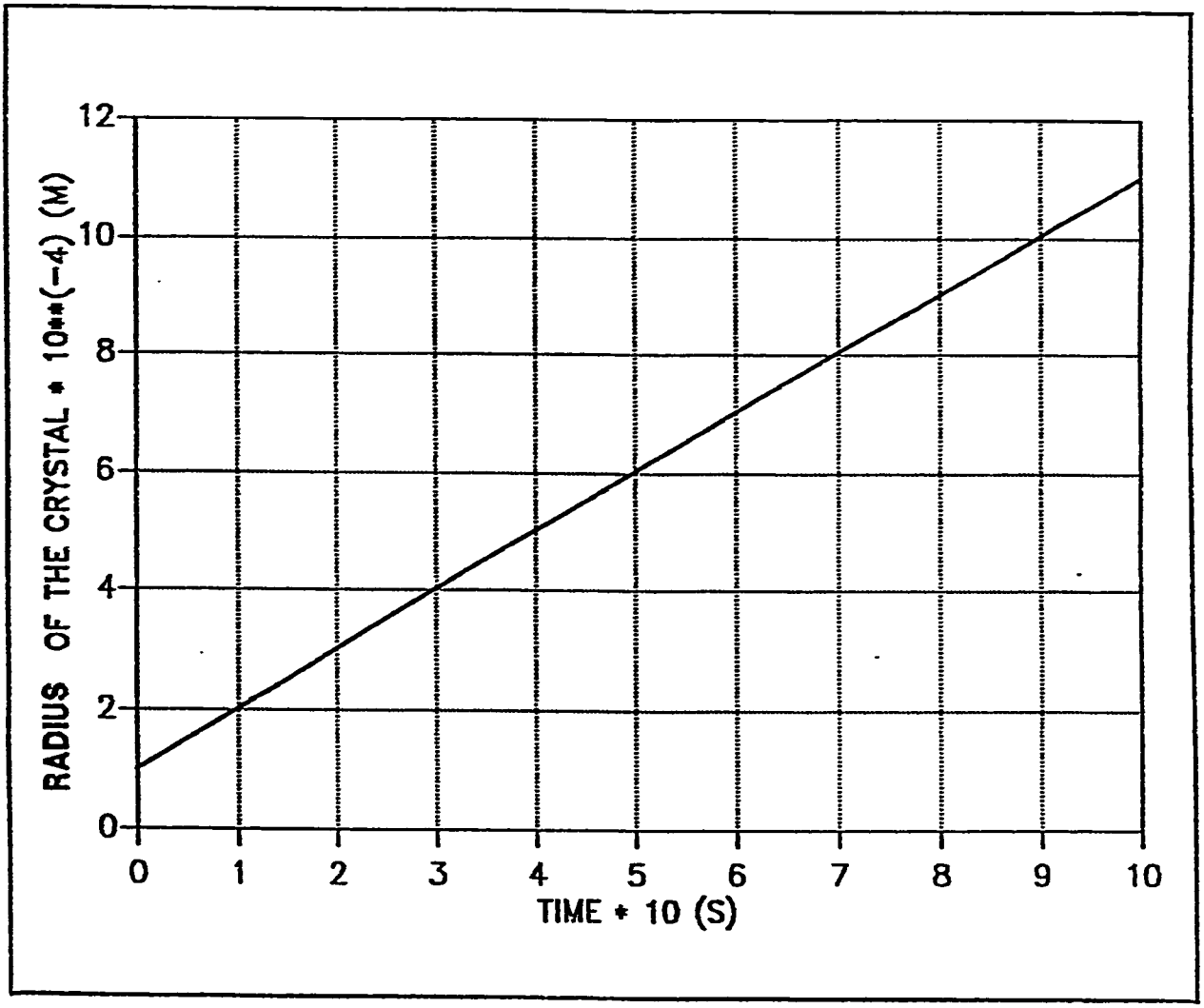

Fig(5.22) Radius of the crystal vs. Time

For cylindrical model .

$r_o = 0.8$, $V_{air} = 2\ m/s$

$T_v = 5.0^oC$. $T_s = (-20)^oC$.

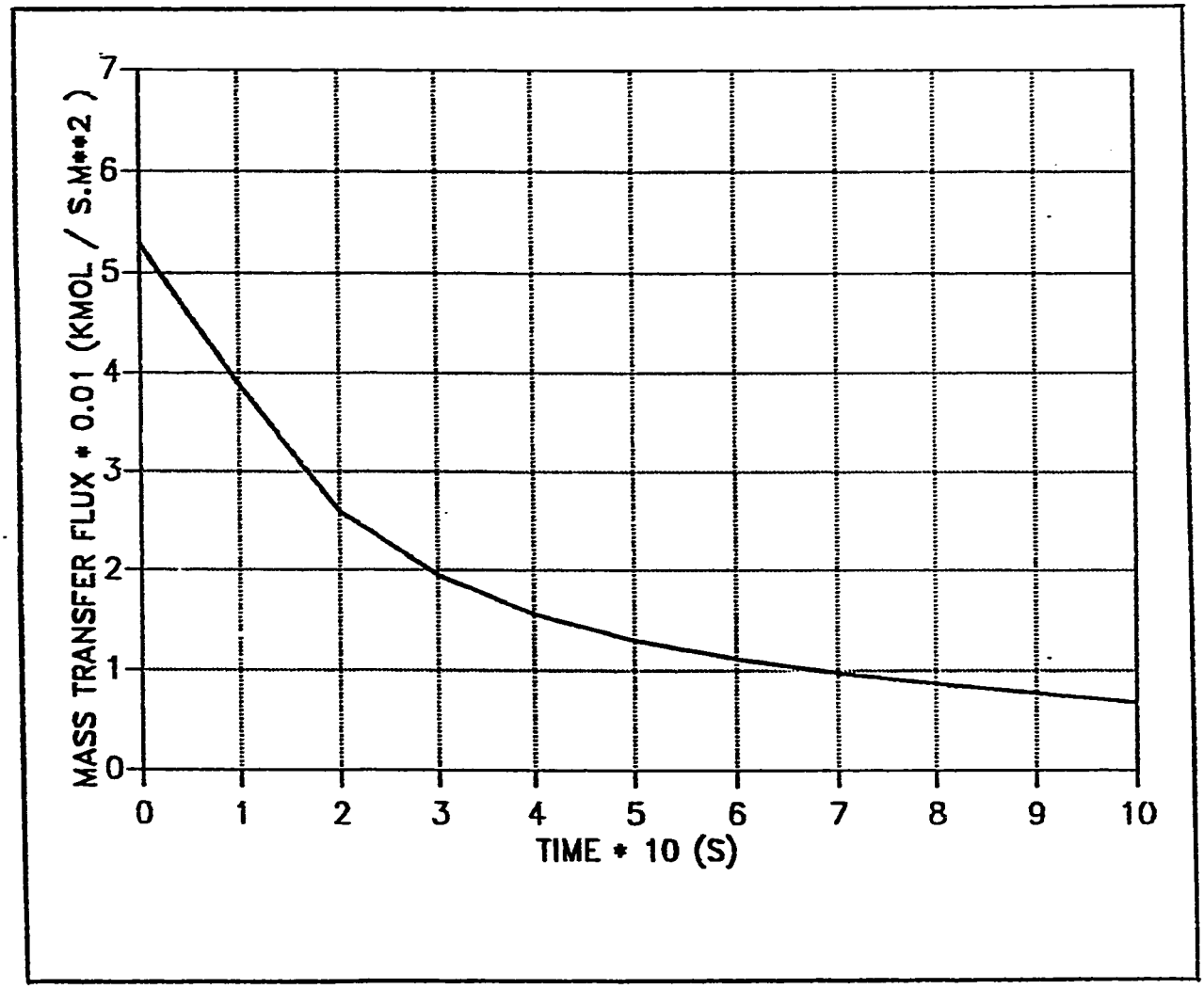

Fig(5.23) Mass transfer flus vs. Time

For cylindrical model.

$r_o = 0.8$, $V_{air} = 2\ m/s$

$T_v = 5.0^oC$. $T_s = (-20)^oC$.

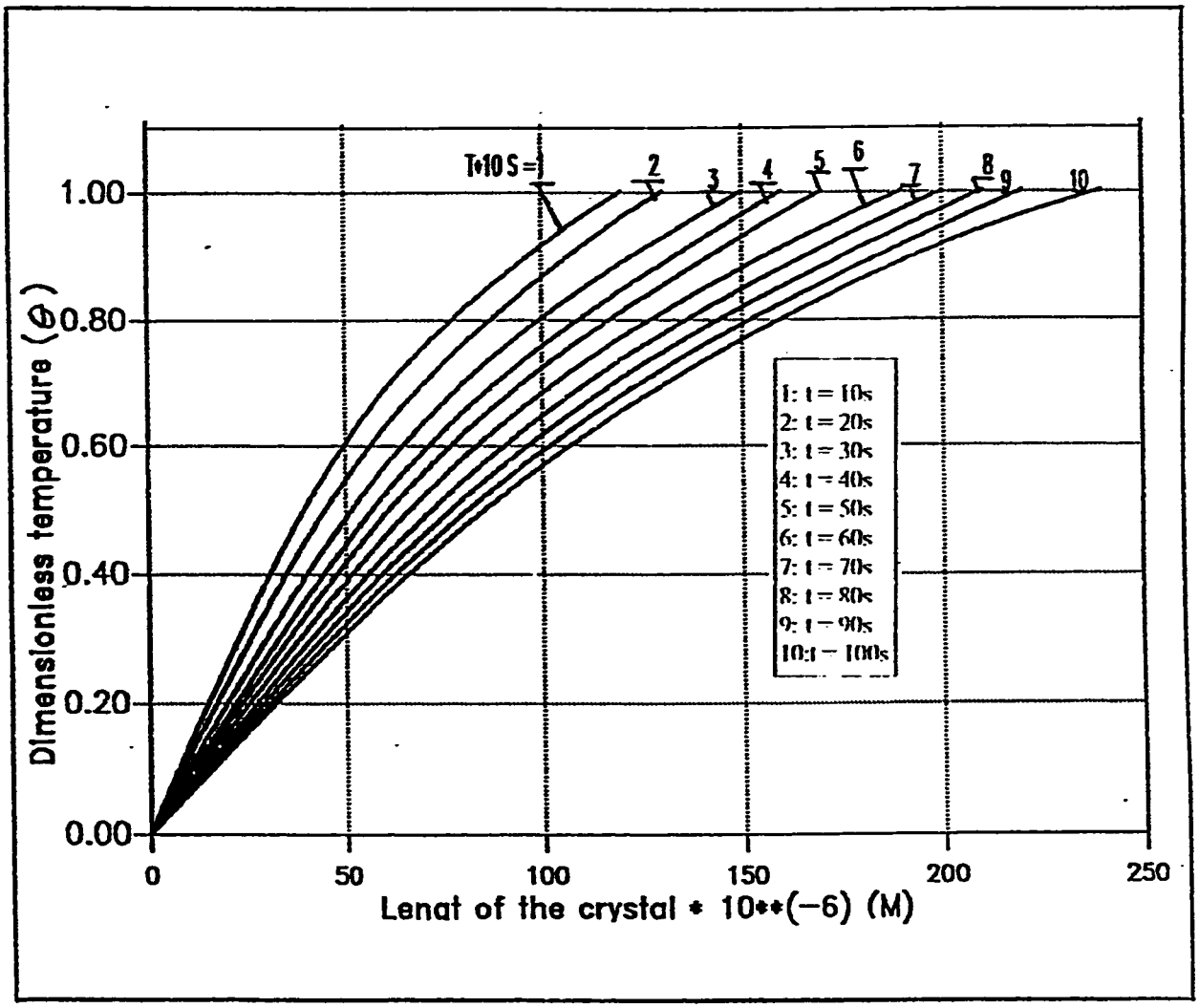

Fig(5.24) Dimensionless temperature vs. length of the crystal. For cylindrical model .

$r_o = 1.0$, $V_{air} = 2\ m/s$

$T_v = 5.0^oC$. , $T_s = (-3)^oC$.

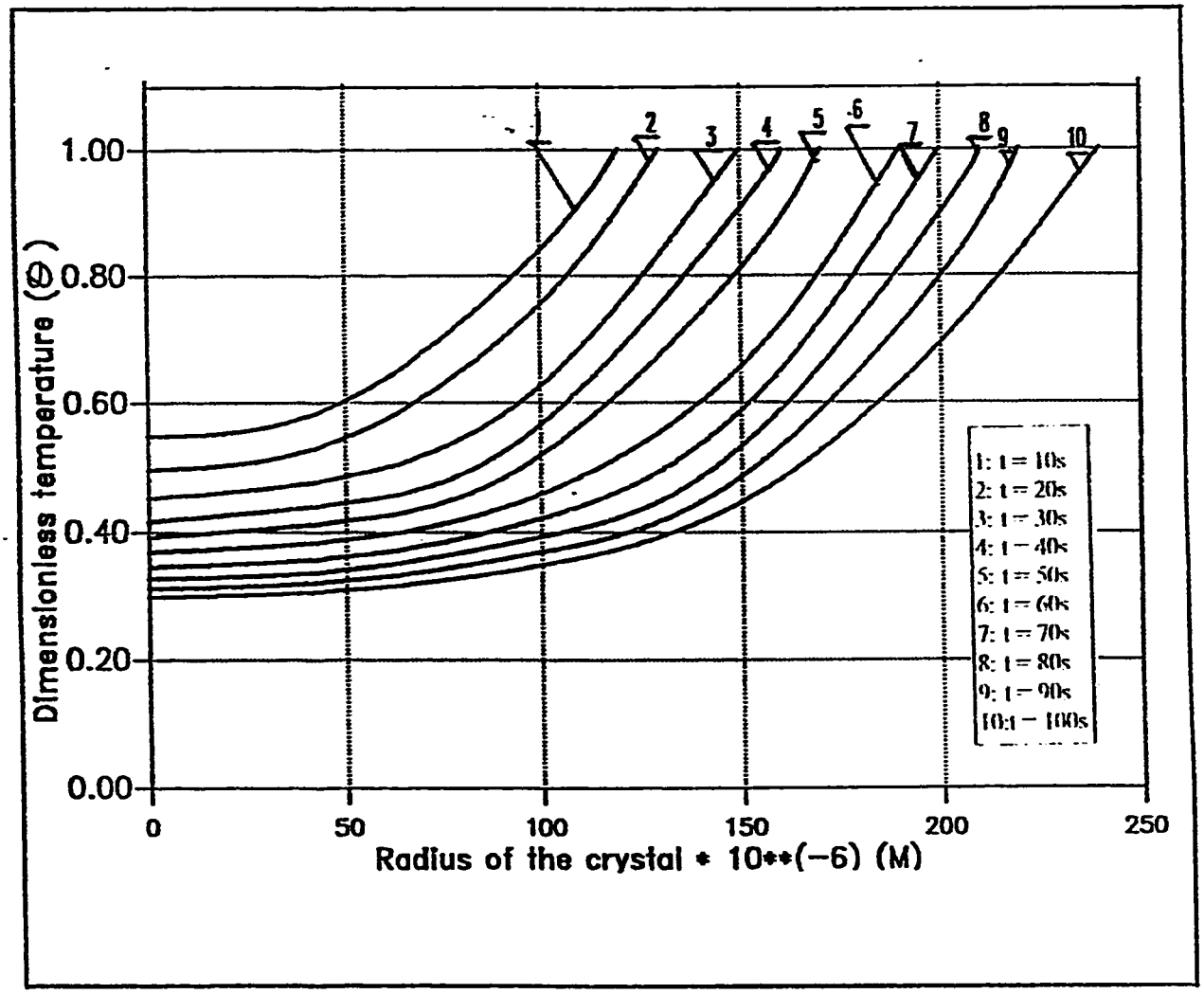

Fig(5.25) Dimensionless temperature vs. raduis of the crystal For cylindrical model.

$r_o = 1.0$, $V_{air} = 2\ m/s$

$T_v = 5.0^oC$. $T_s = (-3)^oC$.

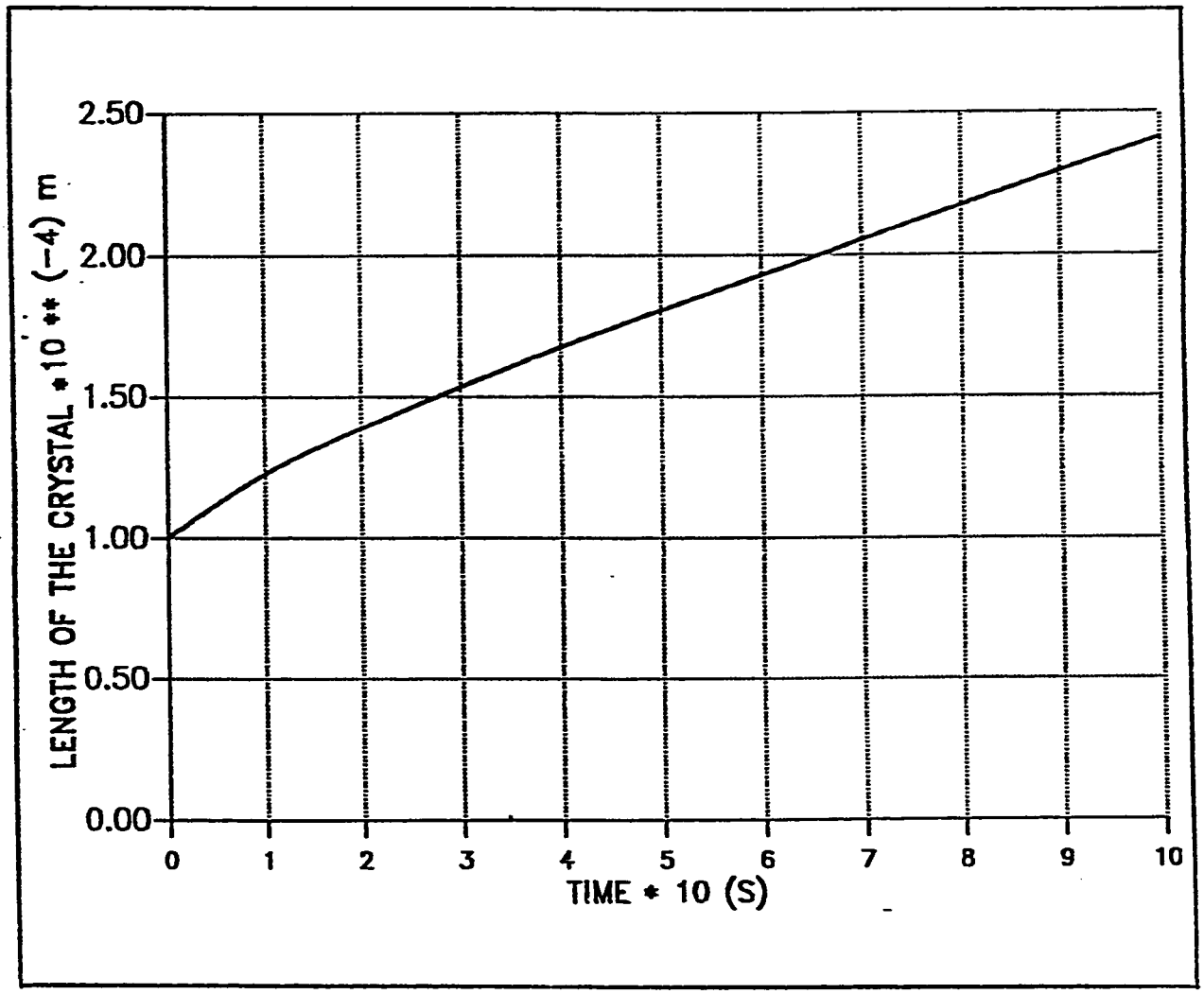

Fig(5.26) Length of the crystal vs. Time

For cylindrical model .

$r_o = 1.0$, $V_{air} = 2\ m/s$

$T_v = 5.0^oC$. $T_s = (-3)^oC$.

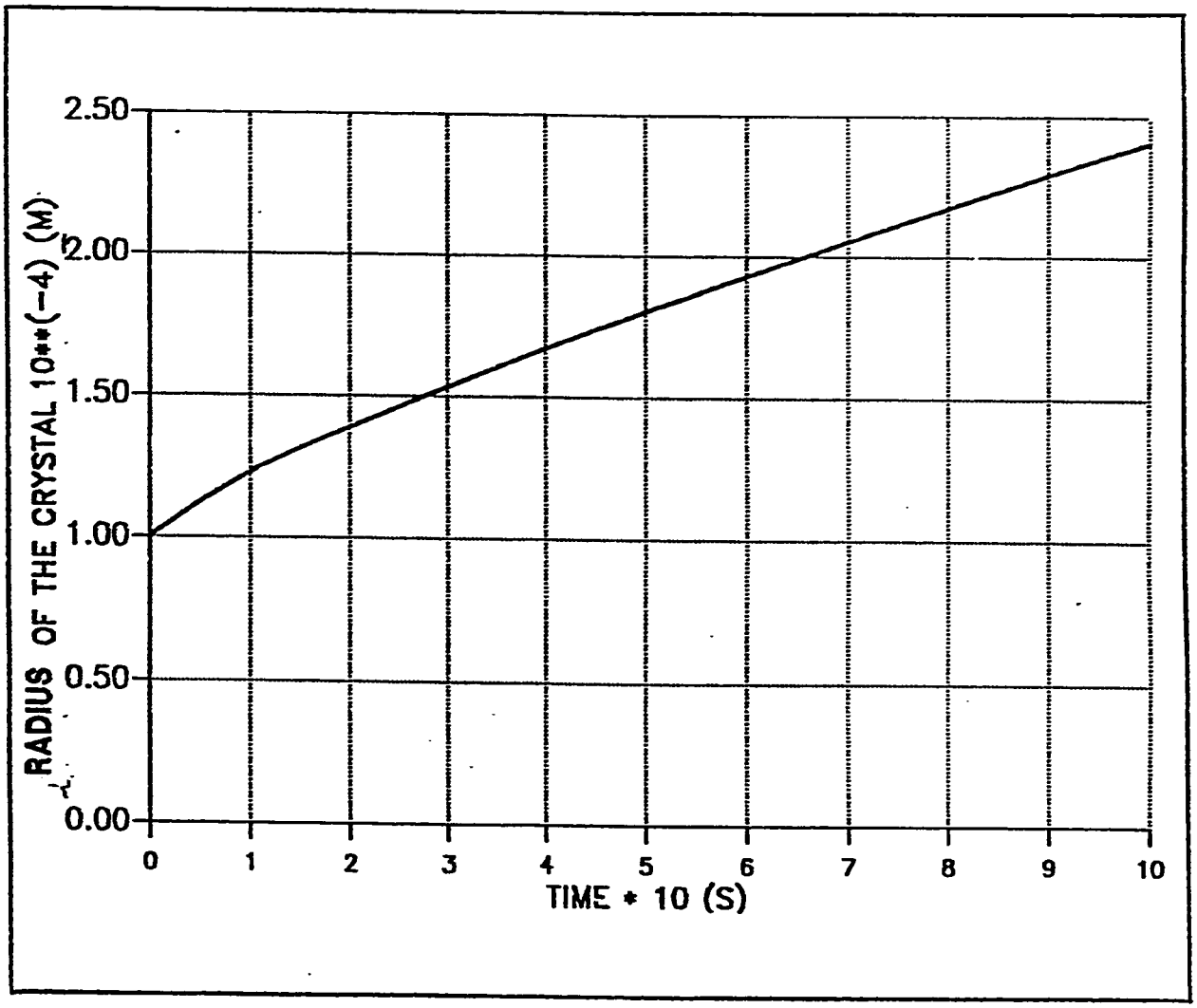

Fig(5.27) Radius of the crystal vs. Time

For cylindrical model .

$r_o = 1.0$, $V_{air} = 2\ m/s$

$T_v = 5.0^oC$. $T_s = (-3)^oC$.

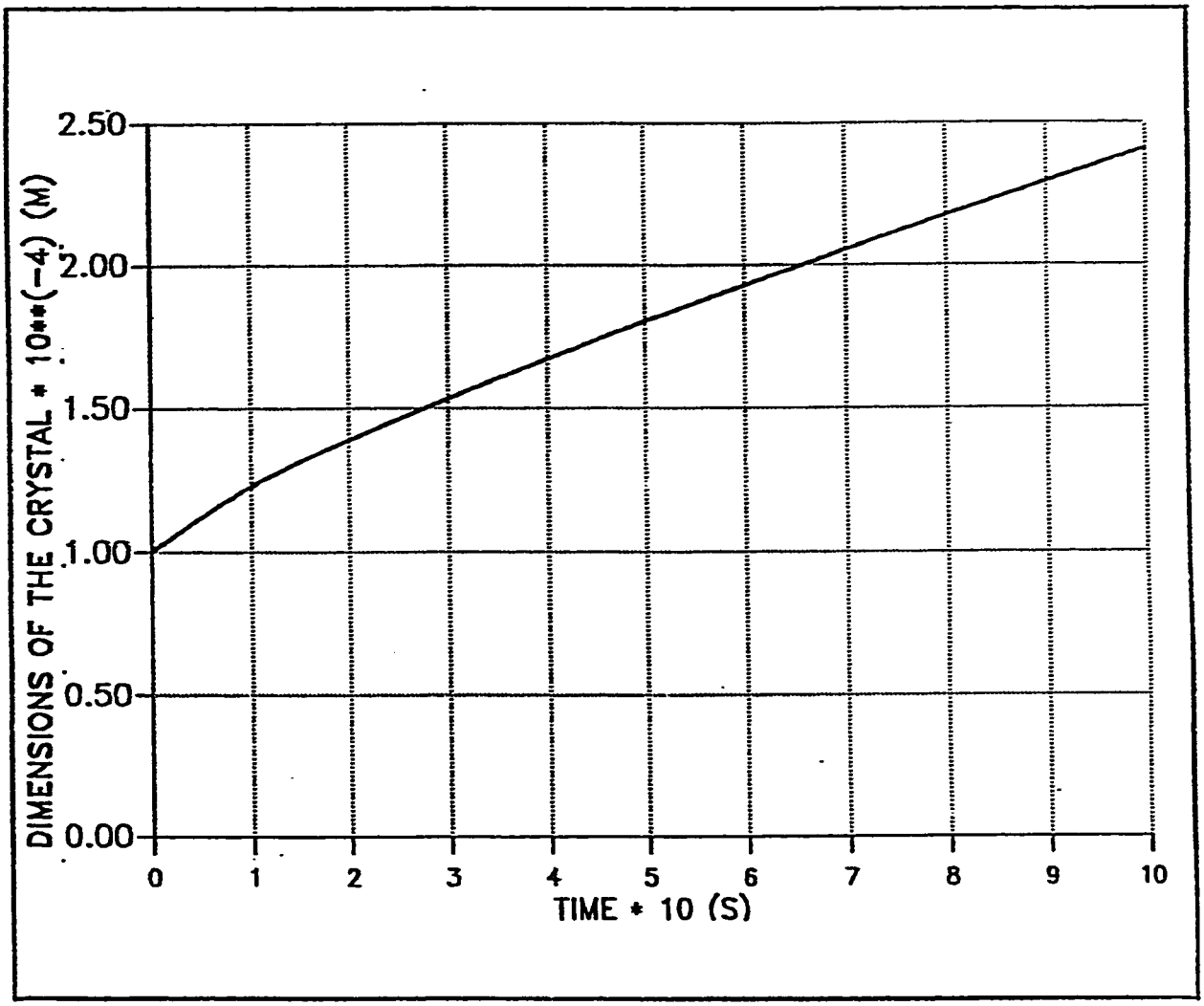

Fig(5.29) Dimensions of the crystal vs. Time

For cylindrical model .

$r_o = 1.0$, $V_{air} = 2\ m/s$

$T_v = 5.0^oC$. $T_s = (-3)^oC$.

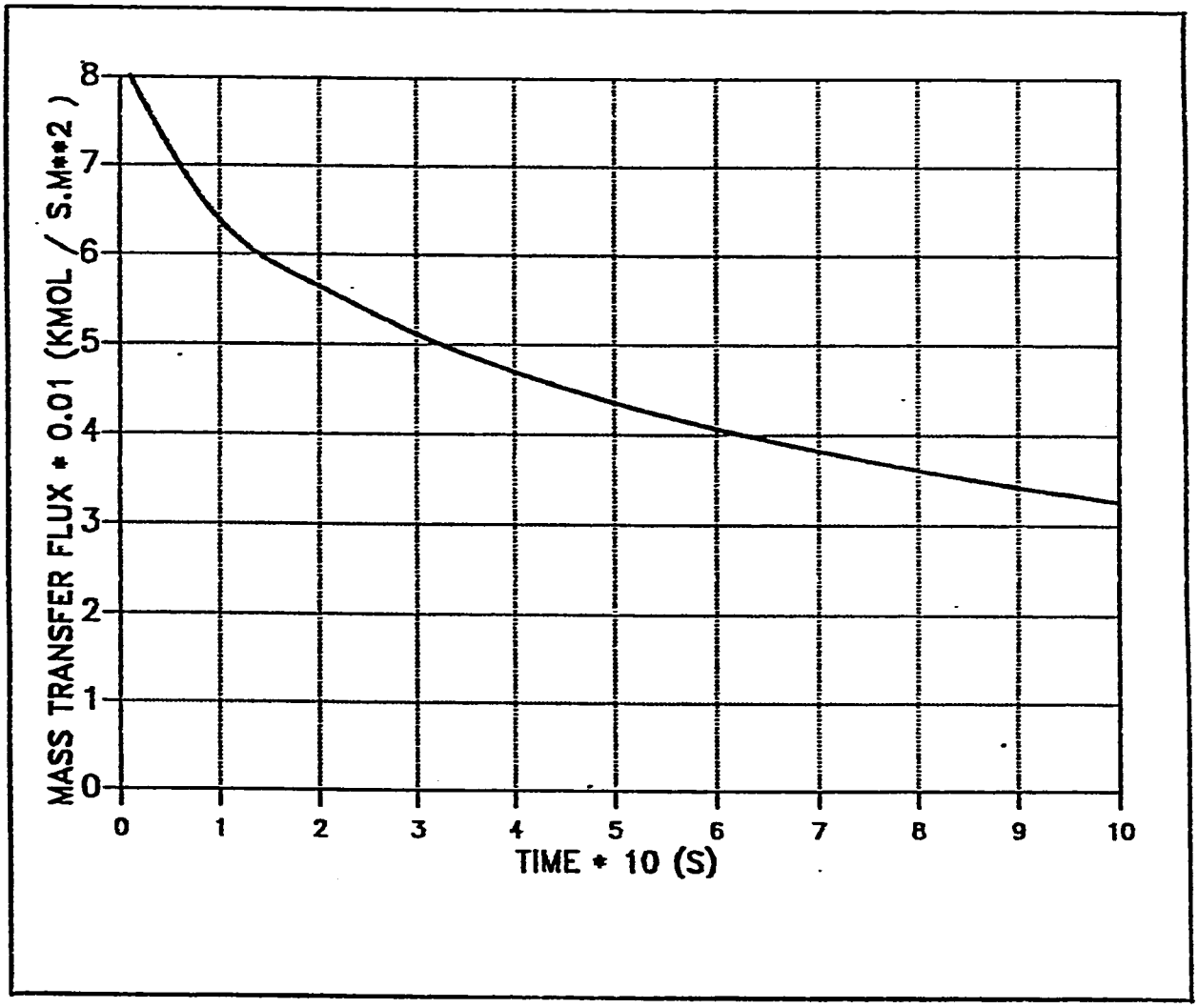

Fig(5.30) Mass transfer flus vs. Time

For cylindrical model.

$r_o = 1.0$, $V_{air} = 2\ m/s$

$T_v = 5.0^oC$. $T_s = (-3)^oC$.

5.1.3 Effect Of Air Velocity

When a crystal grows from the gaseous phase the molecules which form the lattice initially are adsorbed at the crystal surface. Migration along the surface takes place until the local position is reached where the molecules is built into the lattice with maximum decrease in the interfacial energy. So for ice crystal to grow a certain number of molecules is necessary to form through cluster formation . The probability of the ice crystal to become larger, depends on the quantity of water vapour molecules present in the neighbourhood of the cold surface. As the ice crystal grows more water molecules are consumed which are replaced by new molecules coming from the bulk flow. As the air velocity increases the size of the ice crystals growing will increase causing decrease in the temperature distribution in the crystal as shown for the case of temperature distribution in Fig(5.31) and Fig(5.32). When comparing Fig(5.3) and Fig(5.4) with Fig(5.33) and Fig(5.34), it is clear that as the air velocity increases from 2 m/s to 6 m/s the length and radius of the crystal increases. The value of Γ_o in this case is assumed to be 1.2 which enhances the growth of the ice crystal in the radial direction giving a control on the growth in this direction.Fig(5.35) shows the mass flux variation with time. this behavior of the crystal with air velocity agrees with the physical situation represented initially.

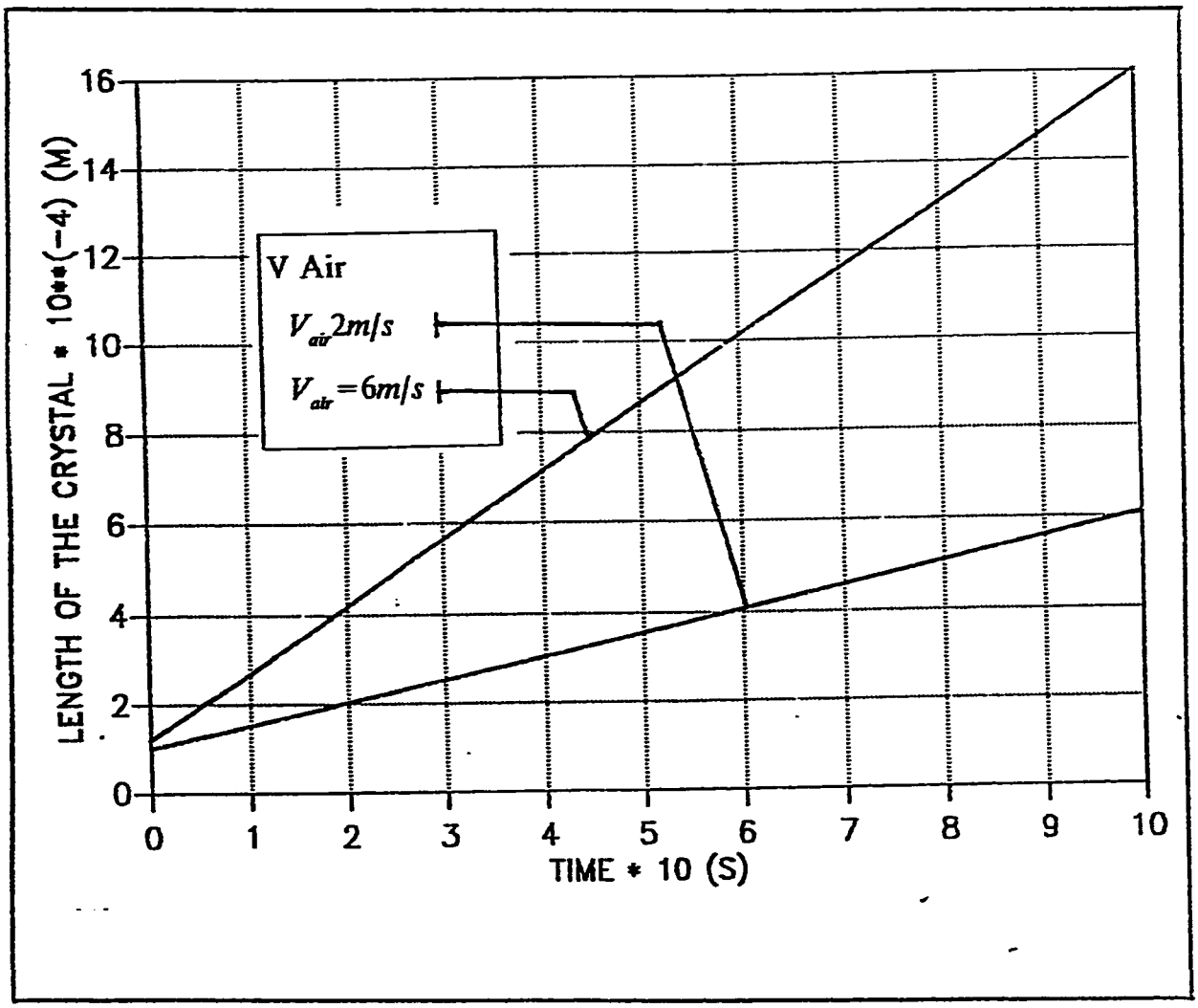

Fig(5.C) Length of the crystal vs. Time for different air velocities

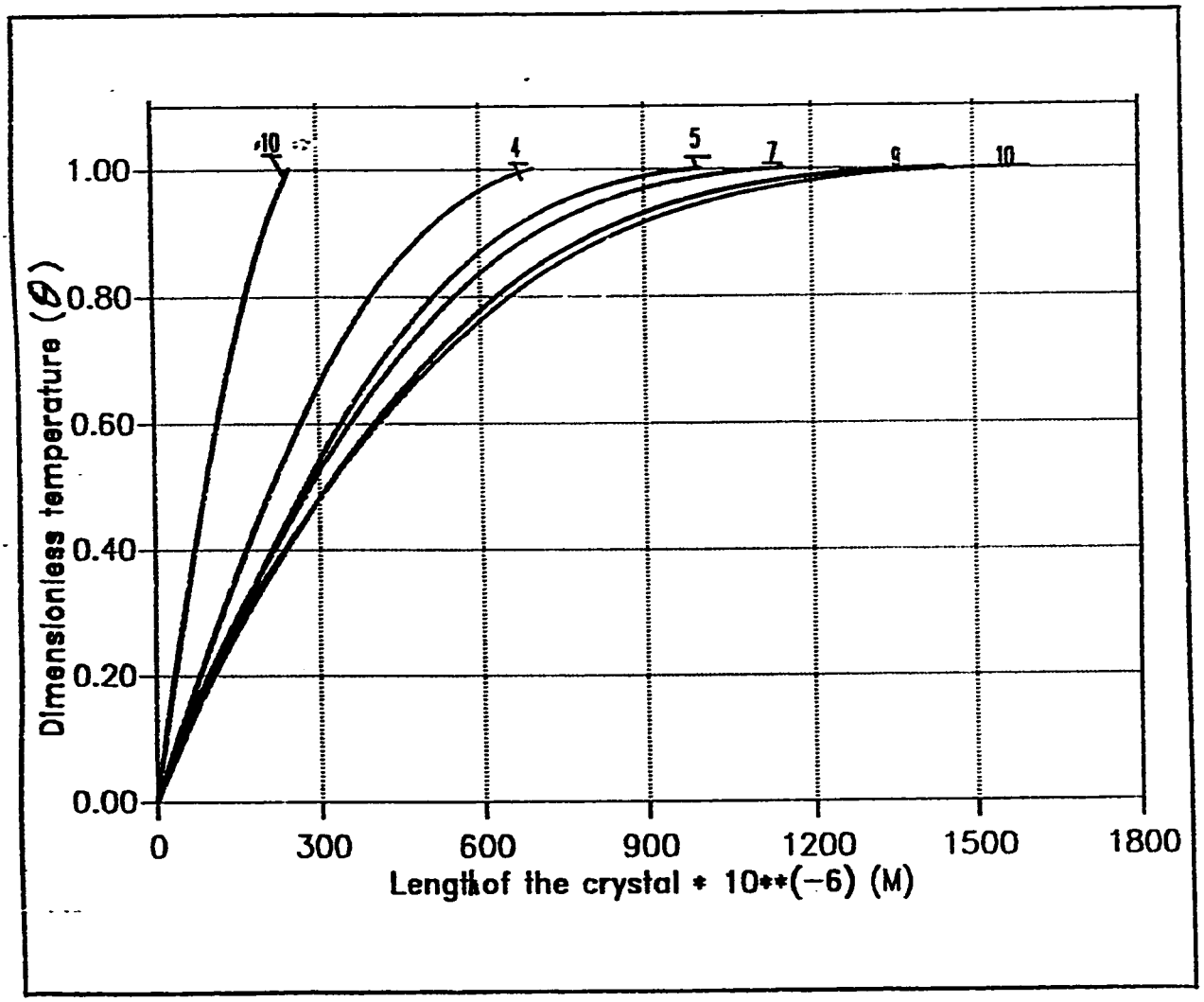

Fig(5.31) Dimensionless temperature vs. length of the crystal. For cylindrical model .

$r_o = 1.2$, $V_{air} = 6 \cdot m/s$

$T_v = 5.0^oC$. , $T_s = (-10)^oC$.

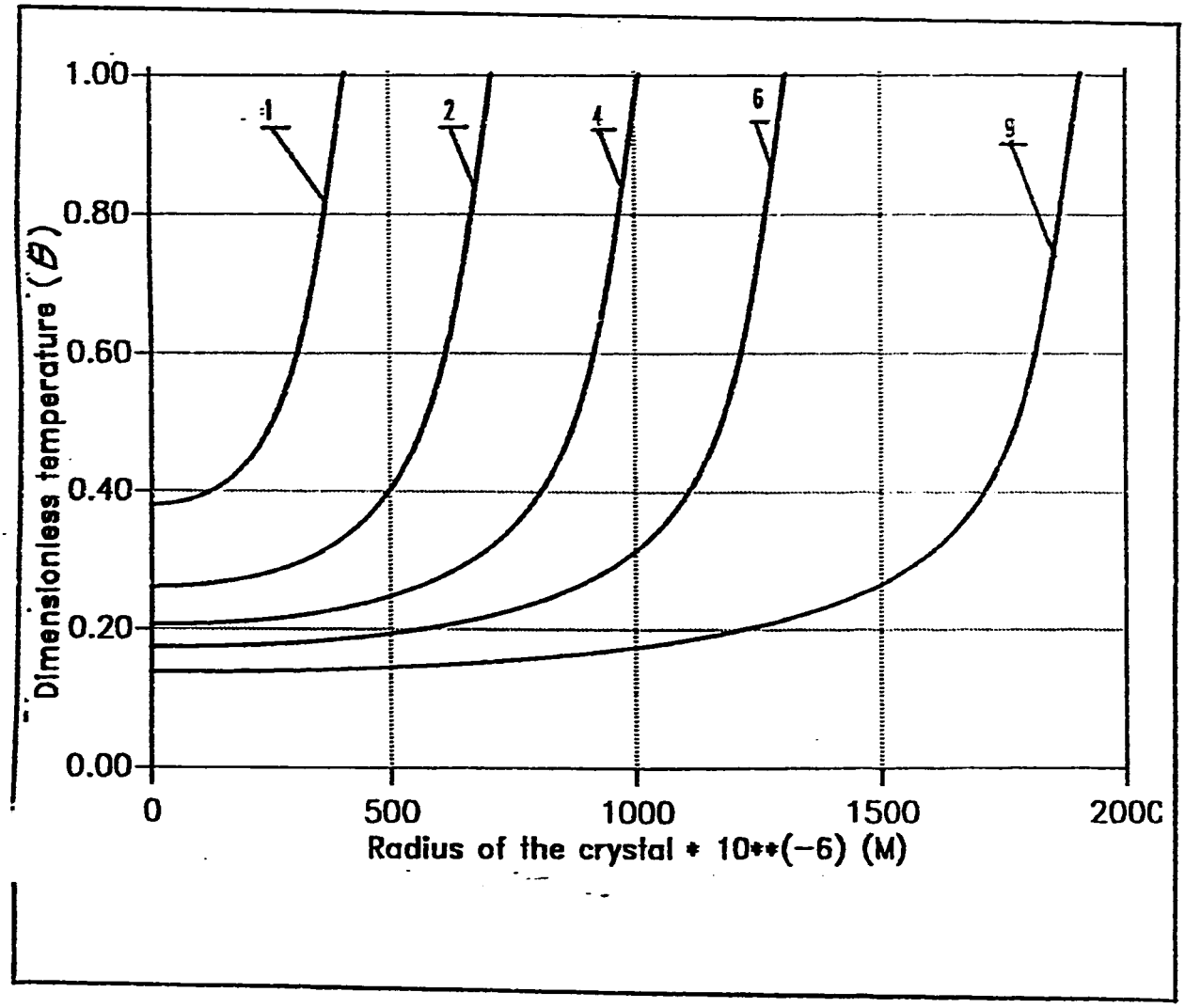

Fig(5.32) Dimensionless temperature vs. raduis of the crystal For cylindrical model.

$r_o = 1.2$, $V_{air} = 6\ m/s$

$T_v = 5.0^oC$. $T_s = (-10)^oC$.

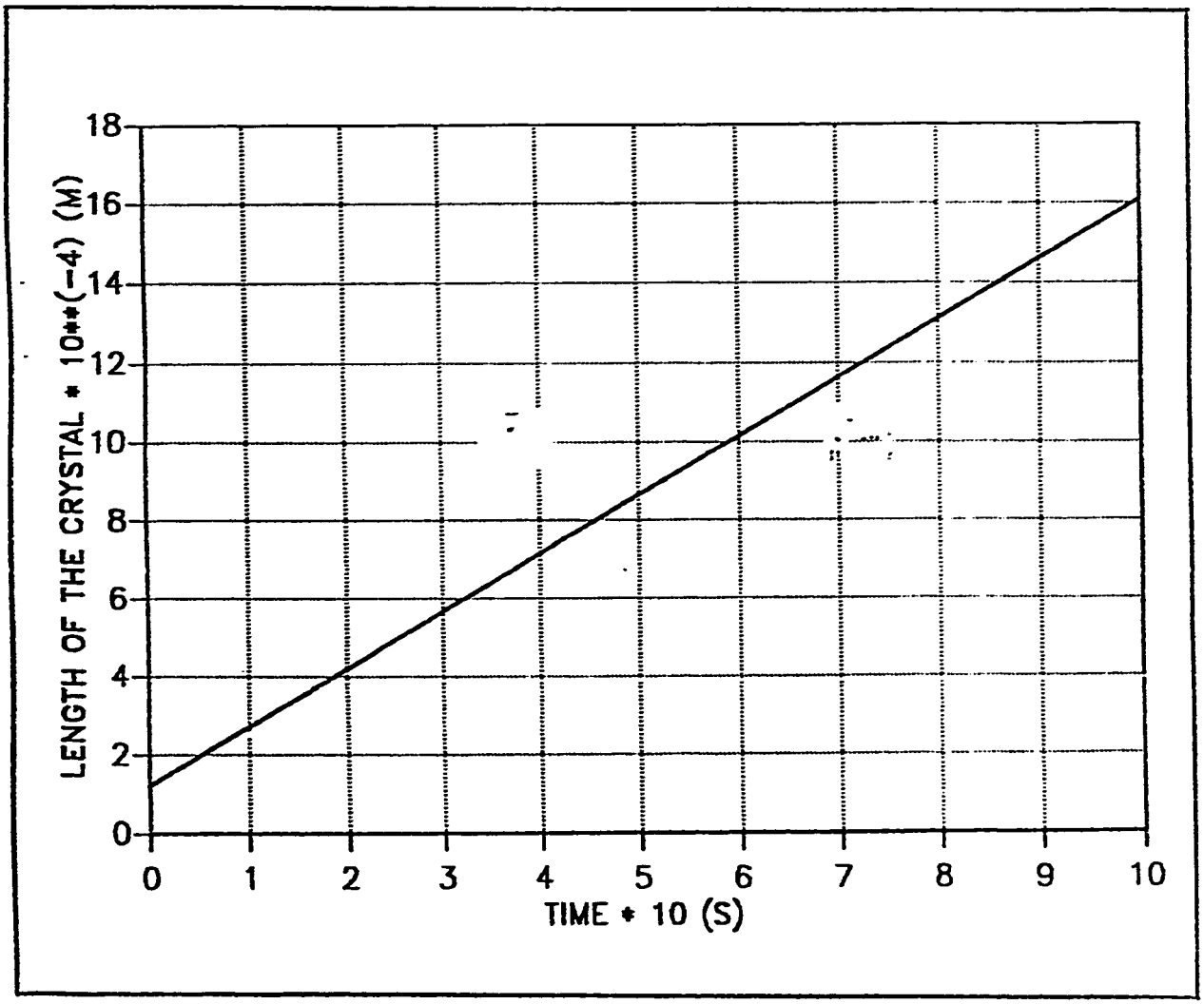

Fig(5.33) Length of the crystal vs. Time

For cylindrical model .

$r_o = 1.2$, $V_{air} = 6\ m/s$

$T_v = 5.0^oC$. $T_s = (-10)^oC$.

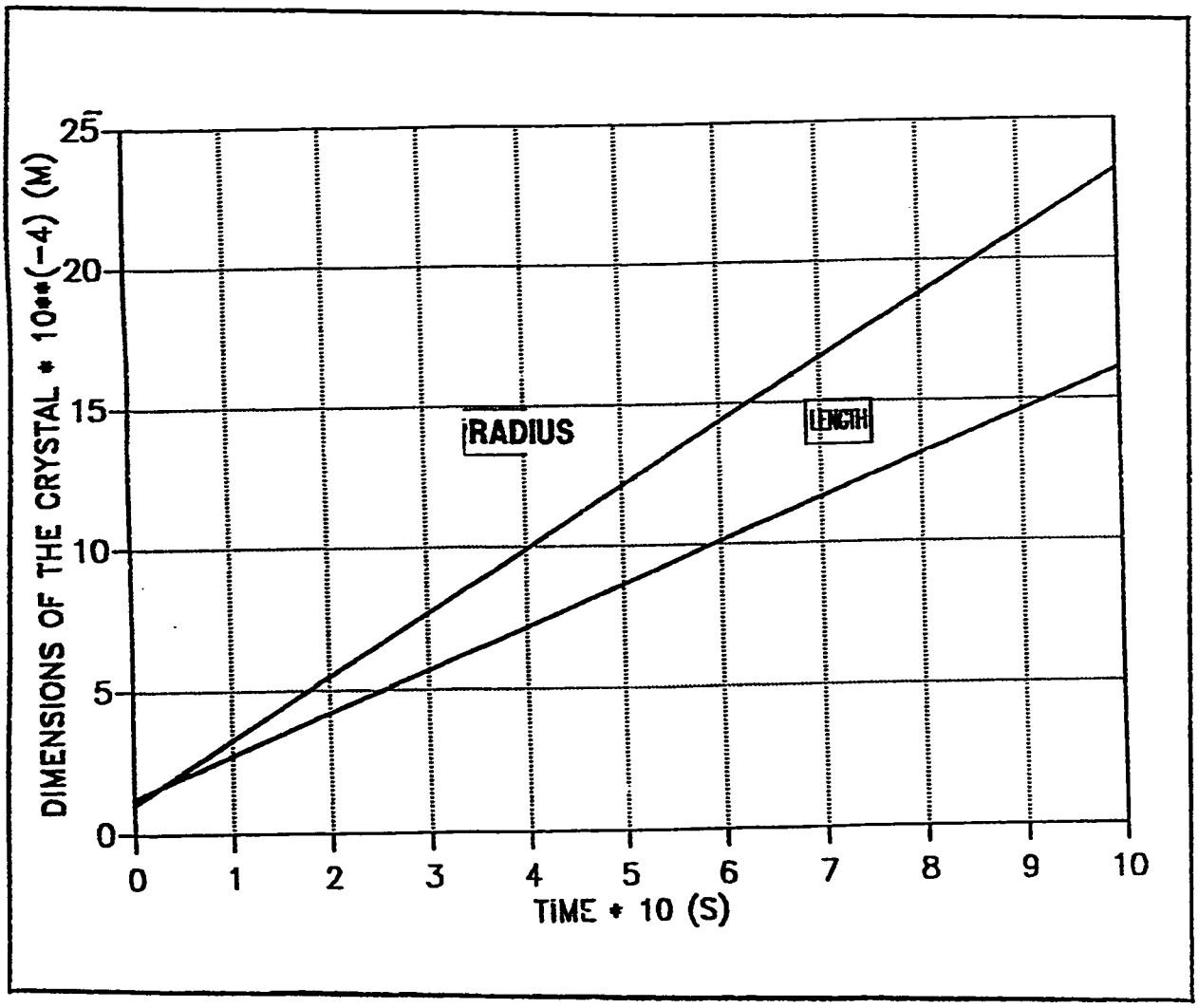

Fig(5.34) Dimensions of the crystal vs. Time

For cylindrical model .

$r_o = 1.2$, $V_{air} = 6\ m/s$

$T_v = 5.0^oC$. $T_s = (-10)^oC$.

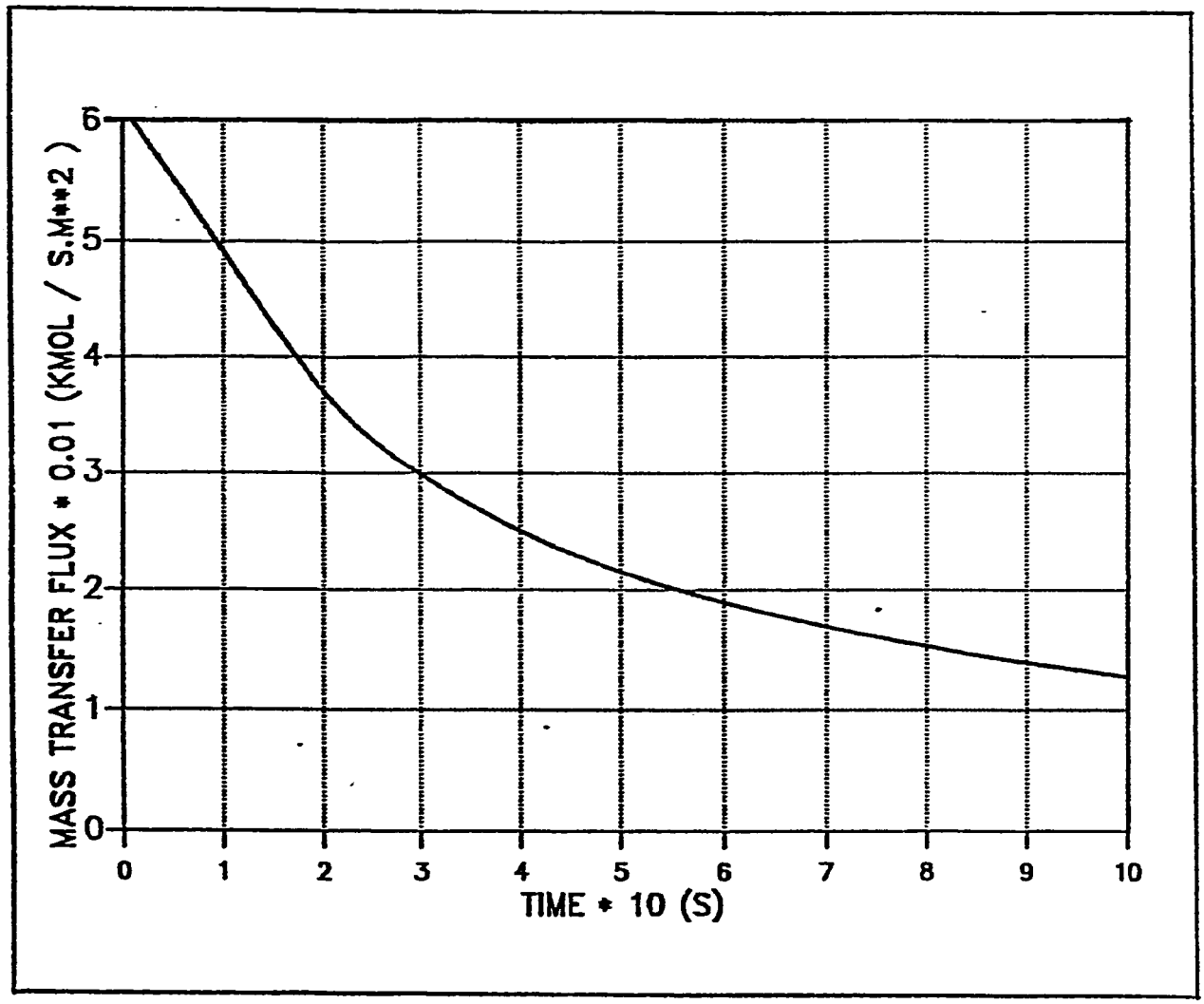

Fig(5.35) Mass transfer flus vs. Time

For cylindrical model.

$r_o = 1.2$, $V_{air} = 6\ m/s$

$T_v = 5.0^{o}C$. $T_s = -10^{o}C$.

5.1.4 Effect Of Initial Ratio

This factor is appearing mainly because of model equations non dimensionalizing so, this is mainly due to model characteristics. It gives a control on the growth of ice crystal in the radial direction. Fig(5.36) and Fig(5.37) shows the temperature distribution in the the ice crystal along it's length and radius. As the length and radius of the crystal is becoming more larger due to higher air velocity Fig(5.38) and Fig(5.3 9) the crystal becomes cooler due to the motion of the boundaries away from the plate of the crystal. Fig(5.40) represents clearly how Γ_o is effecting the radial growth of the crystal. When the crystal is growing in a cluster of crystal the radial growth of the crystal is by the competition occurs between growing crystals. This limits the growth of the crystal in the radial direction. For the model to represent this situation, thier should be some control on the growth in this direction which is provided throw the value of Γ_o. like when there is a large number of ice crystals growing in the same surface, there should be some way to control the radial increase of the crystal because of space limitations, this could be done by controlling the Γ_o

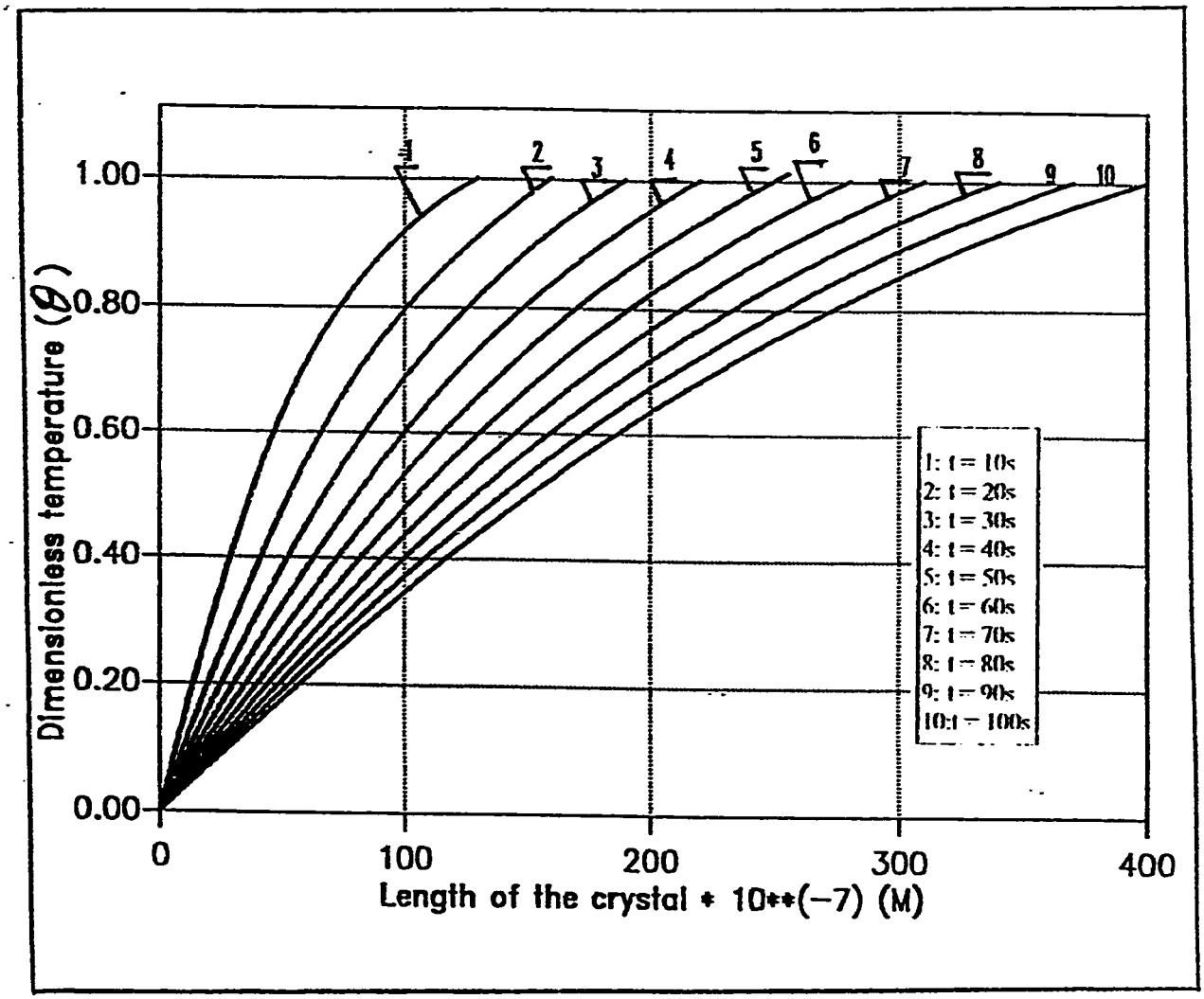

Fig(5.36) Dimensionless temperature vs. length of the crystal. For cylindrical model .

$r_o = 2.0$, $V_{air} = 3\ m/s$

$T_v = 5.0^oC$. , $T_s = (-20)^oC$.

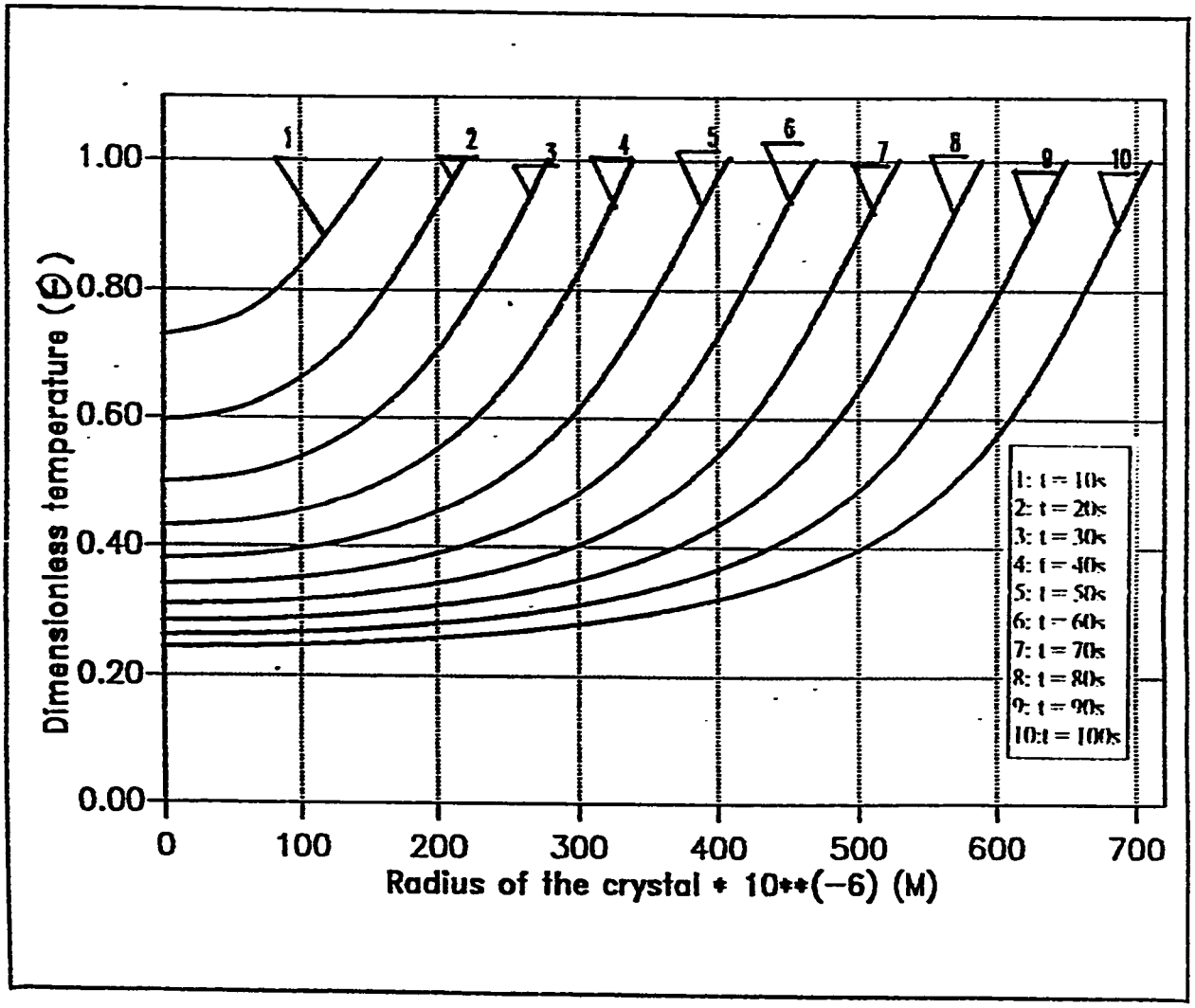

Fig(5.37) Dimensionless temperature vs. raduis of the crystal For cylindrical model.

$r_o = 2.0$, $V_{air} = 3\ m/s$

$T_v = 5.0^{\circ}C$. $T_s = (-10)^{\circ}C$.

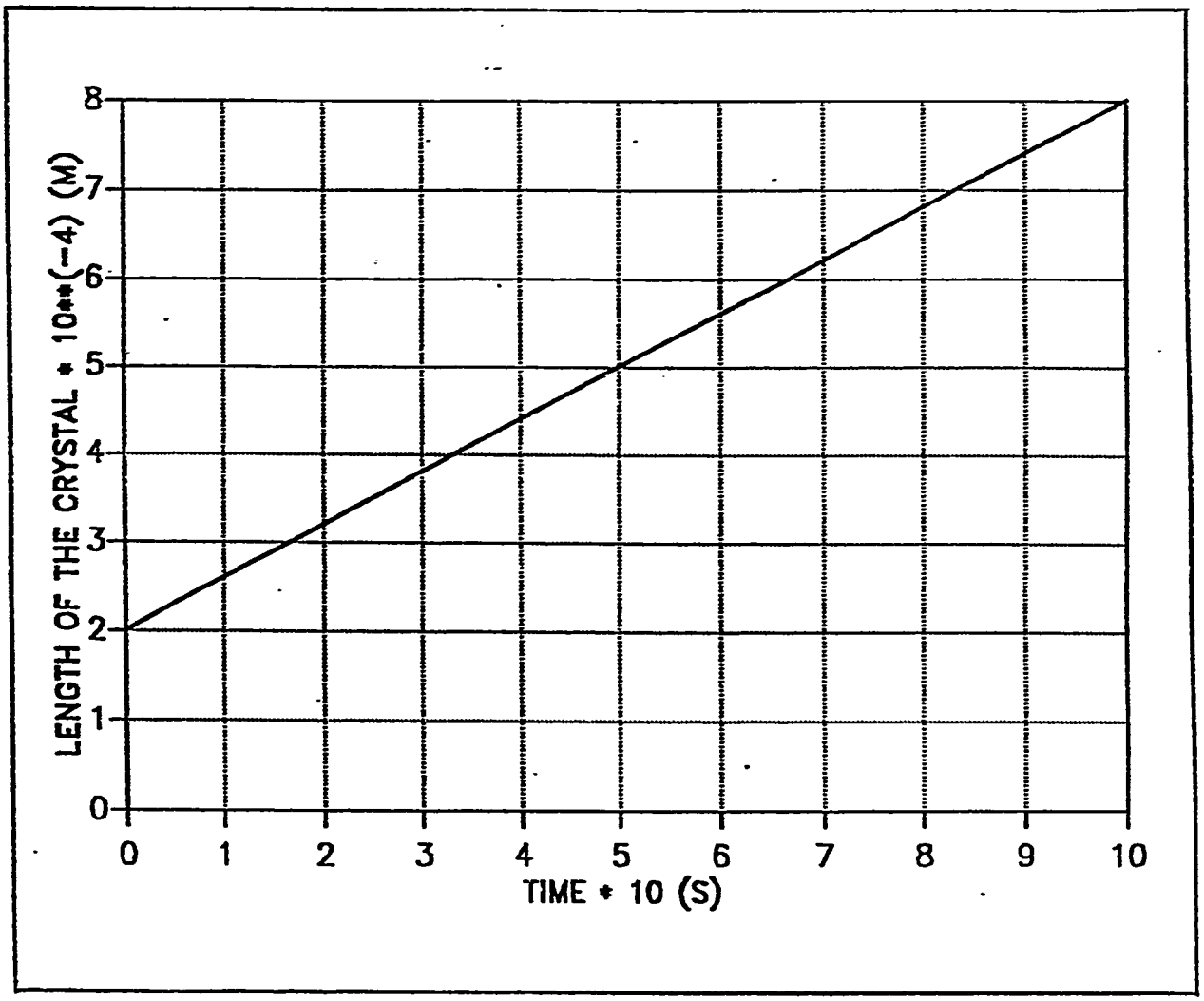

Fig(5.38) Length of the crystal vs. Time

For cylindrical model .

$r_o = 2.0$, $V_{air} = 3\ m/s$

$T_v = 5.0^oC$. $T_s = (-10)^oC$.

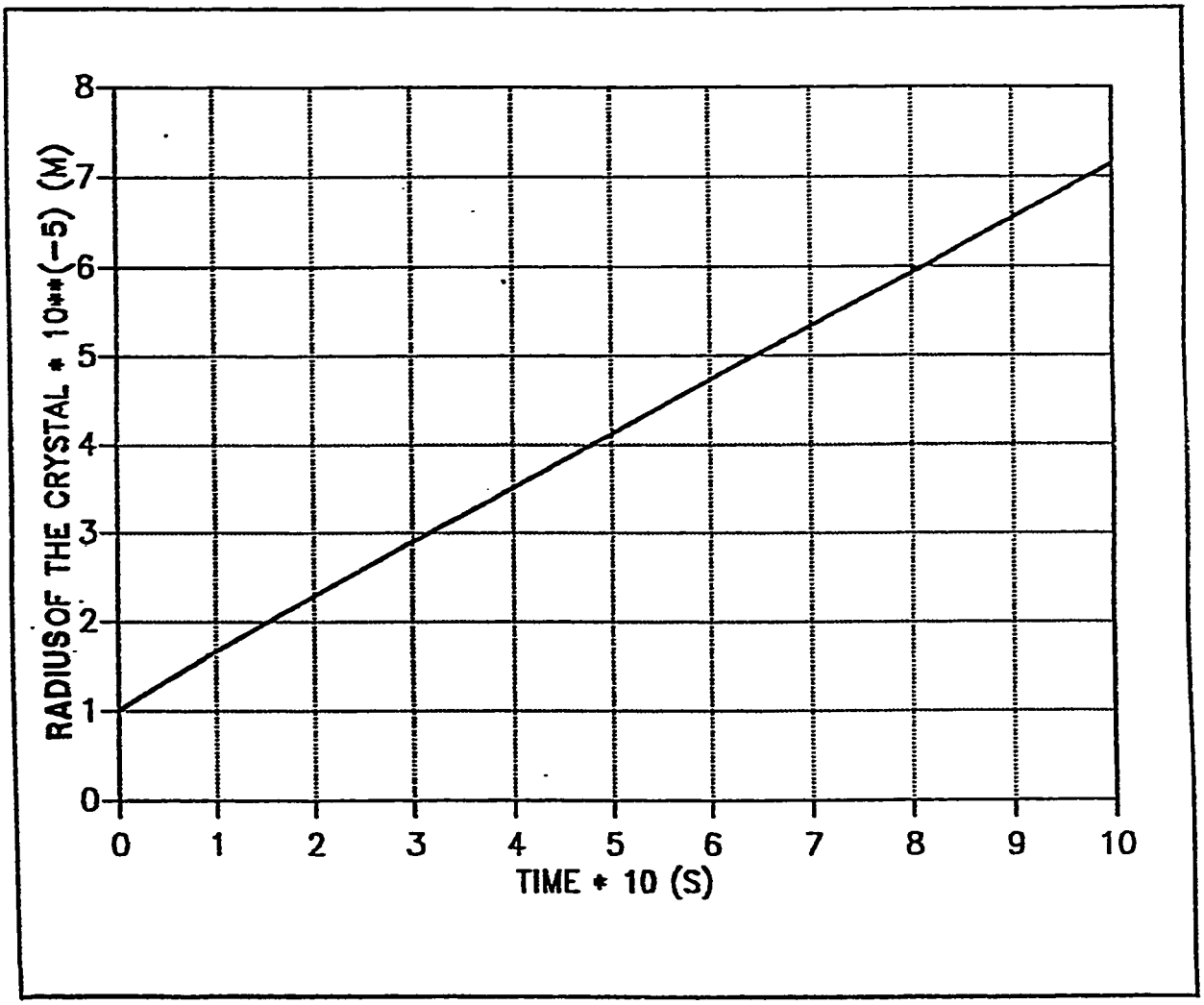

Fig(5.39) Radius of the crystal vs. Time

For cylindrical model .

$r_o = 2.0$, $V_{air} = 3\ m/s$

$T_v = 5.0^oC$. $T_s = (-10)^oC$.

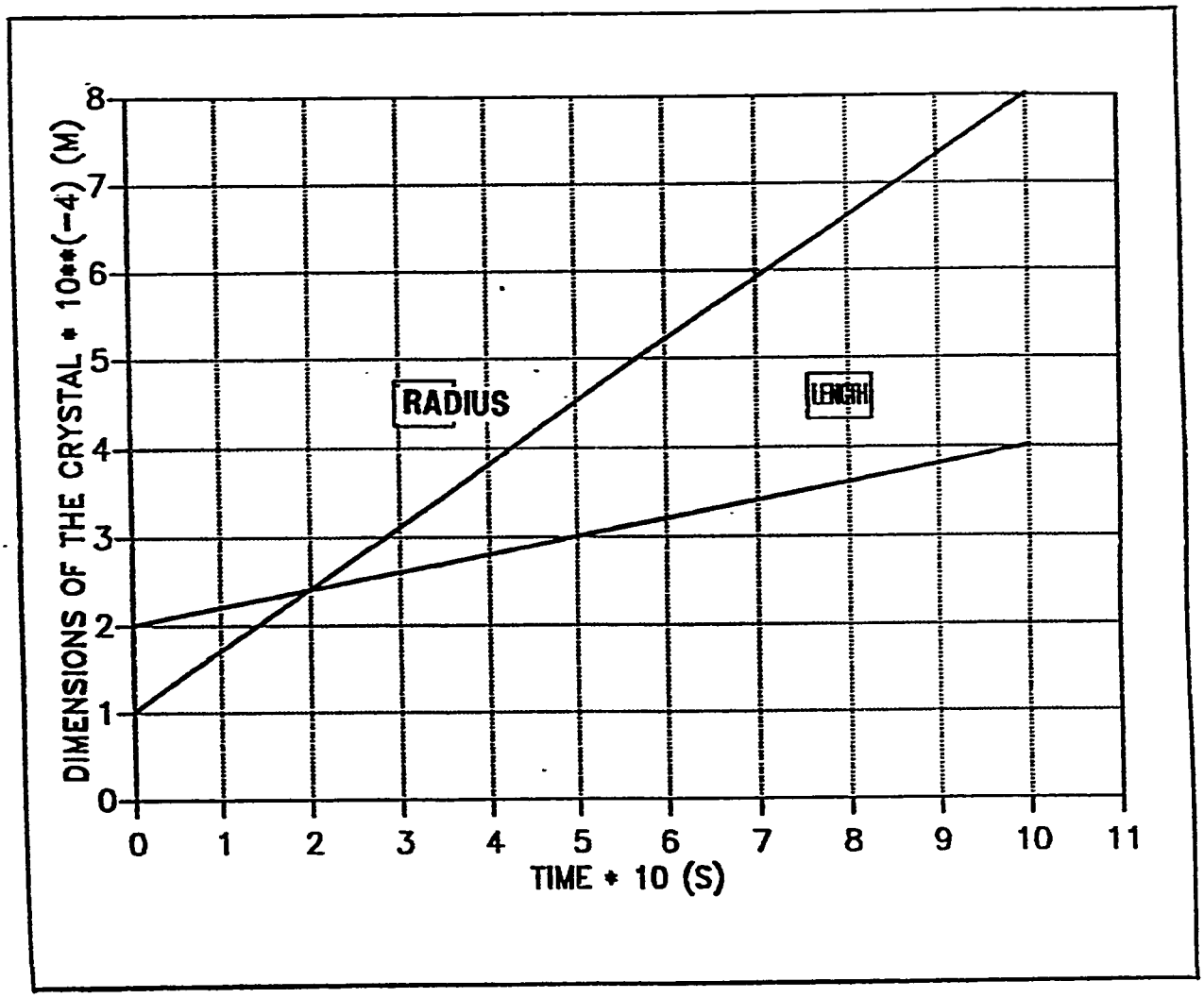

Fig(5.40) Dimensions of the crystal vs. Time

For cylindrical model .

$r_o = 2.0$, $V_{air} = 3\ m/s$

$T_v = 5.0^oC$. $T_s = (-10)^oC$.

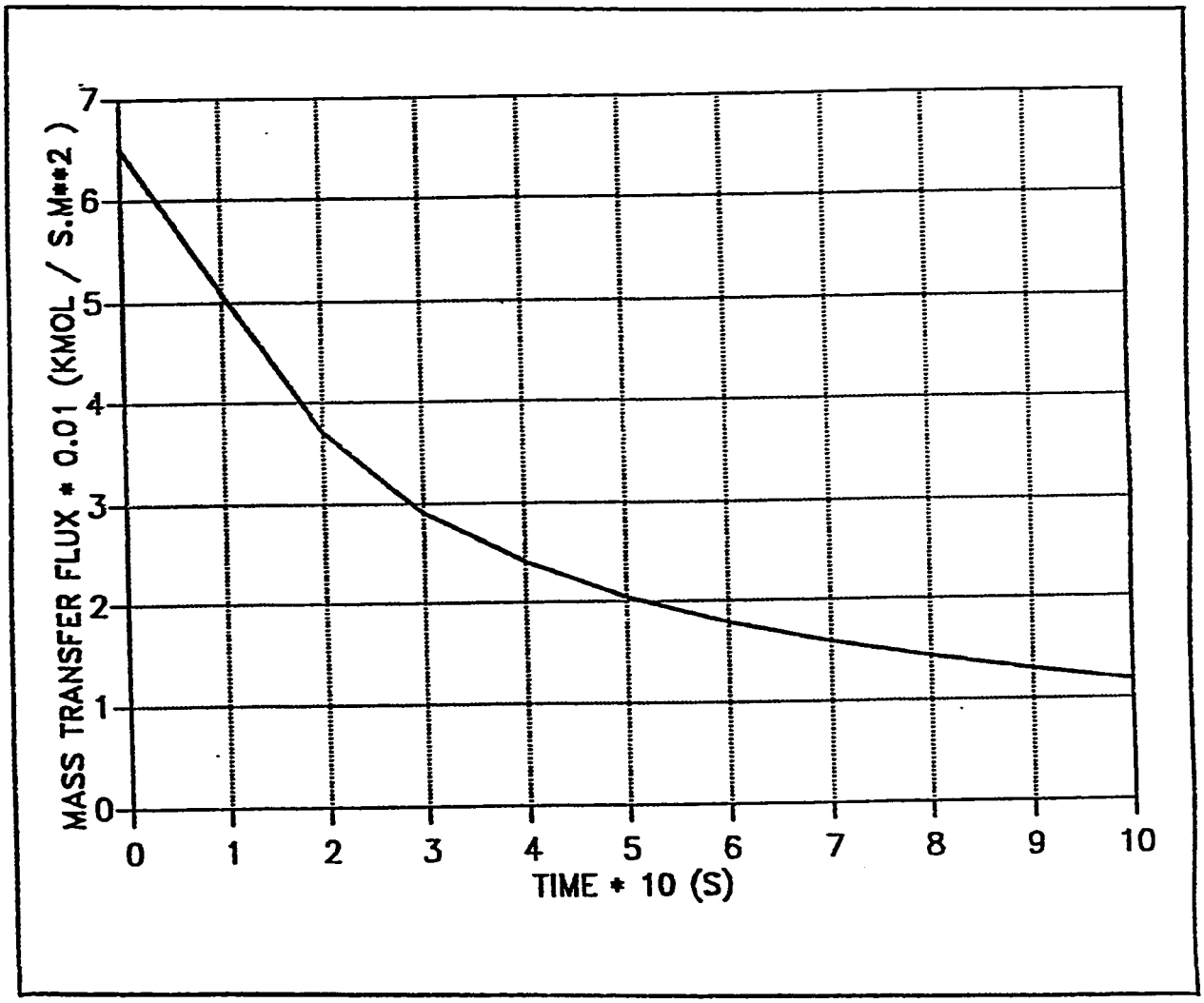

Fig(5.41) Mass transfer flus vs. Time

For cylindrical model.

$r_o = 2.0$, $V_{air} = 3\ m/s$

$T_v = 5.0^{o}C$. $T_s = (-10)^{o}C$.

5.2 Spherical Model

In this model the ice crystal is assumed to grow in hemispherical shape where the height of the crystal is assumed to be R and the base of the crystal is assumed to be (2R) and by this mode the ice crystal is assumed to grow radially and equally with

5.2.1 Effect Of Ambient Temperature

One of the factors that effect the ice crystals growth is the temperature of air-water vapour mixture, since the deposition of water molecules into the crystal is occurring from this temperature. From Fig(5.E)it is very clear that as the ambient temperature is becoming higher the radius of the crystal is also becoming higher . The reasons for this is that the temperature gradient in the boundary layer is greater and therefore the development of ice crystals and phase change of water molecules is faster. As a matter of fact, water molecules passing through the boundary layer encounter a temperature gradient and arrive at the surface of the crystal to take their places in the ice crystal lattice. For small temperature gradients, which means less difference in temperature between the surface temperature and the ambient air temperature more time is required for the development of ice crystals, but for the case of higher temperature gradient less time is required to develop big ice crystals. The radius of the crystal is also effected in the same manner so as the ambient temperature is becoming higher the radius of the crystal is also increasing due to the same reasons mentioned previously. It is also very clear from the figures representing

both the radius and length of the crystal versus time that the crystal is growing in plate like structure . Temperature distributions along the X direction of the crystal is shown in Fig (5.42). It is very clear that as the radius of the crystal is increasing a new temperature distribution is occurring. It is concluded that as the boundary conditions are moving away from the center of the crystal the temperature in the crystal is decreasing with time. Fig(5.43) shows the change of the radius of the crystal with time. The change is linear with the ice crystal growing in radius from 100 μm to 530 μm in 100 seconds. to be equal to one . Fig(5.44) represents the variation of mass flux with time. It is shown that the mass flux inside the ice crystal is decreasing wit time, this implies that their is a variation in the density of the crystal as the crystal is growing but due to the shortage of information about the variation of the density of ice crystals with time, a constant ice crystal density is assumed which is causing a source of error in the model.

In the second case to show the effect of increasing the ambient temperature this temperature is increased in the model up to $7.5°C$. Fig(5.45) the temperature distribution in the crystal along X . The crystal is becoming cooler as it's radius increases due to higher ambient temperature as in Fig(5.46). The density of the ice crystal at higher ambient temperature is becoming lower, due to lower mass flux effect Fig(5.47) the previous discussed behavior of the model variation of ambient temperature is satisfied by the work done by Schneider (1977) where he studied the frost formation process and found that as the ambient temperature increases the frost layer is becoming higher which means the formation of higher ice crystals .

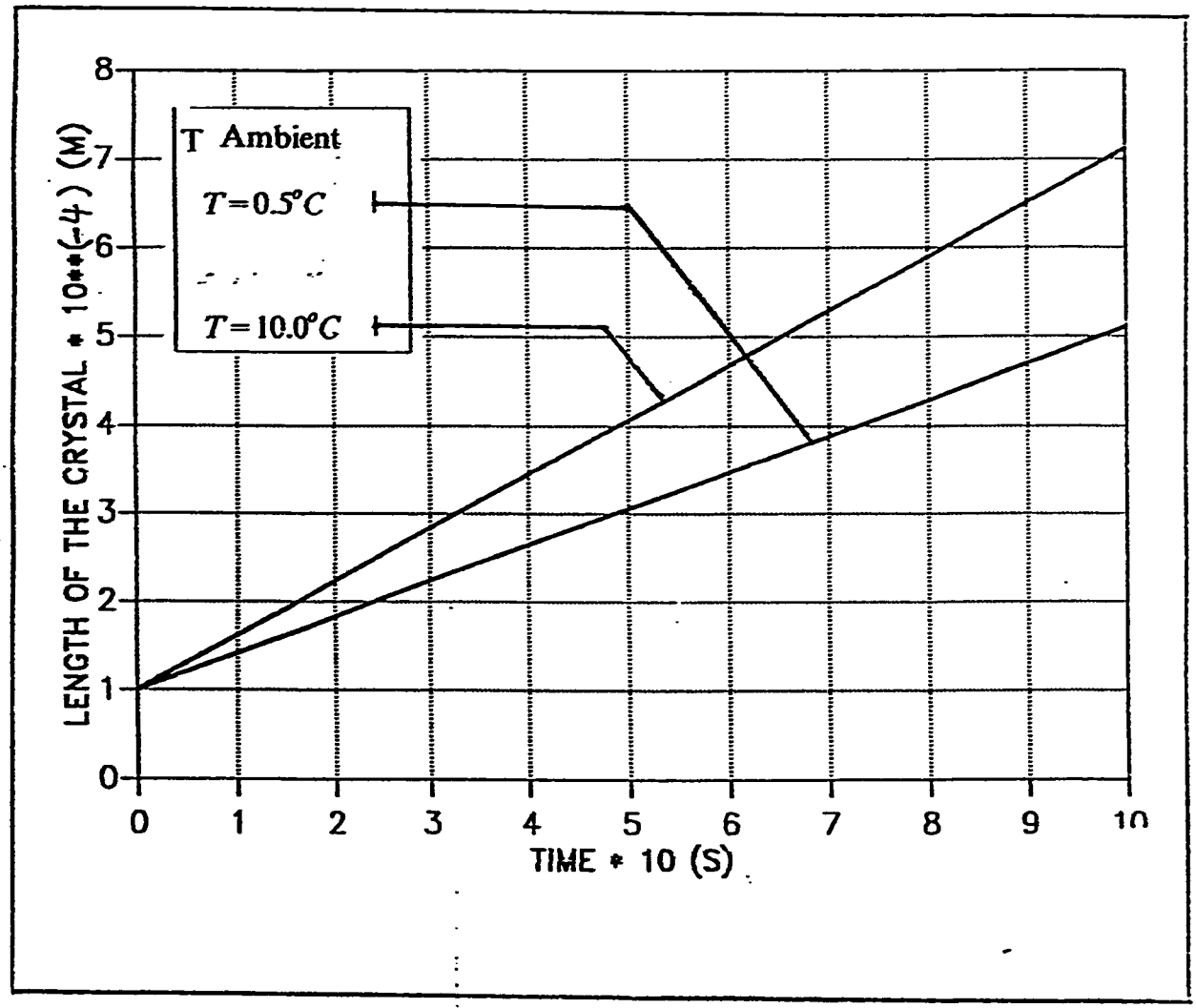

Fig(5.D) Length of the crystal vs. Time for different ambient temperatures

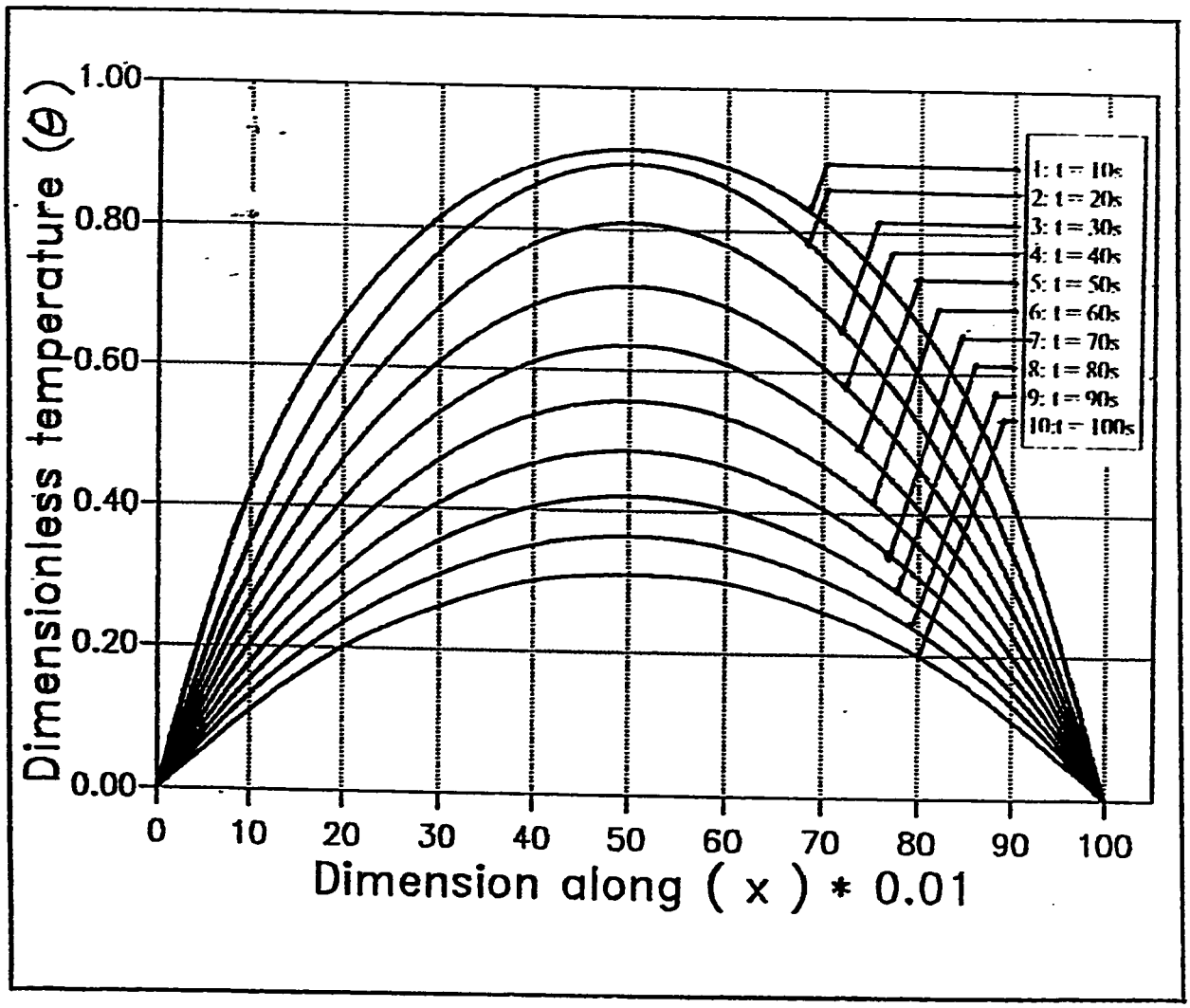

Fig(5.42) Dimensionless temperature vs. X .
For spherical model .
$r_o = 1.0$, $V_{air} = 2\ m/s$

$T_v = 5.0^oC$. , $T_s = (-10)^oC$

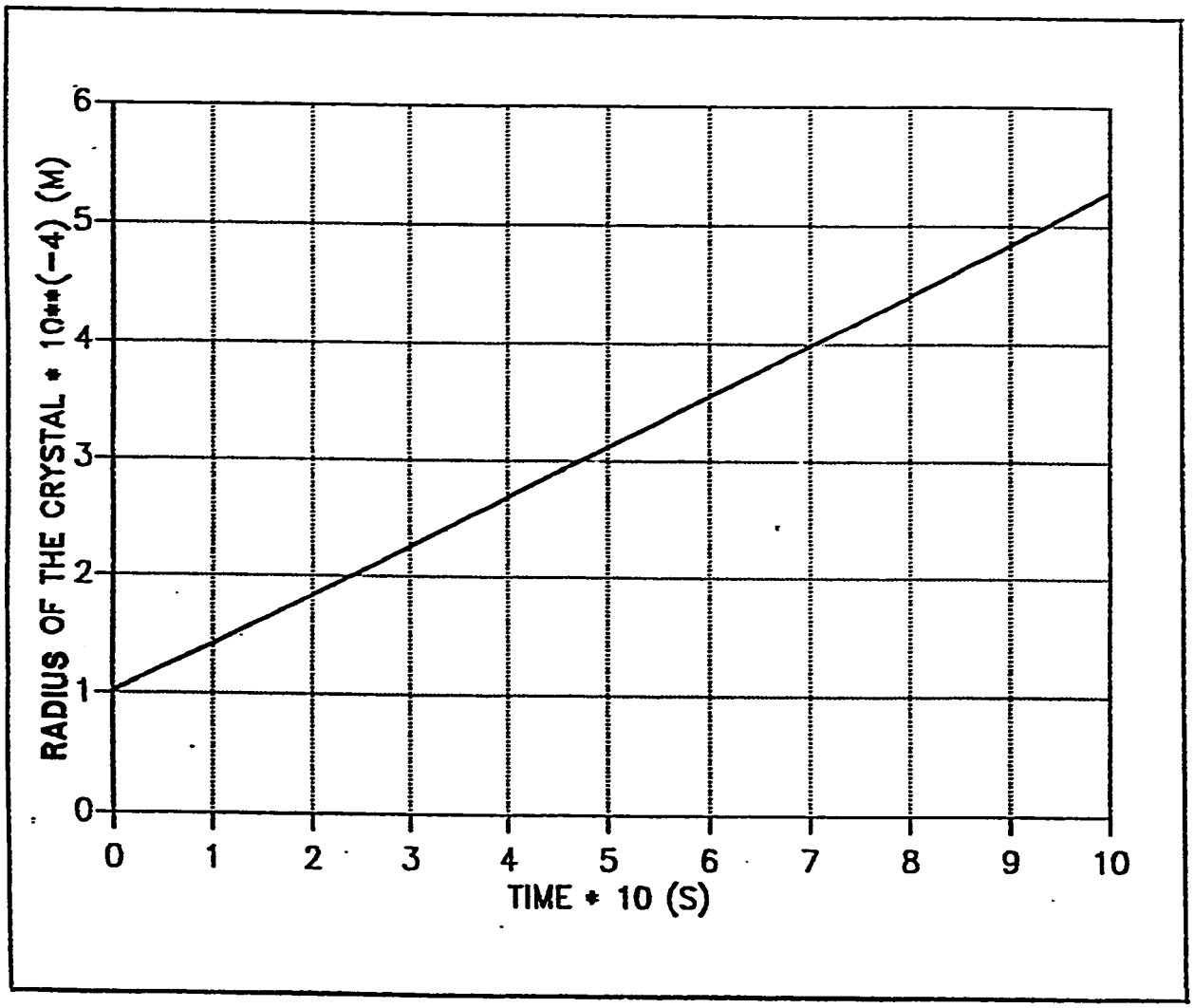

Fig(5.43) Radius of the crystal vs. Time
For spherical model.

$r_o = 1.0$, $V_{air} = 2\ m/s$

$T_v = 5.0^oC$. , $T_s = (-10)^oC$

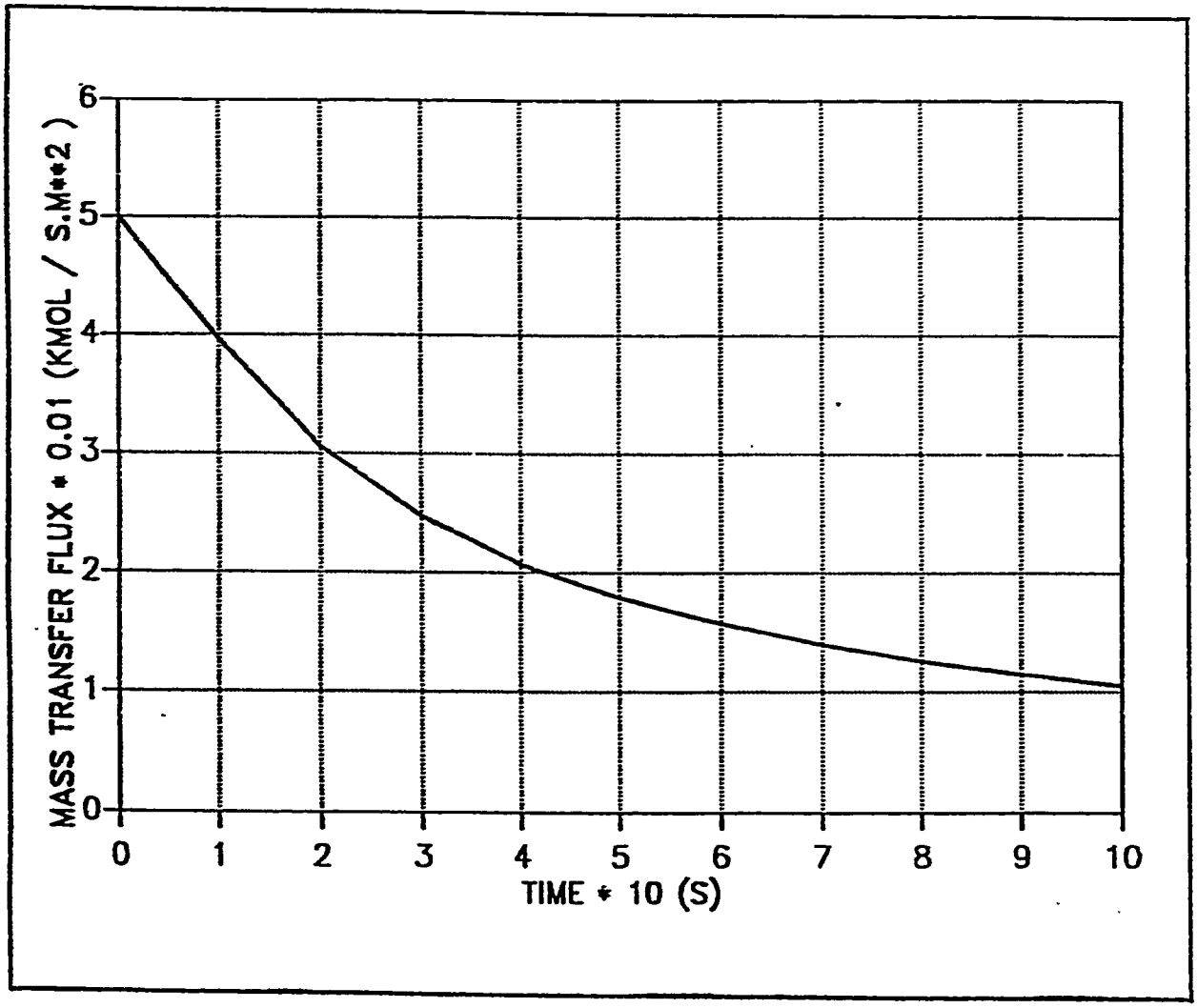

Fig(5.44) Mass transfer flus vs. Time
For spherical model.

$r_o = 1.0$, $V_{air} = 2\ m/s$

$T_v = 5.0^oC$. , $T_s = (-10)^oC$

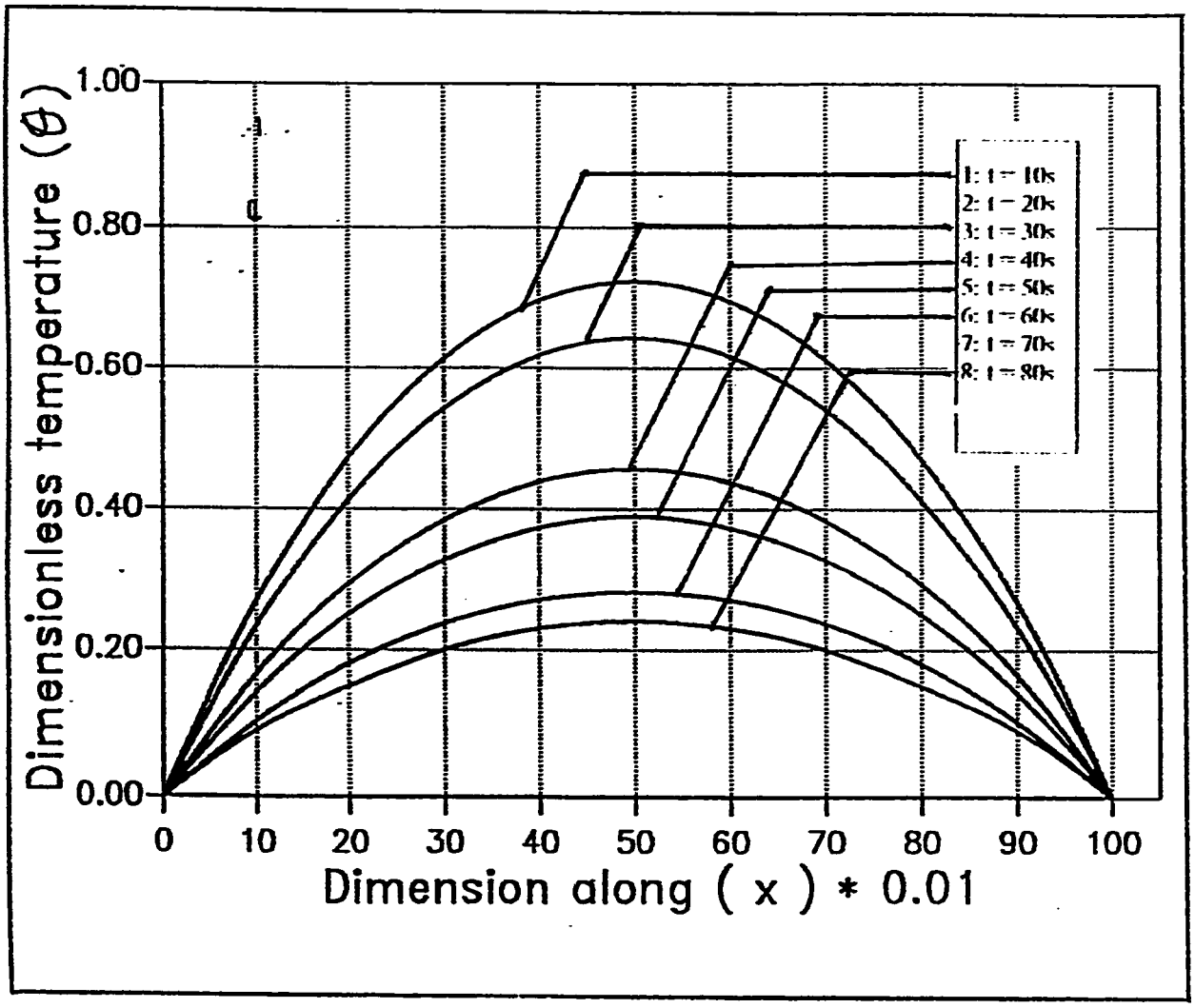

Fig(5.45) Dimensionless temperature vs. X .
For spherical model .
$r_o = 1.0$, $V_{air} = 2\ m/s$

$T_v = 7.5^oC$. , $T_s = (-10)^oC$

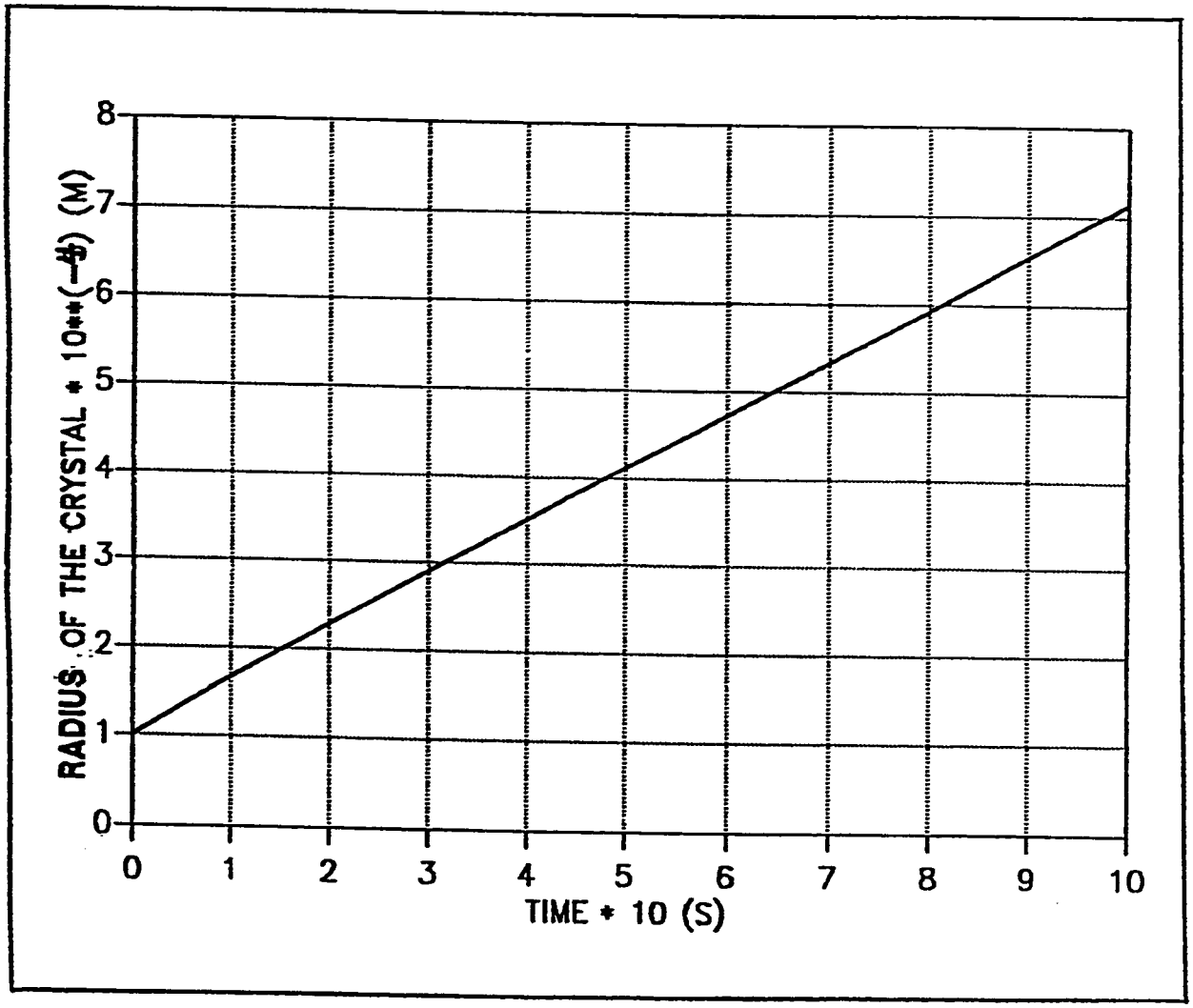

Fig(5.46) Radius of the crystal vs. Time
For spherical model.

$r_o = 1.0$, $V_{air} = 2\ m/s$

$T_v = 7.5^oC$. , $T_s = (-10)^oC$

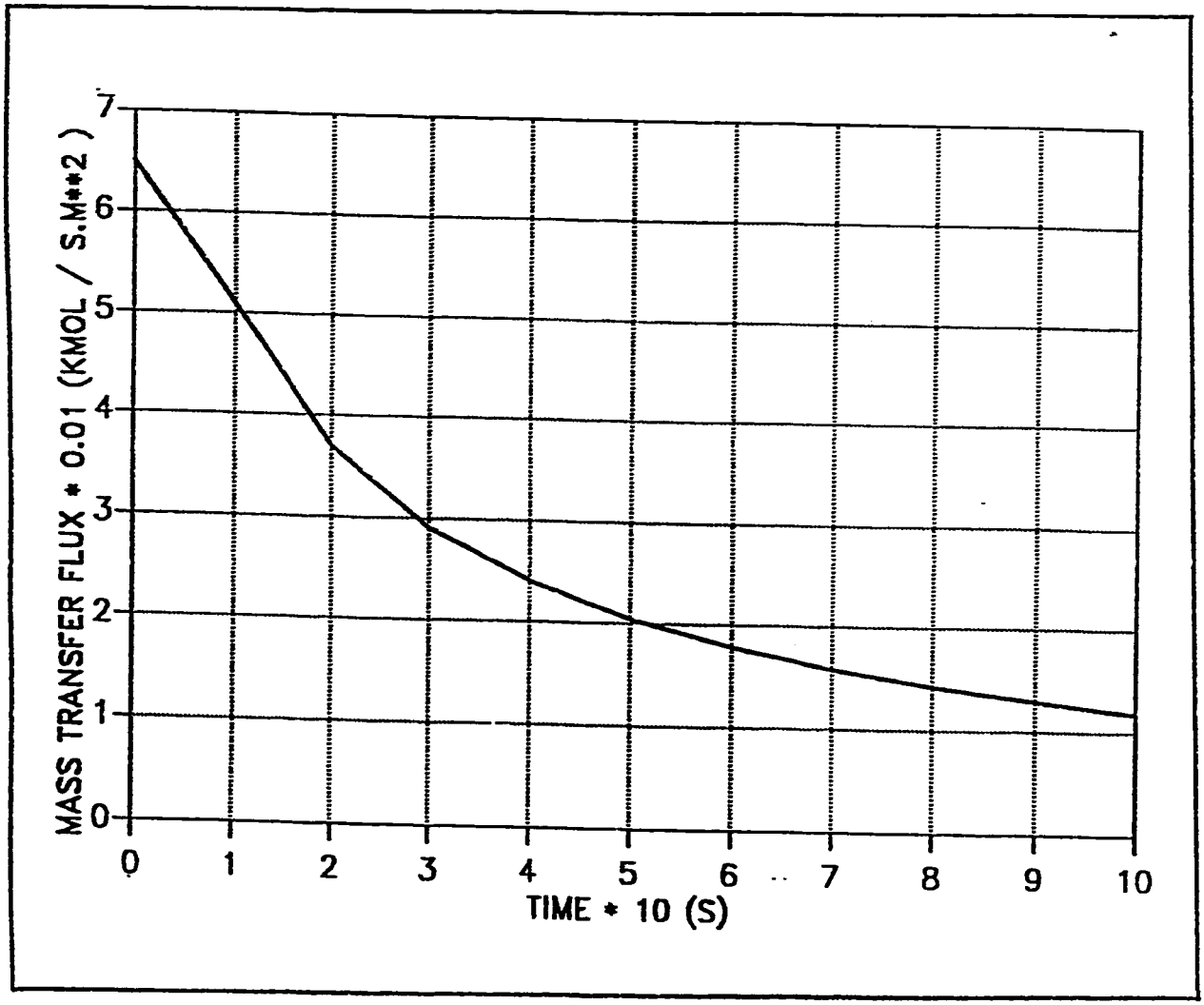

Fig(5.47): Mass transfer flus vs. Time
For spherical model.

$r_o = 1.0$, $V_{air} = 2\ m/s$

$T_v = 7.5^{o}C$. , $T_s = (-10)^{o}C$..

5.2.2 Effect Of Plate Temperature

Another important factor that effect the growth of ice crystals the temperature of the surface over which the crystal grows From Fig(5.F)it is very clear that as the plate temperature becomes lower the radius of the crystal becomes higher . The reasons for this is that the temperature gradient in the boundary layer is greater and therefore the development of ice crystals and phase change of water molecules is faster. As a matter of fact, water molecules passing through the boundary layer encounter a temperature gradient and arrive at the surface of the crystal to take their places in the ice crystal lattice. For small temperature gradients, which means less difference in temperature between the surface temperature and the ambient air temperature more time is required for the development of ice crystals, but for the case of higher temperature gradient less time is required to develop big ice crystals. The radius of the crystal is also effected in the same manner so as the ambient temperature is becoming higher the radius of the crystal is also increasing due to the same reasons mentioned previously. It is also very clear from the figures representing the radius of the crystal versus time that the crystal is growing in plate like structure .

In this case to show the effect of decreasing the plate temperature this temperature is decreased in the model down to $-20°C$. Fig(5.47) the temperature distribution in the crystal along X . The crystal is becoming cooler as it's radius increases due to lower plate temperature as in Fig(5.48). The density of the ice crystal at lower plate temperature is becoming lower, due to

lower mass flux effect Fig(5.49)

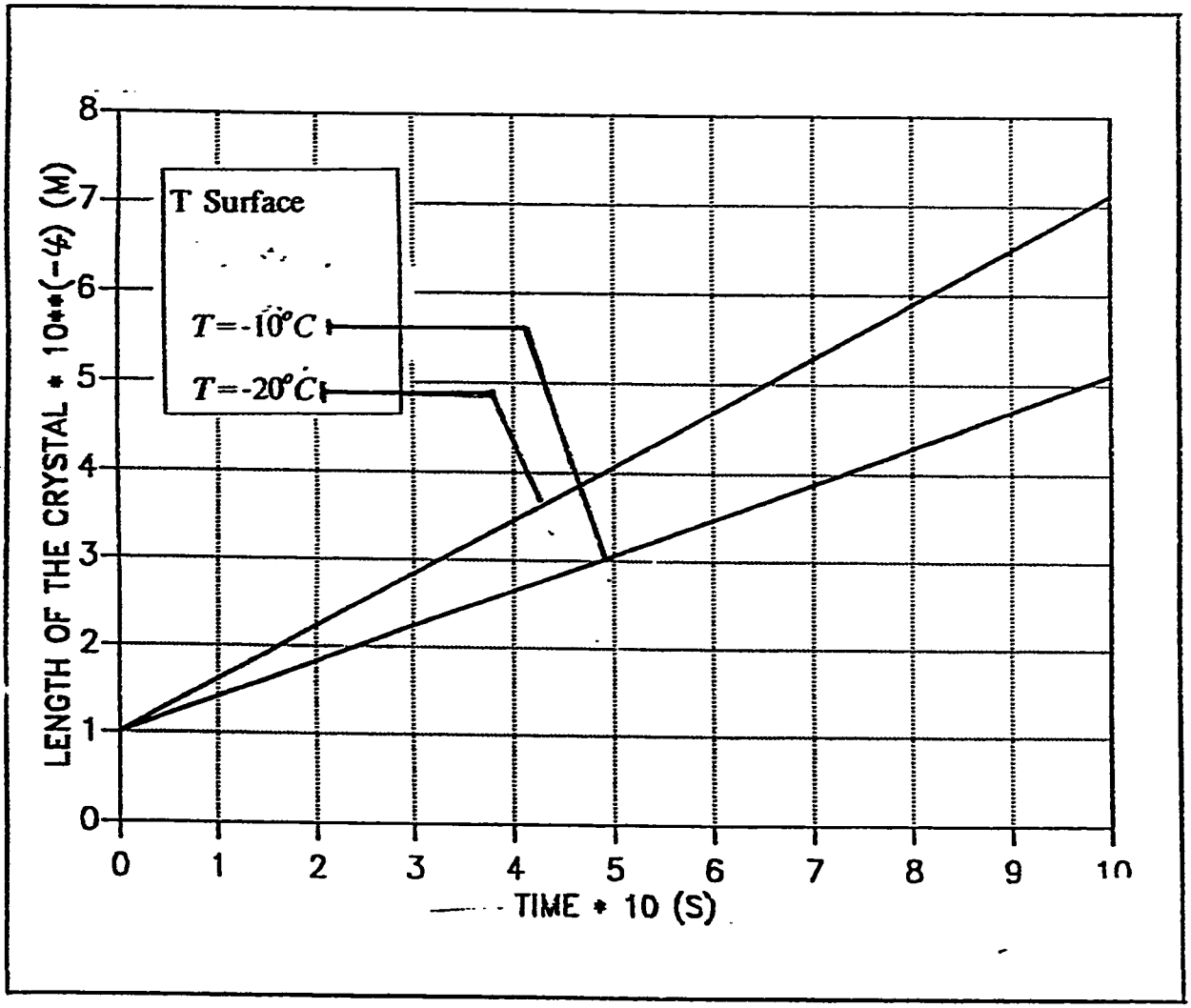

Fig(5.E) Length of the crystal vs. Time for different surface temperatures.

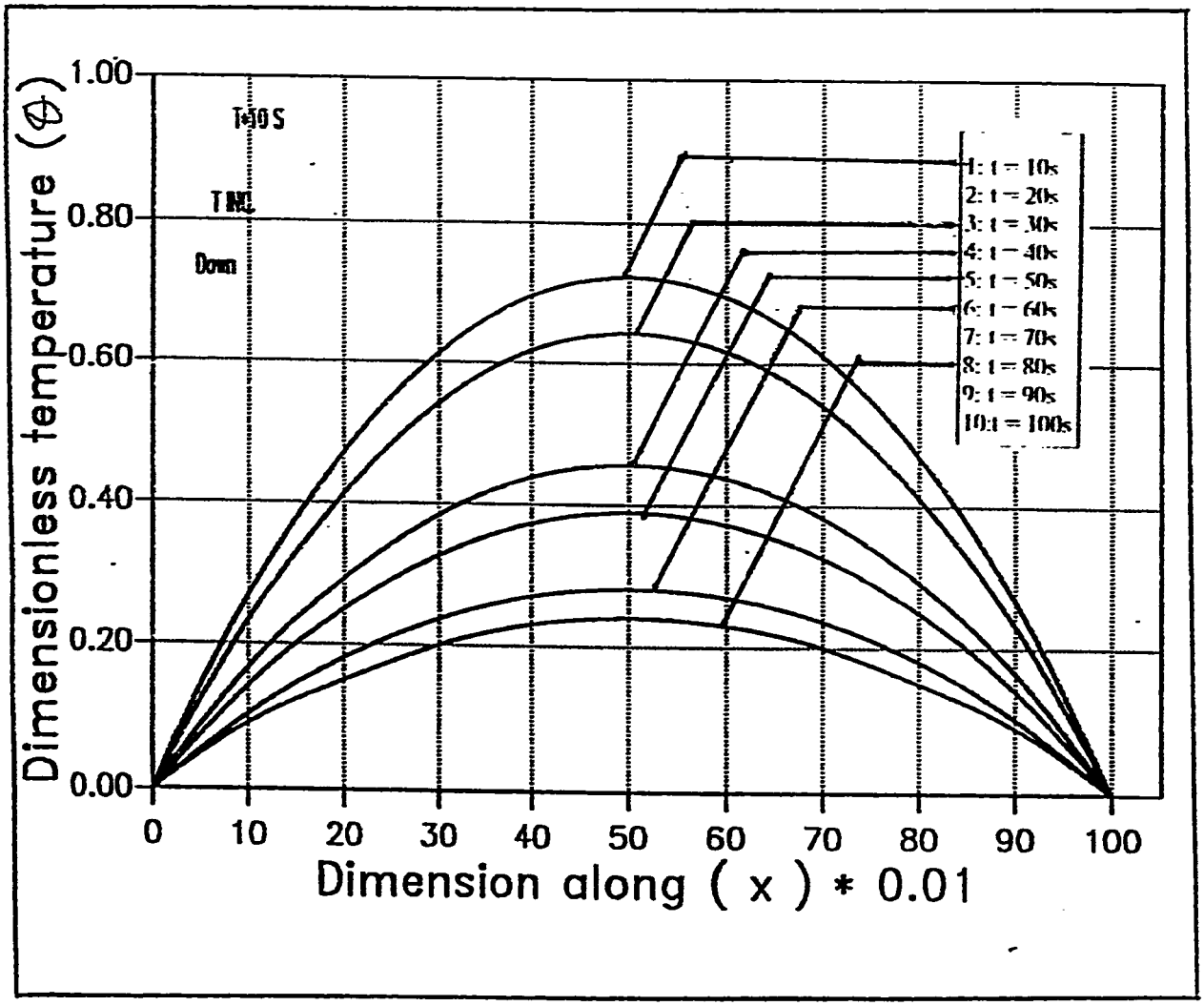

Fig(5.48) Dimensionless temperature vs. X .
For spherical model .
$r_o = 1.0$, $V_{air} = 2\ m/s$

$T_v = 5.0^oC$. , $T_s = (-20)^oC$

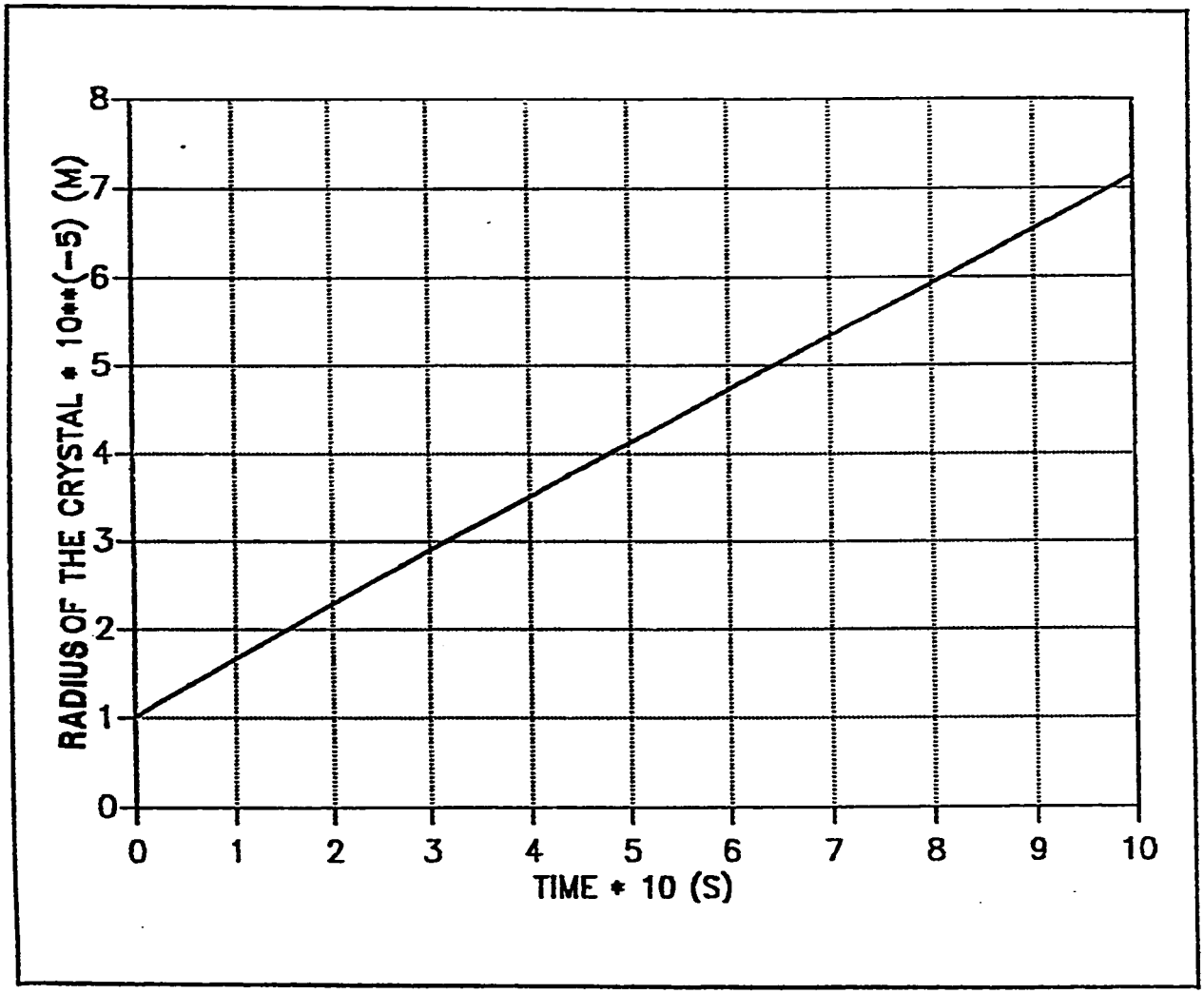

Fig(5.49) Radius of the crystal vs. Time
For spherical model.

$r_o = 1.0$, $V_{air} = 2\ m/s$

$T_v = 5.0^oC$. , $T_s = (-20)^oC$

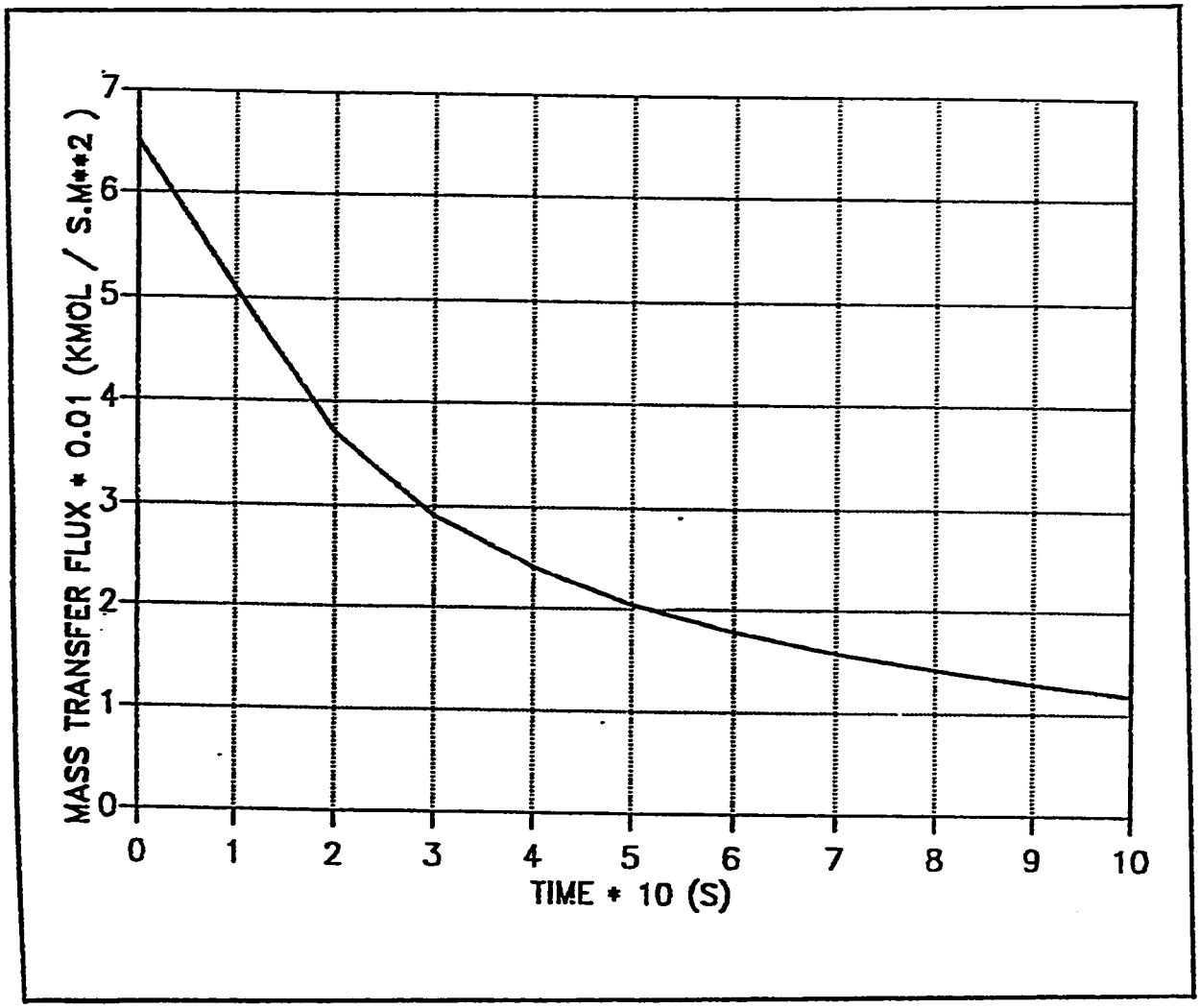

Fig(5.50) : Mass transfer flus vs. Time

For spherical model.

$r_o = 1.0$, $V_{air} = 2\ m/s$

$T_v = 5.0^oC$. , $T_s = (-20)^oC$.

5.2.3 Effect Of Air Velocity

The air velocity's effect on ice crystal radius in noticeable, due to the same reason as mentioned in sec (5.1.3) . Temperature distribution is shown in Fig(5.50) with the (X) direction. Comparing this distribution with that in Fig(5.42) shows that the crystal is cooler in this higher air velocity. This is mainly due to the increase in the radius of the crystal Fig(5.51) when compared with the case of lower air velocity as in the case of Fig(5.43). The change in the mass flux with time is shown in Fig(5.52) where it is very clear that as the air velocity is higher the mass flux decreases with time . This is shown very clearly in fig (5.84), (5.88).

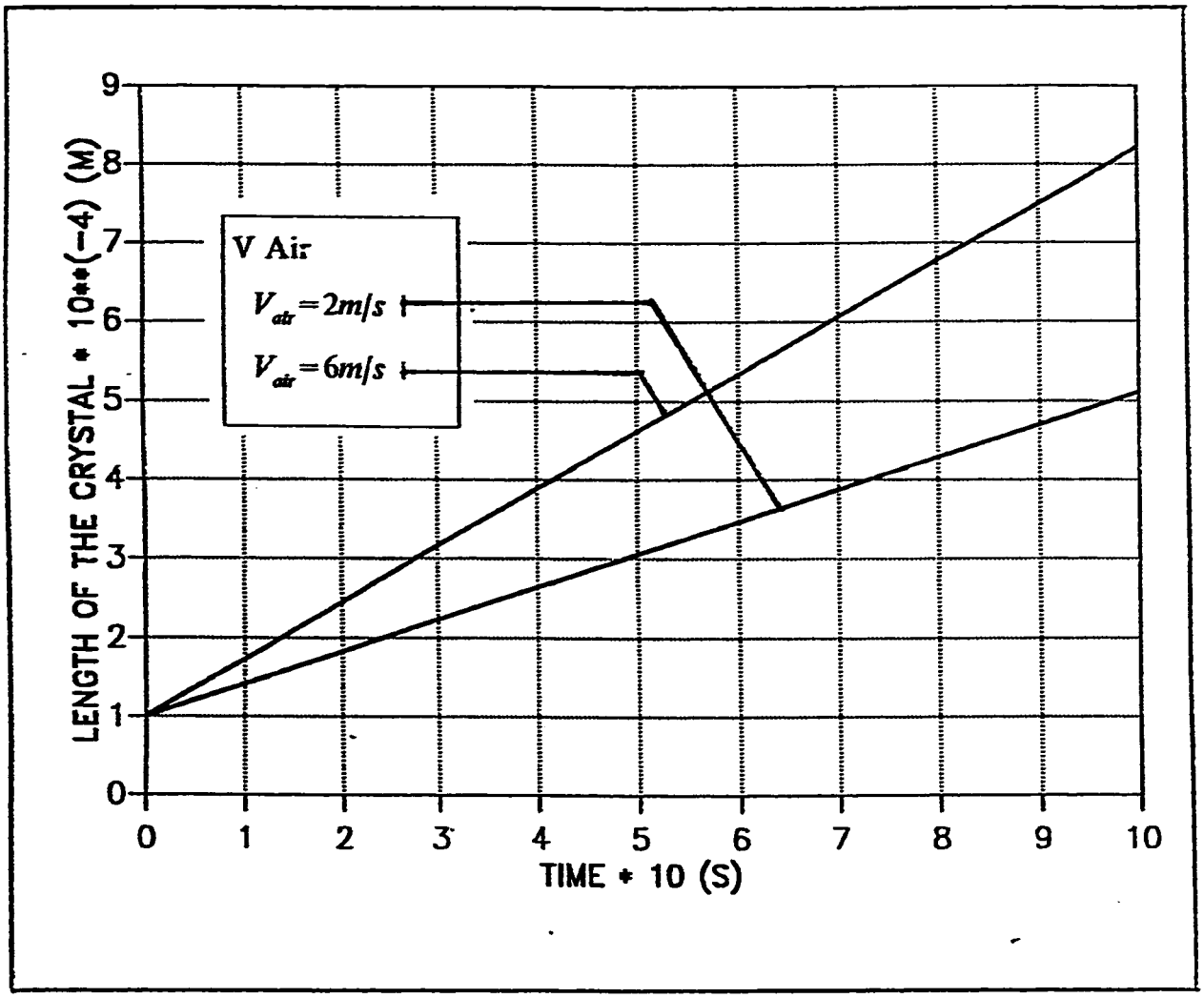

Fig(5.F) Length of the crystal vs. Time for different air velocities

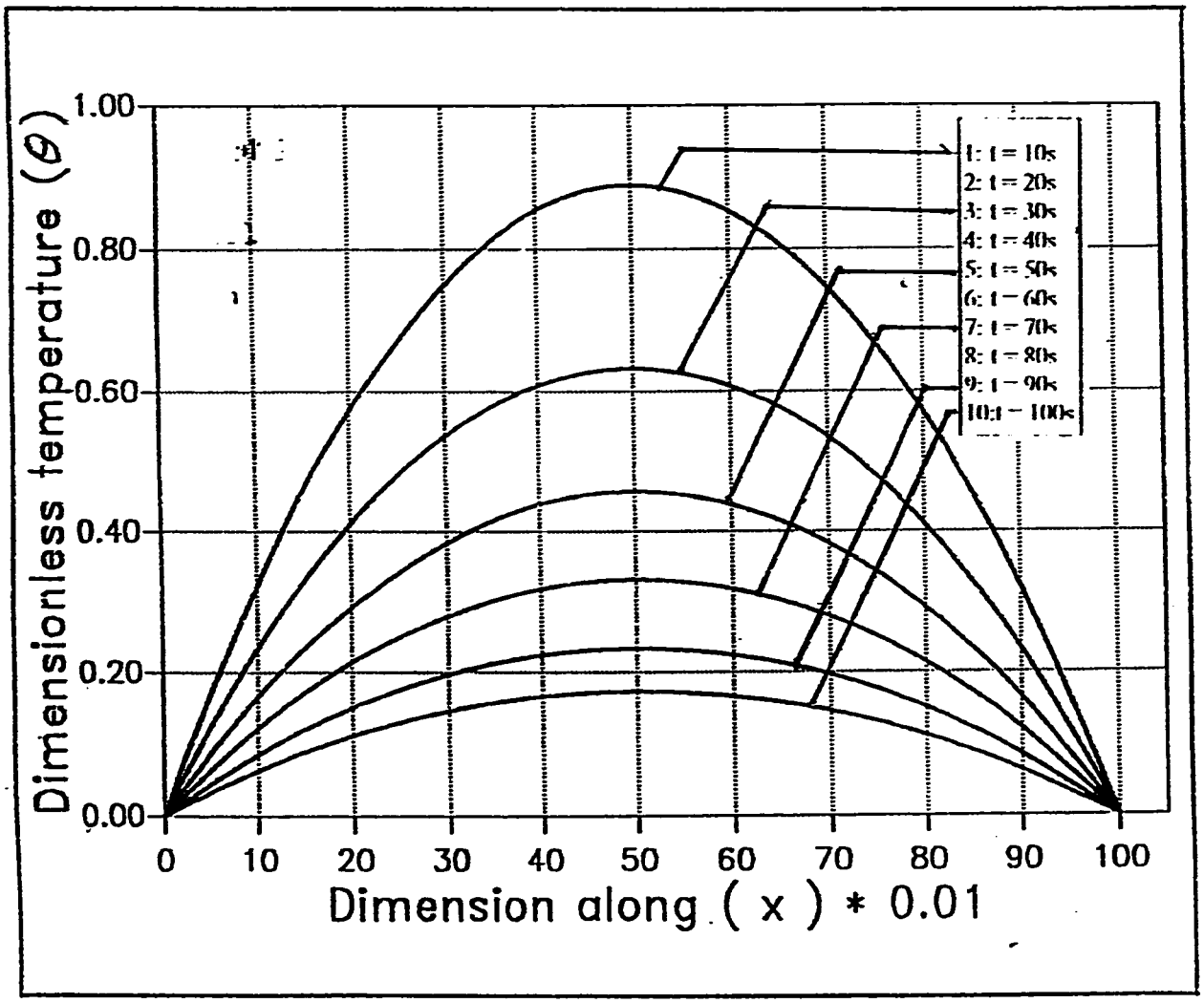

Fig(5.51) Dimensionless temperature vs. X .
For spherical model .
$r_o = 1.0$, $V_{air} = 4\ m/s$

$T_v = 5.0^oC$. , $T_s = (-10)^oC$

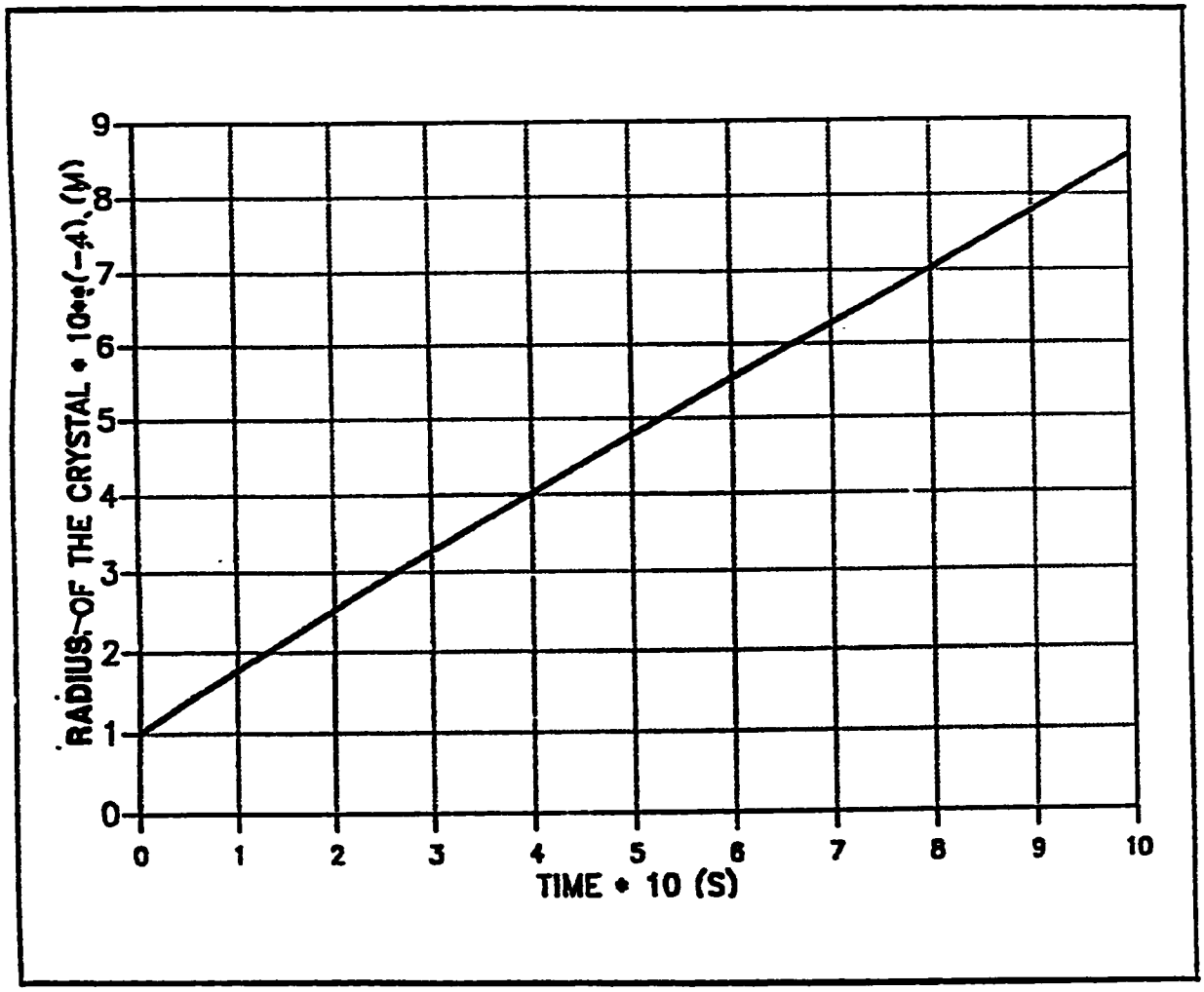

Fig(5.52) Radius of the crystal vs. Time

For spherical model.

$r_o = 1.0$, $V_{air} = 4\ m/s$

$T_v = 5.0^oC$. , $T_s = (-10)^oC$

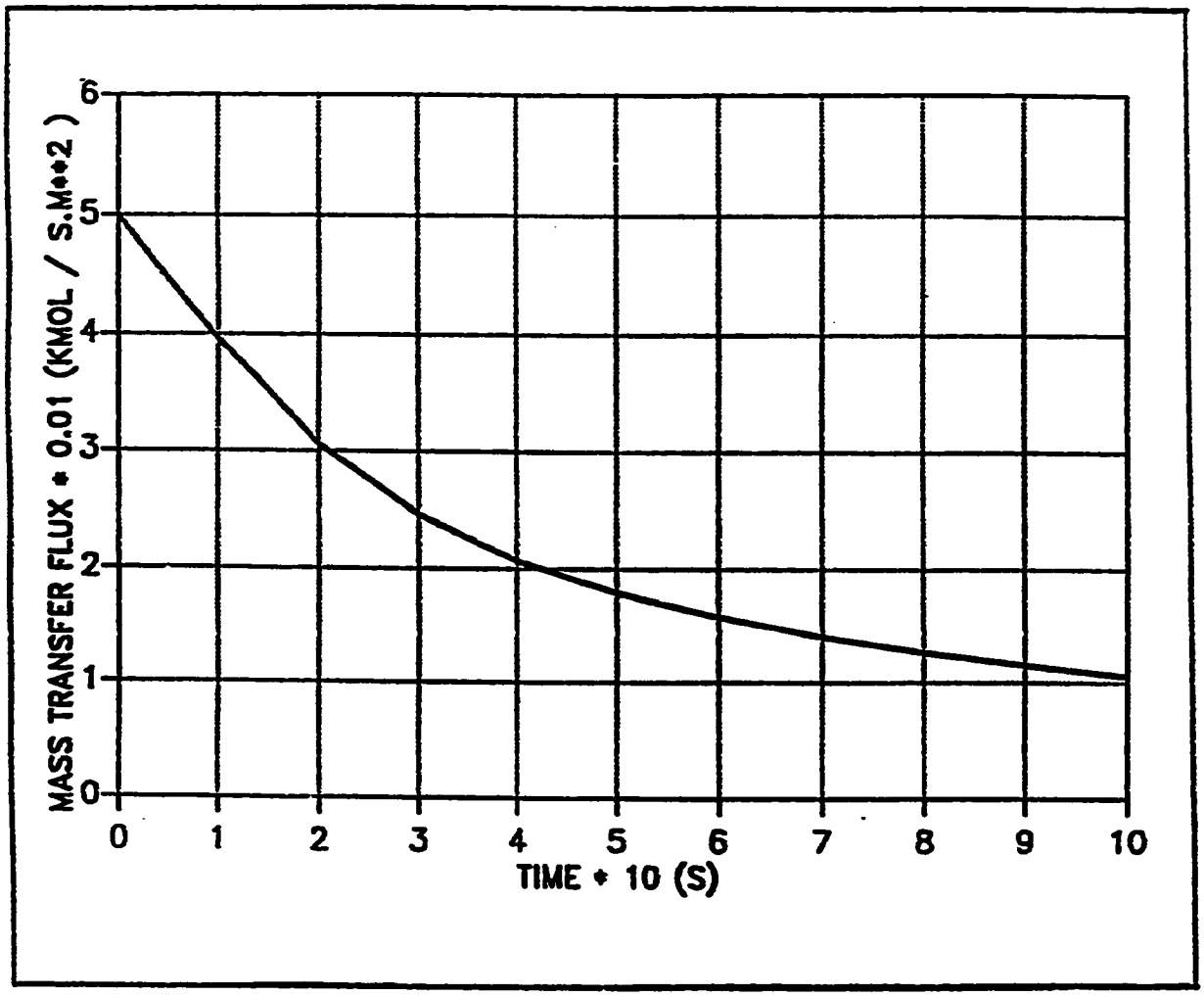

Fig(5.53) Mass transfer flus vs. Time

For spherical model.

$r_o = 1.0$, $V_{air} = 4\ m/s$

$T_v = 5.0^oC$, $T_s = (-10)^oC$.

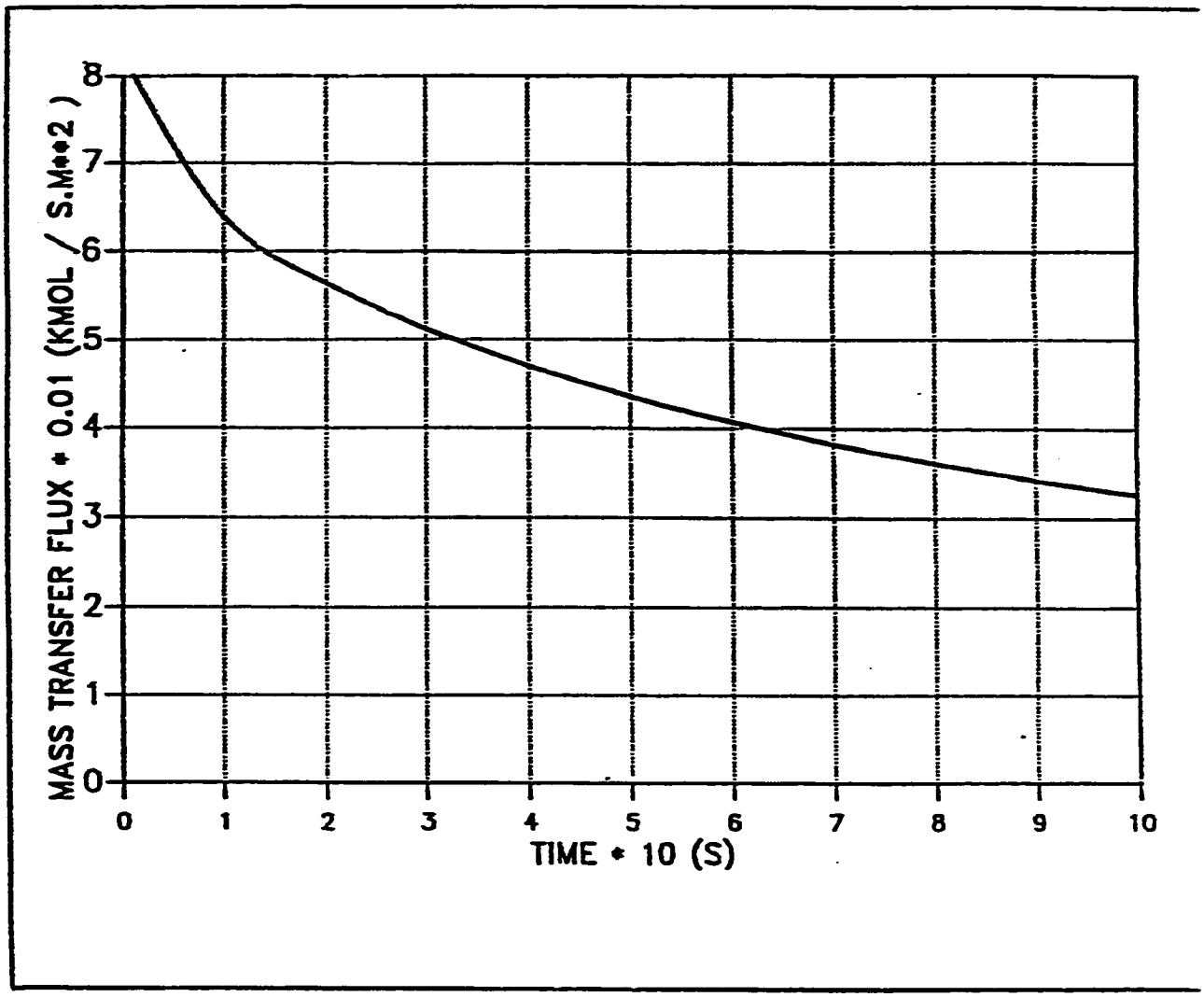

Fig(5.54) Mass transfer flus vs. Time

For cylindrical model.

$r_o = 1.0$, $V_{air} = 2\ m/s$

$T_r = 5.0^oC$. $T_s = (-3)^oC$.

5.3 Experimental Part

As mentioned in chapter (1) the ice crystals grown from vapour phase is taking very complicated and varying shapes and structures (see Appendix (A). This variation in the structure causes the studying of ice crystal wether experimental or theoretical to be very complicated since a small change in the environment where the ice crystal is growing will cause a considerable change in the growth model of the ice crystal resulting in a very complicated crystal shapes

From the previous discussion experimental work that has already been conducted to study the ice crystal growth from vapour phase is very essential in any try to understand the models of growth of ice crystals. In this section a study of the experiments that has been done by different scientist will be presented. One of the experiments has been done by Nakaya (1938) where he grew ice crystals in the laboratory and carried out experiments to investigate the effects of environmental conditions on the habits of the crystal. The ice crystals were grown on a rabbit hair suspended in a convective air stream. The temperature and humidity of the air stream could be varied due to the fluctuation in the convection current. It was difficult for Nakaya to get reproducible results.

A more detailed study of the influence of temperature on the habits of ice crystal growing from vapour phase in the atmosphere was carried out by

Hanajima (1949). He concluded that the most important factor which control the habits of ice crystal is it's temperature. As the temperature of the atmosphere is lowered from about ($-3°C$) to ($-25°C$) transition occurred in the basic habits of ice crystals. He also concluded that the growth mode of ice crystal would be changed by changing it's environmental temperature.

Jaweera (1969) did an experiment where he measured the variation of ice crystal dimensions with time. He concluded that the variation of ice crystal thickness with length will be until certain limit after which the ice crystal will grow in length with no variation along it's thickness. Other experimental work also done by Laplaca and Post (1960) and Brill and Tippe (1967) where they measured the variation of ice crystal dimensions with respect to time for ice crystal grown in the atmosphere, the results of the two experiments are not consistent and this is mainly due to the complicated nature of ice crystal. The only work that was done for the growth of ice crystals over flat plate due to humid flow of a mixture of air water vapour was by Gallily and Neusteader (1987). They studied ice crystals growth under different air mixture constituents. This mixture consists of various organic compounds mixed with air. They first studied the behavior of ice crystals for pure air water vapour mixture under the following conditions.

Ambient air temperature $= 5°C$

Plate temperature $= -10°C$

Air velocity $= 2$ m/s

Then they changed the air mixture by adding some organic gas and observing the ice crystals behavior under these conditions.

In the model the previous environmental conditions were assumed as the base for the comparison of the effect of varying the environmental conditions on ice crystal growth. The values obtained from this experimental data will be compared with the model to get the model justification.

TABLE (5.1) Comparison between the length of the crystal (C-Axis) in the Model and that obtained from experimental results.

Time. (s)	C-Axis Model μm	C-Axis Experiment μm	% difference
10	160	150	6.6
20	270	240	11.0
50	370	330	10.8
80	510	490	4.0
100	610	600	2.0

TABLE (5.2) Comparison between the radius of the crystal (A-Axis) in the Model and that obtained from experimental results. For Cylindrical Model.

Time. (s)	A-Axis Model μm	A-Axis Experiment μm	% difference
10	160	140	12.75
20	270	230	15.0
50	370	330	10.8
80	510	490	4.0
100	610	600	2.0

TABLE (5.3) Comparison between the length of the crystal (C-Axis) in the Model and that obtained from experimental results. For Spherical Model.

Time. (s)	C-Axis Model μm	C-Axis Experiment μm	% difference
10	130	150	15.3
20	220	240	10.0
50	305	330	8.2
80	420	490	14.0
100	530	600	13.2

From the tables (5.1), (5.2) and (5.3) it is evident that the cylindrical model is representing the ice crystal behavior in more realistic manner because the length of the crystal in cylindrical model is closer to experimental results than the other model. Also in cylindrical model more ability to control the growth of ice crystal in the radial direction is available.

The difference between the theoretical and experimental is mainly due to the assumption included in model and finite difference approximation errors . Also the most important source of error is the assumption in the growth mode since we assume in any mode that the growth mode is one mode what so ever the environmental conditions. This is not true since as small variation in temperature is occurring the ice crystals growth mode will be different and also densities will start to grow in the top of the crystal which is not assumed in the case of our model. The crystal is assumed to form from solid with constant density and no porosity which is in violation with the actual case. Since actually after certain limit of growth the ice at the top of the crystal will melt and converted to water, this water will come to the bottom of the crystal and converted to ice causing a more dense ice crystal formulation. Error also is there in the experimental work because of the very complex structure of ice crystals shapes and growth modes. Even though we have all these sources of error the model still represents a good approximation for ice crystal growth, showing very clearly the factors effecting this growth.

CHAPTER SIX

CONCLUSIONS AND RECOMMENDATIONS

Conclusions

The following conclusion can be made based on the numerical modelling studies:

(I) The numerical model developed in this thesis eliminates the inherent difficulties in formulating and applying any other more difficult methods to predict ice crystals growth.

(II) A numerical model for simulating the ice crystal behavior in both modes of growth (i.e. cylindrical and spherical modes) was developed, model solutions were generated for different environmental conditions. In each case, the model predicted the length and diameter of the ice crystal, temperature distribution along the radial and length directions for the cylindrical and spherical models.

(III) Comparison with experimental results is done showing that the maximum percent of error for cylindrical model is 11 % while for spherical model it reaches about 15 % .

(IV) Conclusion was made that the cylindrical model approximates the behavior of ice crystals more accurately that the spherical model, also control could be done on the radial direction growth in the case of cylindrical model which is not there in the case of spherical one.

(V) It is found that the most important factors which effect the crystal growth are the ambient and plate temperatures and air velocity.

Recommendations

(I) Initial frost formation modelling should based on modelling the ice crystal to grow in cylindrical shape.

(II) Better experimental determination of ice crystal growth modes is needed.

(III) Data on crystal dimensions, densities and masses as a functions of times are needed to create more accurate models.

(IV) Initial frost process, where the growth of ice crystals is occurring on flat plate over which passes a humid air, needs more experimental data under different environmental conditions.

APPENDICES

APPENDIX (A)

DIFFERENT SHAPES AND STRUCTURES OF ICE CRYSTALS.

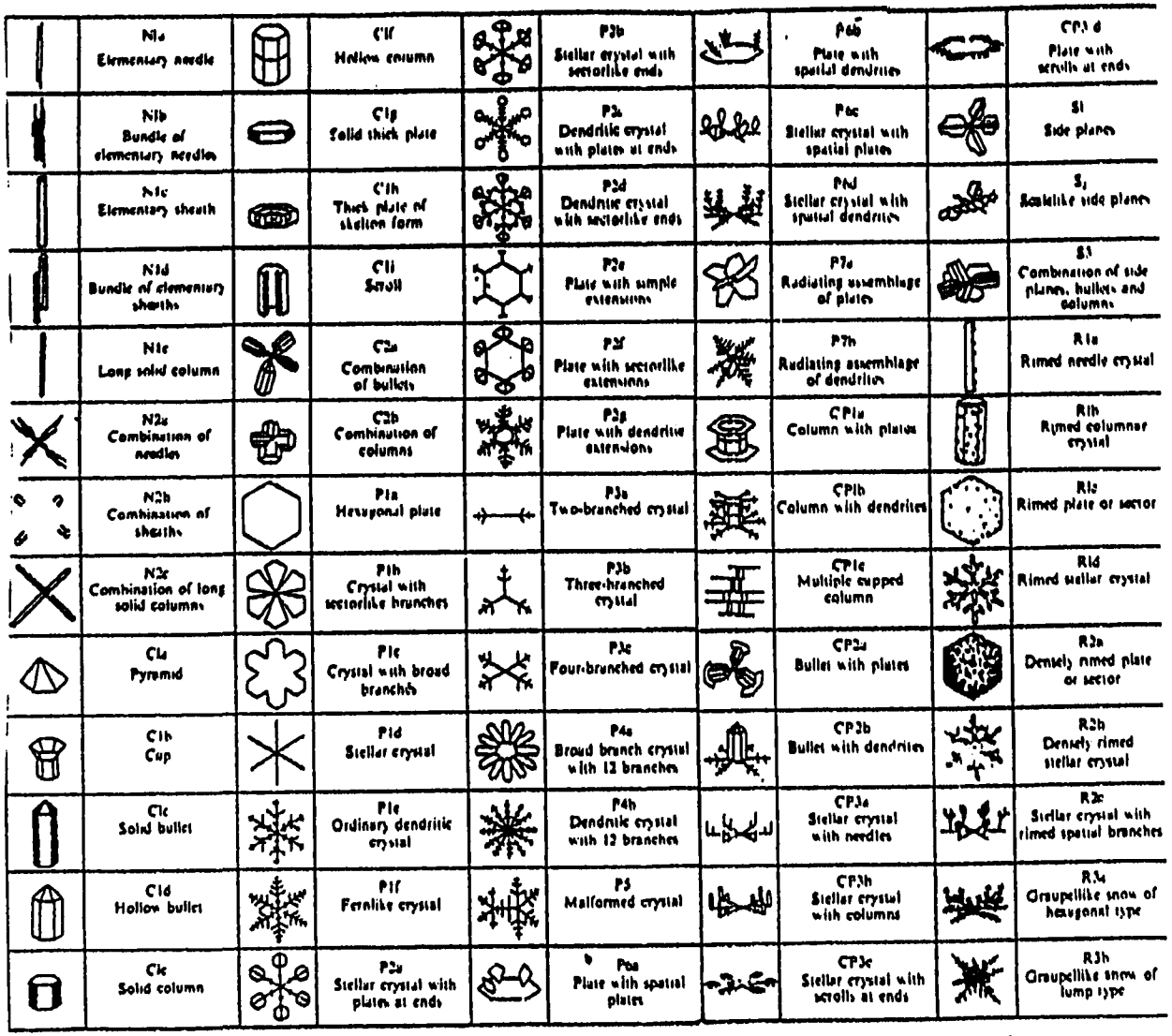

FIG(A.1) Meteorological classification of snow crystals, Mason(1953)

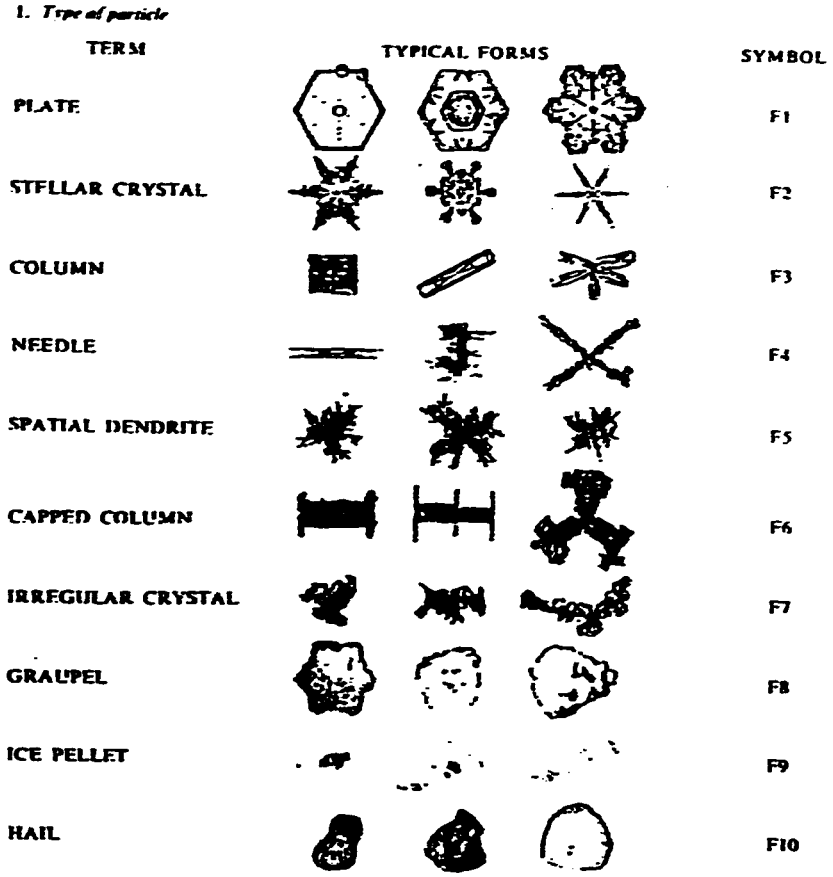

FIG(A.2) Examples of natural snow crystals, Mason(1953)

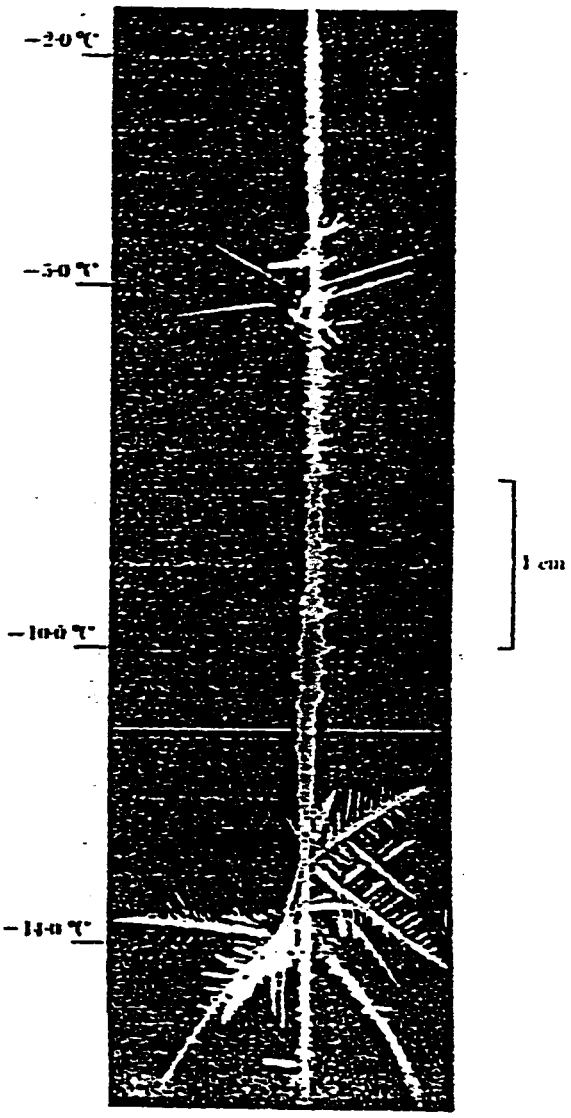

Cont. FIG(A.2) Examples of natural snow crystals, Mason(1953)

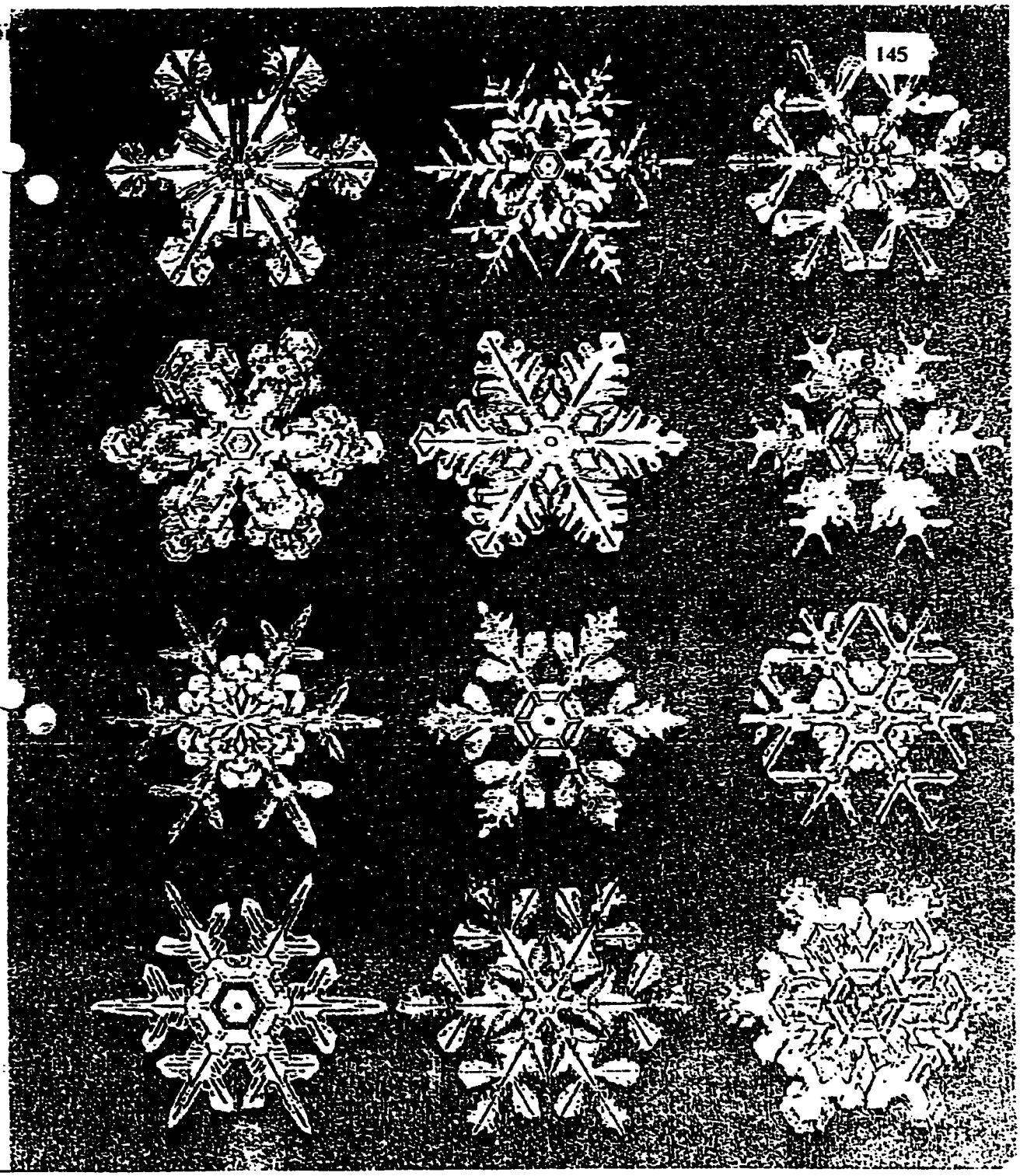

FIG(A.3) Examples of different types of ice crystals, Bently(1962).

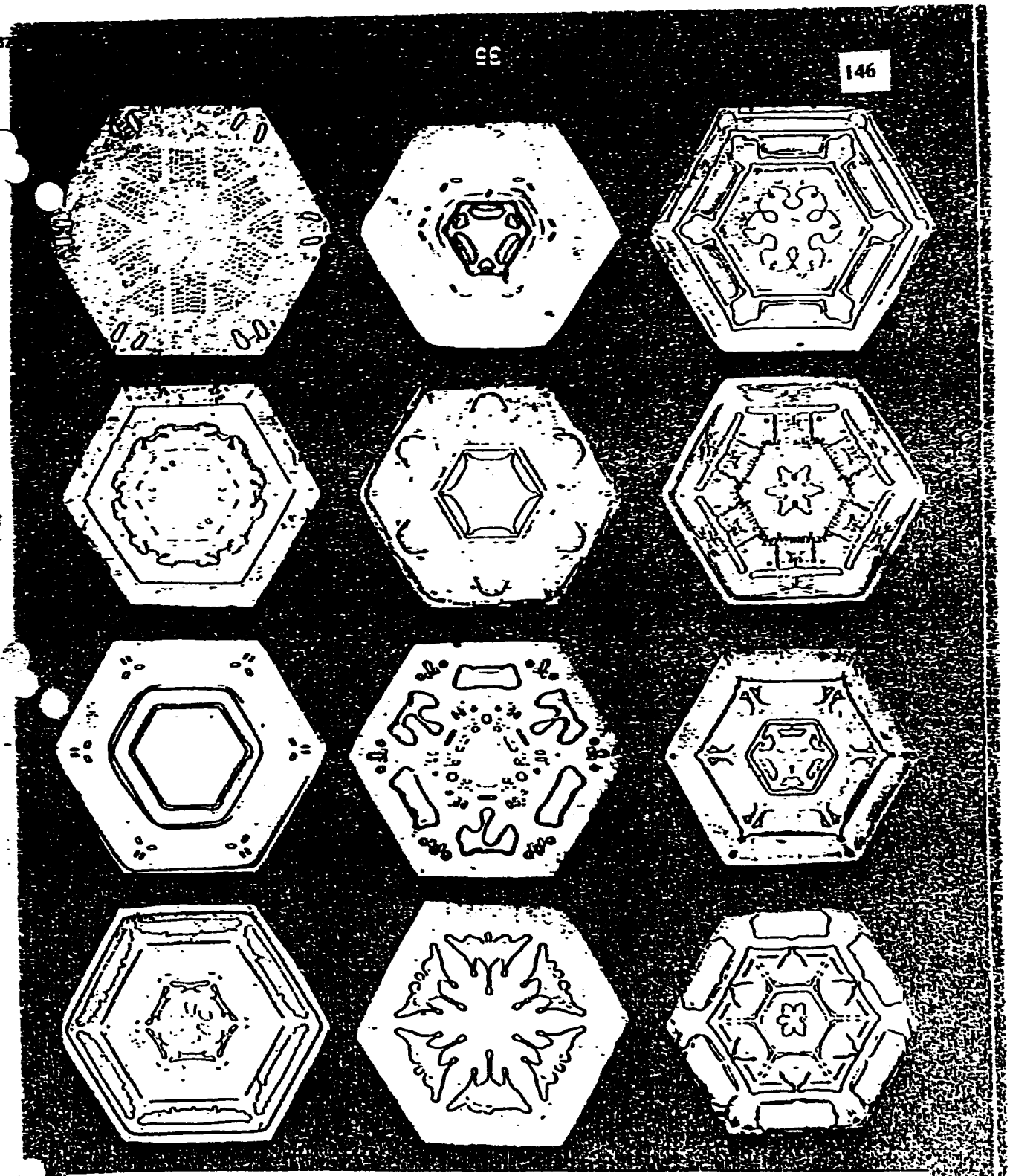

Cont. FIG(A.3) Examples of different types of ice crystals, Bently(1962).

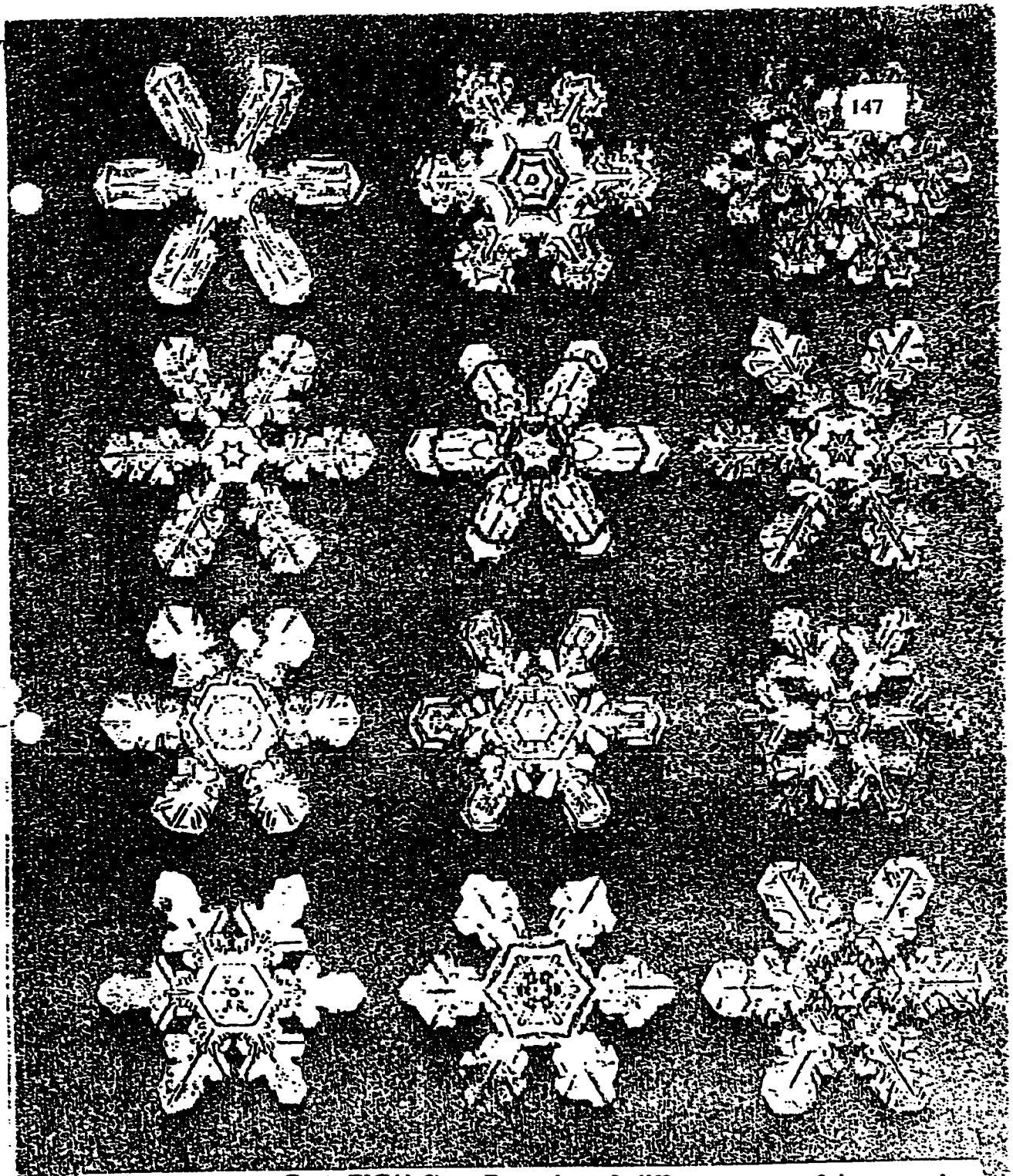

Cont. FIG(A.3) Examples of different types of ice crystals, Bently(1962).

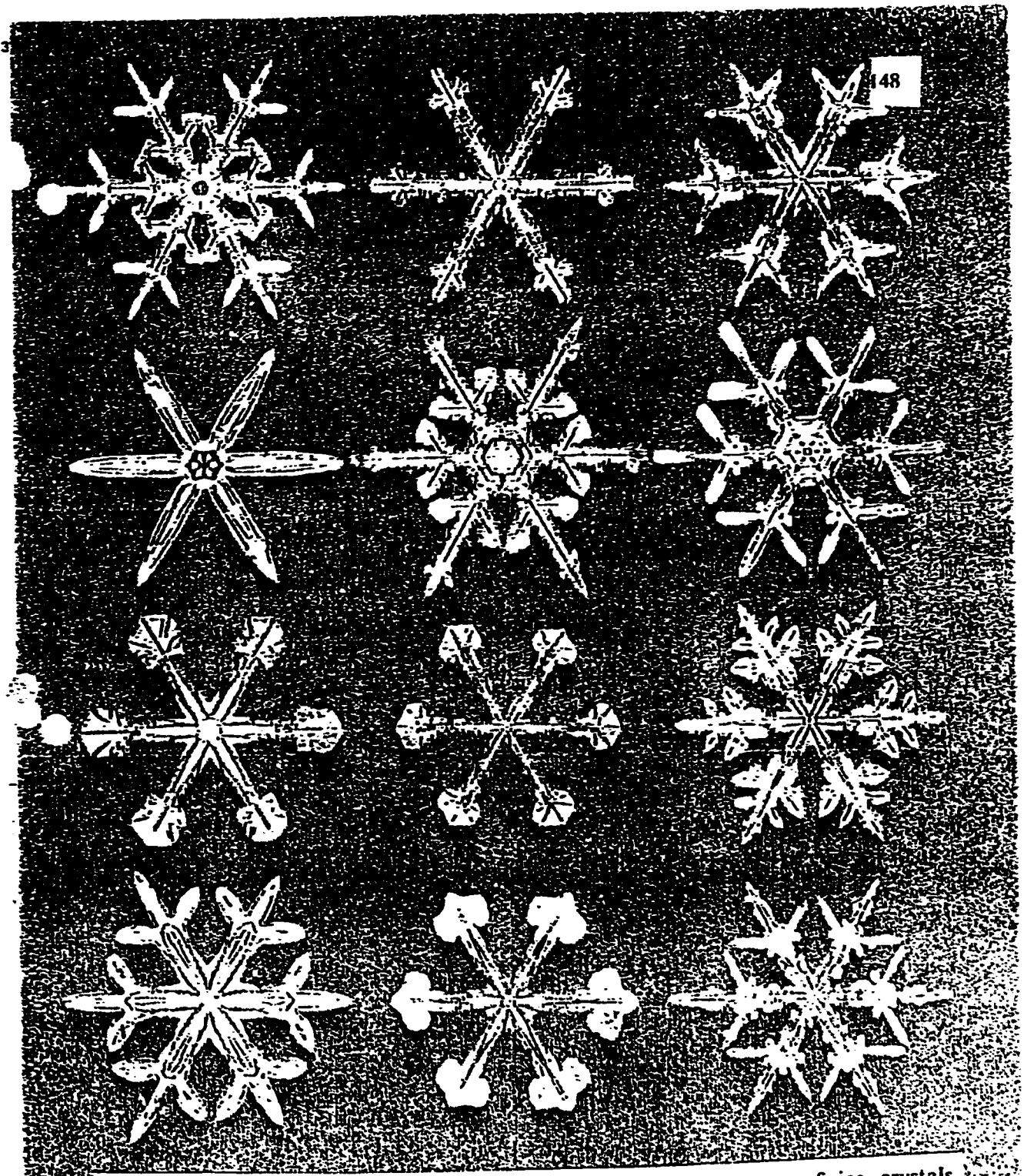

Cont. FIG(A.3) Examples of different types of ice crystals, Bently (1962).

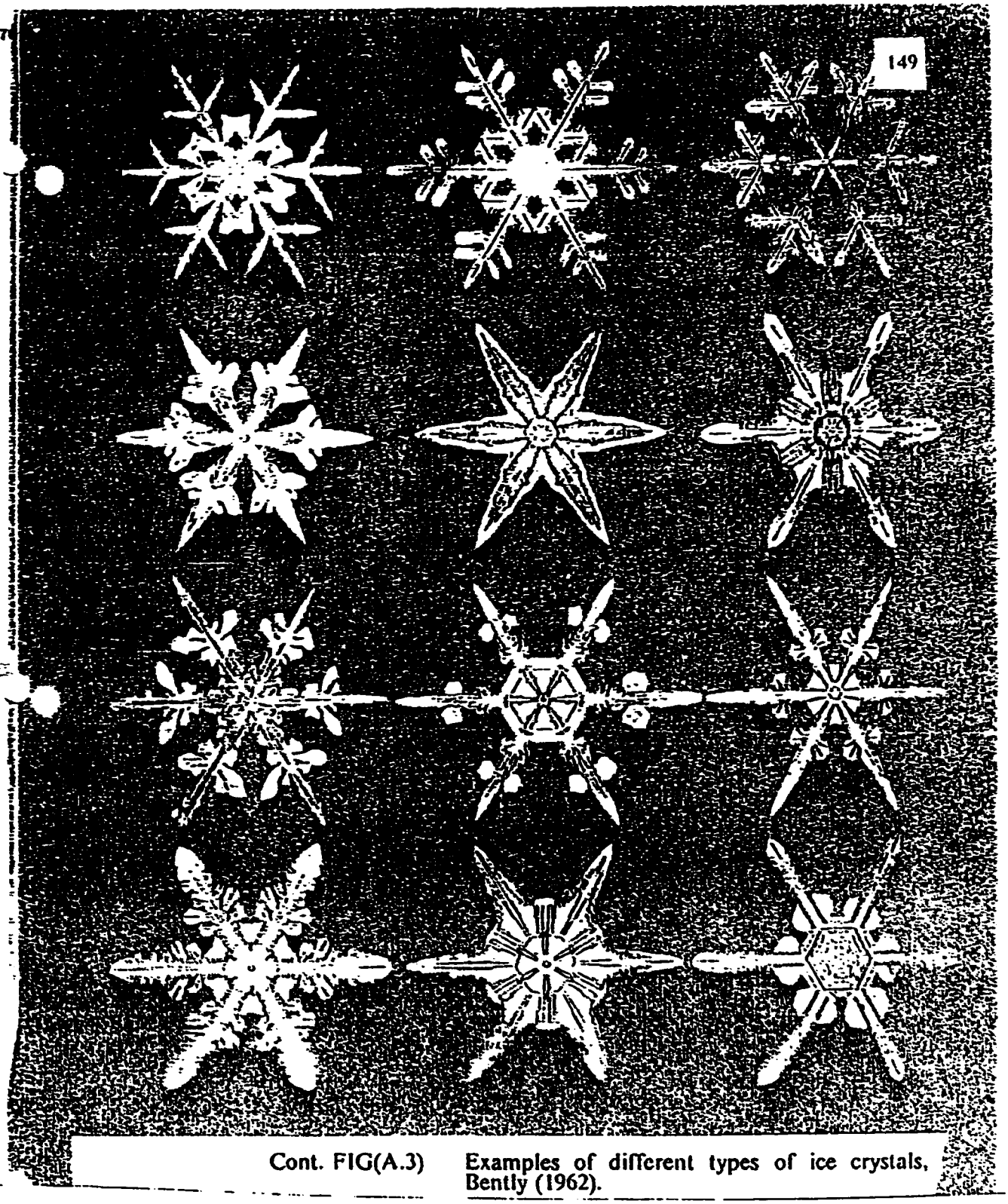

Cont. FIG(A.3) Examples of different types of ice crystals, Bently (1962).

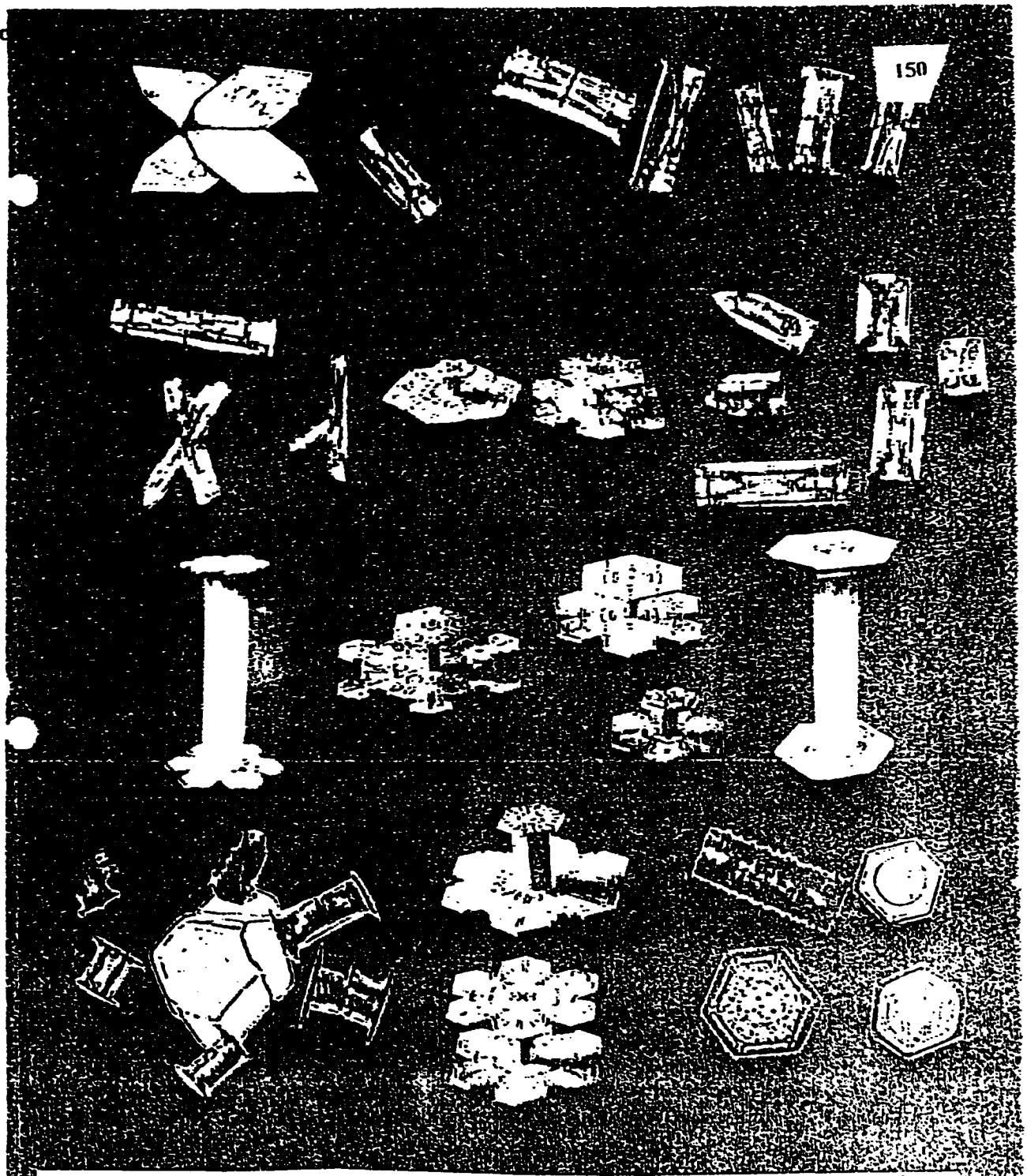

Cont. FIG(A.3) Examples of different types of ice crystals, Bently(1962).

APPENDIX B

MODEL EQUATIONS DERIVATION

B- NON-DIMENSIONALIZING ENERGY AND BOUNDARY EQUATIONS

B.1-Cylindrical Model.

B.1.1-Energy Equation.

The conservation of heat in cylindrical coordinate for two dimensional case where conduction is assumed to be dominant factor for heat transfer in the solid ice.

$$\frac{1}{\alpha_s}\frac{\partial T}{\partial t} = [\frac{1}{r}\frac{\partial}{\partial r}(r\frac{\partial T}{\partial r}) + \frac{\partial^2 T}{\partial z^2}] \qquad \text{(B.1)}$$

Since the dimensioned involved in this problem is very small in order of (μ_m) so a non dimensional equation will be used so non dimensionalizing equation (B.1) using dimensionless variables.

$$R=\frac{r}{r_o}, \quad Z=\frac{z}{z_o} \qquad \text{(B.2)}$$

$$\theta = \frac{T - T_s}{T_{des} - T_s}$$ dimensionless temperature. (B.3)

$$\tau = \frac{\alpha t}{z_o^2}$$ dimensionless time. (B.4)

$$z = Z z_o$$

$$r = R r_o$$

$$\partial z = z_o \partial Z$$

$$\partial z^2 = z_o^2 \partial Z^2$$

$$r = R r_o \rightarrow \partial r = r_o \partial R$$

$$\frac{\partial \theta}{\partial z} = \frac{1}{T_{des} - T_s} \frac{\partial T}{\partial z}$$

$$\frac{\partial T}{\partial z} = (T_{des} - T_s) \frac{\partial \theta}{\partial z}$$

$$\frac{\partial^2 \theta}{\partial z^2} = \frac{1}{T_{des} - T_s} \frac{\partial^2 T}{\partial z^2}$$

$$\frac{\partial^2 T}{\partial z^2} = (T_{des} - T_s) \frac{\partial^2 \theta}{\partial z^2}$$

$$\frac{\partial T}{\partial r} = (T_{des} - T_s)\frac{\partial \theta}{\partial r}$$

so equation (B.1) will become when the previous dimension less parameters are used.

$$\frac{1}{\alpha_s}\frac{\partial T}{\partial t} = [\frac{1}{r}\frac{\partial}{\partial r}(r\frac{\partial T}{\partial r}) + \frac{\partial^2 T}{\partial z^2}]$$

$$(T_{des} - T_s)\frac{\partial \theta}{z_o^2 \partial \tau} = \frac{1}{r_o R}\frac{\partial}{r_o \partial R}[r_o R(T_{des} - T_s)\frac{\partial \theta}{r_o \partial R}] + (T_{des} - T_s)\frac{\partial^2 \theta}{z_o^2 \partial Z^2}$$

$$\frac{1}{z_o^2}\frac{\partial \theta}{\partial \tau} = [\frac{1}{r_o^2}\frac{1}{R}\frac{\partial}{\partial R}(R\frac{\partial \theta}{\partial R}) + \frac{1}{z_o^2}\frac{\partial^2 \theta}{\partial Z^2}]$$

$$\frac{\partial \theta}{\partial \tau} = [\frac{z_o^2}{r_o^2}\frac{1}{R}\frac{\partial}{\partial R}(R\frac{\partial \theta}{\partial R}) + \frac{\partial^2 \theta}{\partial Z^2}]$$

$$\frac{\partial \theta}{\partial \tau} = [\frac{\Gamma_o^2}{R}\frac{\partial}{\partial R}(R\frac{\partial \theta}{\partial R}) + \frac{\partial^2 \theta}{\partial Z^2}] \qquad \text{(B.5)}$$

B.2- Boundary equations

For two dimensional moving boundary problem in cylindrical coordinates and in which the boundary is moving along (r,z) direction.

$$\rho_s \Delta H \frac{\partial Y_z}{\partial t} = [1 + (\frac{\partial Y_z}{\partial r})^2] [h_g(T_{des} - T_s) + k_s \frac{\partial T}{\partial z}] \qquad \text{(B.6)}$$

$$\rho_s \Delta H \frac{\partial Y_r}{\partial t} = [1 + (\frac{\partial Y_r}{\partial z})^2] [h_g(T_{des} - T_s) + k_s \frac{\partial T}{\partial r}] \qquad \text{(B.7)}$$

To nondimensionalize the previous equations the following dimensionless parameters will be used.

$$Y_Z = \frac{Y_z}{z_o} \ , \ Y_R = \frac{Y_r}{r_o} \ , \ \tau = \frac{\alpha_s t}{z_o^2}$$

$$\rho_s \Delta H \, z_o \frac{\partial Y_Z}{\frac{z_o^2}{\alpha_s}\partial \tau} = [1 + (\frac{z_o \partial Y_Z}{r_o \partial r})^2] [h_g (T_{des} - T_s) + k_s (T_{des} - T_s) \frac{\partial \theta}{z_o \partial Z}]$$

$$\frac{\alpha_s \rho_s \Delta H}{z_o} \frac{\partial Y_Z}{\partial \tau} = [1 + (\frac{z_o}{r_o})^2 (\frac{\partial Y_Z}{\partial r})^2] [h_g (T_{des} - T_s) + \frac{k_s}{z_o} (T_{des} - T_s) \frac{\partial \theta}{\partial Z}]$$

$$\frac{\alpha_s \rho_s \Delta H}{z_o} \frac{\partial Y_Z}{\partial \tau} = [1 + \Gamma_o^2 (\frac{\partial Y_Z}{\partial R})^2] [\frac{h_g z_o (T_{des} - T_s)}{T_{des} - T_s} + k_s \frac{\partial \theta}{\partial Z}] * (T_{des} - Ts) * \frac{1}{z_o}$$

$$\frac{\alpha_s \rho_s \Delta H}{T_s} \frac{\partial Y_Z}{\partial \tau} = [1 + \Gamma_o^2 (\frac{\partial Y_Z}{\partial R})^2] [\frac{h_g z_o}{k_s} \frac{(T_{des} - T_s)}{(T_{des} - T_s)} + \frac{\partial \theta}{\partial Z}] * k_s$$

$$G\frac{\partial Y_Z}{\partial \tau} = [1 + \Gamma_o^2(\frac{\partial Y_Z}{\partial R})^2]\ [\frac{\partial \theta}{\partial Z} + B_i(1 - \theta_v)] \qquad \text{(B.8)}$$

$$\text{Where } G = \frac{\Delta H}{C_s(T_v - T_s)} \qquad \text{(B.9)}$$

$$B_i = (\frac{h_g z_o}{k_s}) \qquad B_i = \textit{Biot number} \qquad \text{(B.10)}$$

For the second equation.

$$\rho_s \Delta H\, r_o \frac{\partial Y_R}{\frac{z_o^2}{\alpha_s}\partial \tau} = [1 + (\frac{r_o}{z_o})^2(\frac{\partial Y_R}{\partial Z})^2][\, h_g\, (T_{dis} - T_s) + \frac{k_s}{r_o}(T_{dis} - T_s)\ \frac{\partial \theta}{\partial R}]$$

$$\frac{\alpha_s \rho_s \Delta H}{(T_v - T_s)k_s}(\frac{r_o^2}{z_o^2})\frac{\partial Y_R}{\partial \tau} = [1 + \Gamma_o^2(\frac{\partial Y_R}{\partial Z})^2]\ [\, h_g \frac{r_o}{k_s}\frac{(T_{dis} - T_s)}{T_v - T_s} + \frac{\partial \theta}{\partial R}]$$

$$\frac{G}{\Gamma_o^2}\frac{\partial Y_R}{\partial \tau} = [1 + \frac{1}{\Gamma_o^2}(\frac{\partial Y_R}{\partial Z})]\ [\, B_{ir}(1 - \theta_v) + \frac{\partial \theta}{\partial R}]$$

Where

$$G = \frac{\Delta H}{C_s(T_v - T_s)} \quad , B_{ir} = \frac{B_i}{\Gamma_o}$$

B.2-Spherical Model.

B.2.1-Energy Equation.

The conservation equation for heat and mass transfer

for two dimensional case where conduction is assumed to be the dominant factor for heat transfer in the solid ice.

$$\frac{\partial^2 T}{\partial r^2} + \frac{2}{r}\frac{\partial T}{\partial r} + \frac{1}{r^2 \sin\varphi}\frac{\partial}{\partial \varphi}[\sin\varphi \frac{\partial T}{\partial \varphi}] = \frac{1}{\alpha_s}\frac{\partial T}{\partial t}$$

nondimensionlizing the previous equation

$$R = \frac{r}{r_o} \quad , \quad \theta = \frac{T - T_s}{T_{des} - T_s} \quad , \quad r = r_o R$$

$$\frac{1}{(T_{des} - T_s)}\frac{\partial^2 \theta}{r_o^2 \partial R^2} + \frac{2}{r_o R}\frac{1}{(T_{des} - T_s)}\frac{\partial \theta}{r_o \partial R} + \frac{1}{r_o^2 R^2 \sin\varphi}\frac{\partial}{\partial \varphi}[(\sin\varphi)\frac{1}{(T_v - T_s)}\frac{\partial \theta}{\partial \varphi}]$$

$$= \frac{1}{\alpha_s}\frac{\partial \theta}{\frac{r_o^2}{\alpha_s}\partial \tau}\frac{1}{(T_v - T_s)}$$

$$\frac{\partial^2 \theta}{\partial R^2} + \frac{2}{R}\frac{\partial \theta}{\partial R} + \frac{1}{R^2 \sin\varphi}\frac{\partial}{\partial \varphi}(\sin\varphi \frac{\partial \theta}{\partial \varphi}) = \frac{\partial \theta}{\partial \tau}$$

B.2.2- Boundary equations :

The equation for the ice-liquid interface in spherical coordinates system .

assuming the change in the solid liquid interface is along (R) direction is given by : (φ, t)

$$[1 + \frac{1}{Y_r^2}(\frac{\partial Y_r}{\partial \varphi})^2] [k_s \frac{\partial T}{\partial r} + h_g(T_{des} - T_v)] = \rho_s \Delta H \frac{\partial Y}{\partial r}$$

nondimensioning the previous equation

$$Y_R = \frac{Y_r}{r_o}, \qquad Y_r = r_o Y_R$$

$$[1 + \frac{1}{r_o^2 Y_R^2}(r_o^2 \frac{\partial Y_R}{\partial \varphi})^2] [k_s \frac{\partial \theta}{r_o \partial R} + h_g(1 - \theta_v)] = \rho_s \Delta H \frac{r_o \partial Y_R}{\frac{r_o^2}{\alpha_s} \partial \tau}$$

$$[1 + \frac{1}{Y_R^2}(\frac{\partial Y_R}{\partial \varphi})^2] [\frac{\partial \theta}{\partial R} + \frac{h_g r_o}{k_s}(1 - \theta_v)] = \frac{\Delta H}{C_s(T_v - T_s)} \frac{\partial Y_R}{\partial \tau}$$

assuming that $G = \frac{\Delta H}{C_m(T_v - T_s)}$

so the final form of the previous equation is

$$[1 + \frac{1}{Y_R^2}(\frac{\partial Y_R}{\partial \varphi})^2] [\frac{\partial \theta}{\partial R} + B_{ir}(1 - \theta_v)] = G \frac{\partial Y_R}{\partial \tau}$$

FINITE DIFFERENCE FORMULATION OF MODEL EQUATIONS.

For Cylindrical Model.

$$\frac{\partial\theta}{\partial\tau} = \Gamma_o^2 \left[\frac{1}{R} \frac{\partial}{\partial R} \left(R \frac{\partial\theta}{\partial R} \right) \right] + \frac{\partial^2\theta}{\partial Z^2}$$

To discretize this equation into finite difference form the equation will be expandid and then derivative descretization tables, like the one in finite difference tables will be used to evaluate first and second derivateves.

The discritization of this equation gives

$$\theta_{i,j}^{n+1} = \theta_{i,j}^{n} + \Gamma_o^2(\delta\tau) \left\{ \left[\theta_{i-1,j}^{n} - 2\,\theta_{i,j}^{n} + \theta_{i+1,j}^{n} \right] \frac{1}{(\delta R^2)} + \right.$$

$$\left. + \frac{1}{2\,i\,(\delta R)^2} \left[\theta_{i+1,j}^{n} - \theta_{i-1,j}^{n} \right] \right\} + \frac{\delta\tau}{(\delta Z)^2} \left[\theta_{i,j-1}^{n} - 2\,\theta_{i,j}^{n} + \theta_{i,j+1}^{n} \right]$$

Spherical Model

B.3.1- Model equations descretization :

The Energy Equation

$$\frac{\partial\theta}{\partial\tau} = \frac{\partial^2\theta}{\partial R^2} + \frac{2}{R}\frac{\partial\theta}{\partial R} + \frac{1}{R^2\sin\varphi}\frac{\partial}{\partial\varphi}(\sin\varphi\frac{\partial\varphi}{\partial\varphi})$$

The energy equation now becomes

$$\frac{\partial\theta}{\partial\tau} = \frac{\partial^2\theta}{\partial R^2} + \frac{2}{R}\frac{\partial\theta}{\partial R} + \frac{1}{R^2}\frac{d}{dX}\{(X-X^2)\frac{d\theta}{dX}\}$$

The discritization of the energy equation using finite difference explicit method. where forms of the derivateves are obtained from table(2)

$$\frac{\theta^{n+1}_{ij}-\theta^{n}_{ij}}{\delta\tau} = \frac{\theta_{i+1,j}-2\theta_{ij}+\theta_{i-1,j}}{(\delta R)^2} + \frac{2}{i\delta R^2}(\theta_{i+1,j} - \theta_{i-1,j})$$

$$+\frac{1}{(i\delta R)^2}[(j\delta X - j^2\delta X^2)\frac{(\theta_{i,j+1}-2\theta_{ij}+\theta_{i,j-1})}{(\delta X)^2} + (1-2j\delta X)\frac{\theta_{i,j+1}-\theta_{i,j-1}}{2(\delta X)}$$

$$\theta^{n+1}_{ij} = \theta^{n}_{ij} + \delta\tau\{\frac{i+1}{i\delta R^2}\theta^{n}_{i+1,j} - \frac{2}{(\delta R)^2}\theta^{n}_{ij} + \frac{i-1}{i(\delta R)^2}\theta^{n}_{i-1,j} +$$

$$\frac{1}{(i\delta R)^2}[(j\delta X - j^2\delta X^2)(\frac{\theta^{n}_{i,j+1} - 2\theta^{n}_{ij} + \theta^{n}_{i,j-1}}{(\delta X)^2}) + (1 - 2j\delta X)(\frac{\theta^{n}_{i,j+1} - \theta^{n}_{i,j-1}}{2\delta X})]\}$$

NOMENCLATURE

A : Area of the section in the control volume through which heat flows by conduction.

B_i: Biot number, $\frac{hz_o}{k_s}$.

B_{ir}: Radial Biot number, $\frac{B_i}{\Gamma_o}$

C : Concentration of desubliming component, kmol/ m^3

D_{ij}: Diffusion coefficient for binary mixture, cm^2/s.

F : Mass transfer coefficient, $\frac{DC}{Z}$

G : Dimensionless constant, $\frac{\Delta H}{C_s(T_v - T_s)}$

ΔH: Latent heat of sublimation, J/ kg.

h : Heat transfer coefficient, $W/m^2.k$.

k : Thermal conductivity.

k_i, k_f: Thermal conductivity of pure component.

N : Mass flux, kmole / $m^2.hr$.

N_A, N_B : Mass flux of pure components in a binary mixture, kmole/ $m^2.hr$.

M : Molecular weight of desubliming components, kg / kmole.

M_i, M_j: Molecular weight of pure components, kg / k mole .

r : Radial dimension along the crystal, μm.

r_o: Initial radius of the crystal, μm.

r : Radius of the crystal at any time, μm.

R : Dimensionless radius of the crystal, $\frac{r}{r_o}$.

t : time, s.

T : Temperature.

X : Transformation variable, $\frac{1-Cos\varphi}{Z}$

X_{AO}: Mole fraction of water vapour in the air-water vapour mixture.

X_{Ai}: Mole fraction of water vapour at the solid gas interface.

Yr : A variable in the boundary equation which is equivelant to the radius of the crystal, μm.

Yz : A variable in the boundary equation which is equivelant to the length of the crystal, μm.

z : Dimension along the length of the crystal, μm.

Z : Dimensionless length of the crystal, $\frac{z}{z_o}$.

z_o : Initial starting length of the crystal, μm.

GREEk LETTERS

α : Thermal diffusivity, m^2/s.

α_s : Thermal diffusivity of the ice, m^2/s.

Γ : Ratio between the length of the crystal and it's radius, $\frac{z}{r}$.

Γ_o : Initial ration between the length of the crystal and it's radius, $\frac{z_o}{r_o}$.

δ : Interval taken for numerical solution.

δR : Interval between successive grid points in radial direction , μm.

δS : Dummy spatial variable, μm.

δt : Time increment.

δZ : Interval between successive grid points along the length of the crystal, μm.

$\delta\tau$: Time increment.

Δ : Difference between values.

ε : Collision integral.

θ : Dimensionless temperature, $\frac{T-T_s}{T_{des}-T_s}$.

λ :	Dummy spatial interval .
μ :	Viscosity, kg / m . s .
ρ :	Density, kg / m^3.
ρ_s :	Density of ice crystal kg / m^3.
τ :	Dimensionless time, $\frac{\alpha t}{z_o^2}$
ξ :	Rate of heat flow.
φ :	Angle in spherical coordinate.

SUBSCRIPTS.

des :	Desublimation.
i, j :	Grid location in the radial and axial direction respectively.
V :	Vapour.
r , R :	Radial direction.
z , Z :	Direction along the length of the crystal.
φ :	Angular direction in spherical coordinates.
S :	Surface and solid ice .
O :	Initial value.

SUPERSCRIPTS.

n :	Previous time level.
n + 1 :	Present time level.

REFERENCES

[1] Allen, C.L., "Structural Model For Vitreous Ice.", Physics And Chemistry Of Ice,pp.13-18,1973.

[2] Braham R.R., "Meteorological Basis For Precipitation Developmen", Bull.Amer.Meteo.Soc., V.49, pp.343-353, 1968.

[3] Colbeck, S., "Temperature Dependence Of Equilibrium Form Of Ice.", J.Crystal Growth, V.72, pp.726-732, 1985.

[4] Comini, G. And Bonacina, C., " Numerical Solution To Phase Change Problems.", Int.J.Heat Mass Transfer, V.16, pp1825-1832, 1973.

[5] Cotterill R.M, Martin,J.W., Nielsen, O.V. And Pedersen O.B.," Computer Studies Of Perfect Crystal Properties And Defect structures.", Physics And Chemistry Of Ice, pp.23-27, 1973.

[6] Fletcher, N.H., The Chemical Physics of Ice, Cambridge, 1970.

[7] Frank,K., Principles of heat transfer, third edition, USA, 1973.

[8] Gallily, I And Neusteadter, J., " Some Aspects of Ice Crystal Growth From Vapour Phase.", J.Crystal Growth, V.85, pp.422-432, 1987.

[9] Gallily, I. And Micheali, G., "Mass Growth measurements Of Freely Falling Ice Crystal.", J. Crystal Growth, V.47, pp.219-29, 1960.

[10] Guavin, W.H. And Pasternak, I.S., " Turbulant Heat And Mass For

Stationary Particles ", Cond.J. Chem.Eng., pp.5-42, April 1960.

[11] Gray, D.M. and Male, D.H., Hand Book of Snow, Canada, 1981.

[12] Hallett, J. And Cho, N., "Ice Crystal Growth.", J. Crystal Growth, V.69, pp.325-334, 1984.

[13] Hamphregs, W.J. and Bentley, W.A.,Snow Crystals, Newyork, 1962.

[14] Hastaoglu, M.A., "Numerical Solution To A Moving Boundary Problem, Application To Melting And Solidification.",Int.J. Heat Mass Transfer, V.29, pp.495-499, 1986.

[15] Hastaoglu, M.A., "Numerical Solution To A Three Dimensional Moving Boundary Problem, Melting And Solidification With Blanketing Of A Third Layer.", Chem.Eng.Sci., V.42, pp.2417-2423, 1986.

[16] Hindman,E.E. And David Johnson, "Numerical Simulation Of Ice Paticle Growth In A Cloud Of Super Cold Water", J.Atmos. Sci., V.29, pp.1313-1320, 1972.

[17] Heymsfield,A., "Cirrus Uncinus Generating Cells And The Evolution Of Cerriform Clouds", J.Atmos.SCI., V.32, pp820-829, 197

[18] Hobbs, P.V.And Fraster, a.b., "A Theoritical Study Of The Flow Of Air and The Fall Out Of Solid Precipitation Over Mountainous Terrain Part II ", J.Atmos.Sci, V.30, pp.813-823, 1973.

[19] Hobbs, P. Ice physics, Oxford, 1974.

[20] Hobler T, Mass Tansfer and Absorbers, Canada, 1966.

[21] Jayaweera, K.O., "Calculation Of Ice Crystal Growth", J.Atmos.Sci, V.28, pp.728-736, 1968.

[22] Kajikawa, M. and Heymsfield, A. ,"Aggregation Of Ice Crystals." ,J.Atmos.Sci., V.46, pp.3108-3121, 1989.

[23] Kallungal, J.P. And Barduhn, A.J.,:"Effect Of Forced And Natural Convection On Ice Crystal Growth", AICHE, V.23, pp.256-265, 1977.

[24] Kamb,B.,"Crystallography Of Ice.", Physics And Chemistry Of Ice, pp.2-41, 1973.

[25] Klinger,J.,"Thermal Conductivity of Ice Single Crystal.", Physics And Chemistry Of Ice, pp.114-116, 1973.

[26] Knight, A.C., "Comments On The Role Of Cubic Structure In Ice Nucleation.", J. crystal Growth ,V.62,pp633-634, 1983.

[27] Laudise, R.A. And Barns, R.L.,"Size And Prefections Of Ice Crystals", J.Atmos.Sci., V.38, pp.458-469, 1979.

[28] Lazaridis, A.," Numerical Solution Of The Multidimensional Solidification Or Melting Problem.",Int.J.Heat Mass Transfer , pp.1459-1477, January 1970.

[29] Mason, B.J., "The Growth Of Ice Crystal In Super Cold Water Cloud", Quant.J.Royal.Meteor.Soc., V.79, pp.104-111, 1953.

[30] Miller, t.And Young, k., "Numerical Simulation of Ice Crystal Growth From Vapour Phase, " J.Atmos.Sci., V.36, pp.458-469, 1978.

[31] Ono, A, "Growth Mode Of Ice Crystals In Natural Clouds", J.Atmos.Si,V.27, p p.649-658, 1970

[32] Perry, R.H. , Perry's Chemical Engineering Hand Book, sixth edition , Newyork, 1984.

[33] Pruppacher, H. And Hall W.d., " The Survival Of Ice Particles From Cirrus Clouds In Subsaturated Air", J.Atmos.Sci., V.33, pp.1995-2006, 1976.

[34] Reynolds,S.E., " Ice Crystal Growth", J.Meteor., V.9, pp.36-40, 1952. Lake Ice", J.Crystal Growth, V.71, pp.104-110, 1984.

[35] Sahin,A, Nucleation Of Frost On Cold Surfaces, PHD, University Of Michigan, 1988.

[36] Sherwood, T.K., Mass Transfer, USA, 1973

[37] Skelland, H., Diffusional Mass Transfer, Newyork, 1974.

[38] Smith, T., Numerical Solution To PDE, Newyork, 1975.

[39] Stoyanova, V, Nenow, D. And Genadier,N., " Instability Of Vapour Grown Ice Crystals.", J. crystal Growth, V.69, pp.489- 492, 1984.

[40] Sunderland, E. And Cho, S.H., " Phase Change Of Spherical Bodies.", Int.J.Heat Mass Transfer, 1969.

[41] Termizi, H.And Gill, N., " Effect Of Natural Convection On Growth Velocity And Morphology Of Dendretic Ice Crystals ". J.Crystal Growth, V.85, pp.488-502, 1987.

[42] Trybal, R.E., Mass Transfer Operations, USA, 1980.

[43] Tryde, P., Physics and Mechanics of Ice, Newyork, 1980.

[44] Whally,E., Jones, S.J. and Gold, L.W., Physics and Chemistry of ice, Ottawa, 1973.

VITA

NAME: EBALL HIFTHY ABD-AL-RAHEEM AHMAD

ADDRESS: KFUPM P.BOX#539

DHAHRAN 31261

SAUDI ARABIA

NATIONALITY: JORDANIAN

EDUCATION

1989-DATE

KING FAHD UNIVERSITY OF PETROLEUM & MINERALS (KFUPM),

MECHANICAL ENGINEERING DEPARTMENT, DHAHRAN, SAUDI ARABIA.

Expected to graduate by february 1992 with a Master's Degree in Mechanical Engineering. I took graduate courses related to heat conduction, heat convection advanced fluid mechanics, advanced mass transfer, numerical solution to PDEs and advanced engineering mathematics.

My M.S. thesis was related to a factor which affects air-conditioning and refrigeration systems .My thesis title is **Numerical Simulation Of Ice Crystals Growth** . In this thesis both heat and mass transfer problem was solved numerically using finite difference method.

Having a very good knowledge in numerical work which

involve any finite difference or finite element techniques.

Very interested in researches related to heat and mass transfer, air-conditioning and energy applications.

Having an excellent knowledge in many programming languages like : **Pascal, Fortran, Assembly and Prolog** since I took many courses related to these languages.

Familiar with P.C. usage and many technical PC programs.

Having an excellent knowledge in digital logic design, computer design and computer microprocessors .

I designed a complete PC set in a microprocessors course.

Familiar with machine design and design concepts .I designed a gear box and other design projects in machine design courses.

1983-1989

KING FAHD UNIVERSITY OF PETROLEUM & MINERALS (KFUPM),

MECHANICAL ENGINEERING DEPARTMENT, DHAHRAN, SAUDI ARABIA.

Graduated in 1989 in Mechanical Engineering with a GPA of 3.34 on 4.00 scale with HONORS.

Familiar with concepts of AIR-CONDITIONING and SOLAR ENERGY applications.

Familiar with PUMPING MACHINERY, MACHINES

VIBRATIONS , SYSTEMS STABILITY and MACHINES DESIGN.

I am also familiar with CLASSICAL and MODERN CONTROL.

My senior project was (Comfort Verification at KFUPM Academic Buildings) which was supported by Energy Research Lab and it was supervised by DR.Mohammad Abdulrahman from energy research lab.